Iron and manganese in Antarctic bivalves:
Indicators of change in near-shore biogeochemistry?

Eisen und Mangan in antarktischen Muscheln:
Indikatoren für Änderungen der küstennahen Biogeochemie?

Dissertation zur Erlangung des
Doktorgrades der Naturwissenschaften
(Dr. rer. nat.)

an der
Fakultät für Mathematik und Naturwissenschaften
der Carl von Ossietzky Universität Oldenburg
- angenommene Dissertation -

von
Harald Poigner

geboren am 21.5.1984 in Wien

gewidmet im Andenken an meinen Großvater,
Johann Diernegger
* 15.11.1930   † 27.11.2013

Preface

This study was conducted in the framework of the priority program SPP 1158 „Antarktisforschung", funded by the Deutsche Forschungsgemeinschaft (DFG) and was associated to the IMCOAST-project (AP-9; www.imcoast.org). The present work is submitted as dissertation and was supervised by PD Dr. habil. Doris Abele (Alfred Wegener Institute Helmholtz Centre for Polar and Marine Research, Bremerhaven, Germany) and Prof. Dr. Hans-Jürgen Brumsack (Institute for Chemistry and Biology of the Marine Environment, Oldenburg, Germany) and instructed by Dr. Dorothee Wilhelms-Dick (Alfred Wegener Institute Helmholtz Centre for Polar and Marine Research, Bremerhaven, Germany).

The cumulative thesis includes five manuscripts (one published, one under review and three in preparation for submission) to which a general introduction is prefixed in chapter 1. The introduction reviews (i) the characteristics of the clam *Laternula elliptica* and (ii) the consequences of glacial retreat on the Western Antarctic Peninsula (WAP) to the coastal areas as well as the objectives of the thesis (chapter 1). Chapter 2 focuses on the particle selection and nutrition of *L. elliptica* to discuss the consequences on trace metal uptake by the bivalve which is relevant in the subsequent chapters. Within chapters 3 and 4, both research articles, the influence of the bivalve environment (sediment, pore water, and seawater) on Fe and Mn concentrations in the hemolymph and on tissue contents is discussed to define the major Fe and Mn sources for the clam. To assess the suitability of the bivalves' chondrophore as archive to monitor the glacial retreat (i) the mineralogical composition of the condrophore was analyzed to determine the polymorph depended incorporation of trace elements (chapter 5), (ii) trace metal concentrations along seasonal growth layers of the chondrophore (containing only aragonite) were analyzed (chapter 6). In chapter 7, I summarize the main results of the thesis, draw conclusions, and highlight the main findings and the open questions to be answered by further research.

During the PhD thesis I cooperated in a German-Ukranian project (Toxicological effect of Ni^{2+} and Co^{2+} on the goldfish, *Carassius auratus*) and contributed to three further publications. The abstracts of these publications are presented in chapter 8.

Table of contents

List of figures

(abbreviated)

List of tables

(abbreviated)

Abbreviations

95% CI	95% confidence interval
ACC	amorphous calcium carbonate
AE	assimilation efficiency
AFM	atomic force microscopy
Ar	aragonite (in chapter 5 only; otherwise the chemical element Argon)
ASW	Atlantic seawater
ATP	Adenosine-5'-triphosphate
a.u.	arbitrary units
AWI	Alfred Wegener Institute Helmholtz Centre for Polar and Marine Research
b.d.l.	below detection limit
cmbsf	cm below seafloor
conc.	concentrated/ concentration
CP	carbonyl proteins
CRM	confocal raman microscopy
DFG	Deutsche Forschungsgemeinschaft (German Research Foundation)
DG	digestive gland
DT	digestive tract
e.g.	exempli gratia (for example)
EMP	electron microprobe
ENSO	El Nino Southern Oscillation
EPF	extrapallial fluid
G	gills
HR	high resolution
ICBM	Institute for Chemistry and Biology of the Marine Environment
i.e.	id est (that is)
ICP	inductively coupled plasma
ICP-MS	ICP-mass spectrometry
ICP-OES	ICP-optical emission spectroscopy
IPCC	Intergovernmental Panel on Climate Change
KGI	King George Island
LA	laser ablation
LOOH	lipid peroxides
l.o.q.	limit of quantification
LR	low resolution
L-SH	low molecular mass thiol-containing compounds

MR	medium resolution
n.c.	not certified
n.d.	not determined
OA	ocean acidification
p.a.	pro analysi (reagent grade)
PE	polyethylene
PFA	perfluoroalkoxy
pH	potential hydrogen
PP	polypropylene
PTFE	polytetrafluoroethylene (Teflon[®])
Q	quadrupole
r	Pearson correlation coefficient
R^2	determination coefficient
ROS	reactive oxygen species
S	siphon
SD	standard deviation
SF	sector field
SST	sea surface temperature
SPM	suspended particulate matter
u.a.	unter anderem
Va	vaterite
WAP	Western Antarctic Peninsula
XANES	X-ray absorption near edge structure
XRD	X-ray diffraction
z.B.	zum Beispiel

List of publications submitted for the thesis

The main part of the thesis includes five articles, whereas one is already published (chapter 5), one article is under review (chapter 3), and three articles (chapter 2, 4, 6) are in preparation:

Publication I (Chapter 2)

Particle ingestion of the Antarctic clam *Laternula elliptica* in Potter Cove, King George Island

H. Poigner, M. Hernando, D. Wilhelms-Dick, and D. Abele

Article in preparation for submission.

Own contribution:

- Concept development.

- Sample preparation and analyses of the smear slides.

- Data evaluation and interpretation together with all coauthors.

- The first draft of the manuscript was written by myself and revised together with all coauthors.

Publication II (Chapter 3)

Influence of the pore water geochemistry on Fe and Mn assimilation in *Laternula elliptica* at Potter Cove (King George Island, Antarctica)

H. Poigner, P. Monien, D. Monien, M. Kriews, H.-J. Brumsack, D. Wilhelms-Dick, and D. Abele

Submitted to the journal of Estuarine and Coastal Shelf Science, 24.01.2013.

(under review)

Own contribution:

- Concept development together with D. Abele, D. Wilhelms-Dick, and P. Monien.

- Sample preparation and analyses (ICP-MS measurements together with D. Wilhelms-Dick).

- Data evaluation and interpretation together with all coauthors.

- The first draft of the manuscript was written by myself and revised together with all coauthors.

Publication III (Chapter 4)

Stable Fe isotopes (δ^{56}Fe) in the hemolymph of the clam *Laternula elliptica* as indicator for sources of assimilated Fe

H. Poigner, D. Wilhelms-Dick, D. Abele, Michael Staubwasser, and S. Henkel
Article in preparation for submission.

Own contribution:

- Concept development, Sample preparation and analyses together with S. Henkel.

- Data evaluation and interpretation together with all coauthors.

- The first draft of the manuscript was written by myself and revised together with all
  coauthors.

Publication IV (Chapter 5)

Coexistence of three calcium carbonate polymorphs in the shell of the Antarctic

clam *Laternula elliptica*

G. Nehrke, H. Poigner, D. Wilhelms-Dick, T. Brey, and D. Abele (2012)

Geochemistry, Geophysics, Geosystems, 13, 5.

(G. Nehrke and H. Poigner are both first authors)

Own contribution:

- Concept development together with T. Brey and G. Nehrke.

- Sample preparation and analyses together with G. Nehrke.

- Data evaluation and interpretation together with all coauthors.

- The first draft of the manuscript was written by myself and revised together with all
  coauthors.

Publication V (Chapter 6)

Trace metal incorporation into the chondrophore of *Laternula elliptica*: Indicator of

change in nearshore biogeochemistry?

H. Poigner, A. Klügel, G. Nehrke, D. Abele, and D. Wilhelms-Dick

Article in preparation for submission.

Own contribution:

- Concept development together with D. Abele and D. Wilhelms-Dick.

- Sample preparation.

- Sample analyses together with A. Klügel and G. Nehrke.

- Data evaluation and interpretation together with all coauthors.

- The first draft of the manuscript was written by myself and revised together with all
  coauthors.

Abstract

During the last decades global climate change caused a strong rise in air temperature on the Western Antarctic Peninsula (WAP) which provoked a decreasing period of sea ice cover, increasing glacial retreat, and an increasing release of freshwater and lithogenic material into coastal waters. In Maxwell Bay (King George Island; KGI) the sediment accumulation rates tripled during the last century – resulting in changing environmental conditions for benthic filter feeders, like the circum Antarctic clam *Laternula elliptica*.

Iron (Fe) and manganese (Mn) tissue contents in *L. elliptica* are higher compared to other bivalve species and vary by more than one order of magnitude around the Antarctic continent. Several authors related both, the high contents and the variability, to the high input of terrigenous, lithogenic material released by glacial melt, because Fe and Mn content in lithogenic material exceed dissolved metal concentrations in sea water several orders of magnitude. Based on this assumption, a potential suitability of Fe and Mn as proxies for glacial melting is considered.

This thesis focuses on the assimilation of metals by *L. elliptica* and their incorporation into the carbonate shell. In particular, the present work surveys the suitability of the two elements Fe and Mn as proxies for the melt water driven element load into the coastal environment of Potter Cove (KGI).

Laternula elliptica assimilates bioavailable Fe and Mn from many different dissolved and particulate sources (e.g. planktonic and benthic microalgae, detritic and inorganic particulate matter, seawater, pore water). Therefore, possible assimilation pathways need be known to verify a direct relationship between the potential proxies (Fe, Mn in the shell of *L. elliptica*) and the changing environmental process (melt water driven import of lithogenic matter into coastal waters).

In a first step, ingested material retrieved from siphon, gills, and the digestive tract of *L. elliptica* was qualitatively analyzed for its particle composition (chapter 2). Lithogenic particles rarely exceeded 5 µm diameter. Visible organic particles were bigger (10 – 250 µm) and consisted mainly of diatoms. Nevertheless, they appeared strongly diluted by lithogenic material. Comparisons with existing literature suggest suspended organic matter mainly of detritic origin and to a lesser extend benthic diatoms as major food sources for *L. elliptica* in Potter Cove. The discrepancy among particle sizes of ingested lithogenic and organic particles support an active selection and the rejection of sediment particles as pseudo feces, which is in agreement with existing literature. This physiological control on the ingestion likely affects the assimilation of Fe and Mn and complicates their potential use as environmental proxies.

Iron and Mn analysis of the hemolymph and tissues of *L. elliptica* and comparisons to pore water and seawater concentrations as well as sediment contents in Potter Cove were accomplished to determine the environmental influence on element assimilation in the bivalve (chapter 3). Low experimental Fe concentrations caused a rapid decline of high initial Fe concentrations in the hemolymph, indicating an environmental control on Fe hemolymph concentrations. Further analysis revealed that on average only 30% of the total hemolymphmatic Fe concentration was bound cellular within hemocyte cells. Seawater Fe concentrations ($0.01 - 0.76$ µmol L^{-1} Fe) were, however, too low to explain high Fe concentrations in the hemolymph ($5.6 - 458$ µmol L^{-1} Fe). Based on similarly high Fe concentrations in the hemolymph and pore water samples ($1.4 - 192$ µmol L^{-1} Fe; from sediment surface down to 5 cm below seafloor) from selected sampling sites in the Cove pore water appears to be the main Fe source for *L. elliptica*. Mn concentrations in hemolymph ($0.1 - 4.0$ µmol L^{-1} Mn) showed a discrimination against pore water concentrations ($0.8 - 60$ µmol L^{-1} Mn), but were distinct enriched compared to seawater Mn concentrations ($0.01 - 0.09$ µmol L^{-1} Mn). No significant differences in hemolymph and tissue Fe and Mn concentrations were found between two sites of high and lower input of lithogenic debris.

Differences in the geochemical environment of the sediment and resulting concentrations of dissolved Fe and Mn in pore water at different sampling sites seem to be responsible for the high variability of Fe and Mn concentrations in tissues of *L. elliptica*. This result strongly contradicts an unambiguous relationship between the amount of lithogenic particulate matter and metal assimilation by *L. elliptica*, since several factors related to sediment diagenesis such as the content of organic matter, oxygen penetration depth, remineralization rate, and bioirrigation regulate the concentrations of dissolved Fe and Mn in pore water and the flux across the benthic boundary.

To support the conclusion, that Fe concentrations of the hemolymph are depend on pore water concentrations, Fe isotope signatures of bivalve hemolymph and environmental Fe sources (sediment, pore water) were analyzed as well. Stable Fe isotopes, however, can only be applied as proxy for Fe dietary sources, if physiological fractionation processes (during assimilation, storage, transport) within *L. elliptica* can be identified or excluded. This thesis presents the first characterization of the Fe stable isotope signature (δ^{56}Fe) in bivalve hemolymph (chapter 4).

The shell of *L. elliptica* was tested for homogeneity in calcium carbonate polymorph composition (chapter 5) prior to the analysis of incorporated trace elements, because trace elements fractionate among different polymorphs. Within this study we show for the first time the coexistence of three calcium carbonate polymorphs (aragonite, calcite, and

vaterite) within a marine calcifying organism. Annual shell growth layers continued through different polymorphs (suggesting a simultaneous mineralization) which complicates the suitability of trace element based proxies in the chondrophore of *L. elliptica*, due to a polymorph dependent trace metal incorporation (verified for Sr and Mg). As consequence, mineralogical analyses are additionally necessary to exclude mineralogical control on trace metal incorporation. Therefore, we selected only individuals composed exclusively of aragonite for the quantification of trace elements within the chondrophore (chapter 6). The incorporation of B, Mg, and Sr showed a strong seasonality with distinct maxima in winter growth layers, coinciding with concentration minima of Ba. Contents of Fe and Mn dropped during the first years of bivalve lifetime, which is consistent with an earlier study, and underwent the limits of quantification. Differences in elemental patterns among the five replicates cannot be attributed to the external environment (e.g. temperature, salinity, sediment load, food availability), because all individuals, about the same age, were sampled from the same location and did not show any analogy to climatic change. The results, further, suggest a strong physiological control on trace element incorporation through metabolic activity and/or growth rate.

Overall, several factors restrict the applicability of Fe and Mn in the shell of *L. elliptica* as proxies for melt water driven trace element load into the coastal environment, namely:
(i) The Fe and Mn assimilation from lithogenic particulate matter – imported by glacial melt waters – was not confirmed within this study. Moreover, pore water appears as important source of Fe and Mn for the assimilation by *L. elliptica*.
(ii) The coexistence of up to three calcium carbonate polymorphs and the polymorph dependent element incorporation necessitate additional, time- and cost-consuming mineralogical analysis of the chondrophore.
(iii) Contents of Fe and Mn in the chondrophore of *L. elliptica* are too low, to enable analyses of metal incorporation within growth layers in the required high spatial (temporal) resolution even if a sector field ICP-MS is used.
(iv) The strong physiological influence on element incorporation into the shell matrix readily overprints potential environmental influences.

Kurzfassung

In den letzten Jahrzehnten verursachte der globale Klimawandel auf der westlichen Antarktischen Halbinsel (WAP) einen starken Anstieg der Lufttemperatur, der zu einer Verkürzung der Meereisbedeckung, einem zunehmenden Rückzug der Gletscher und einem steigenden Eintrag von Schmelzwasser und lithogenen Materials in die Küstengewässer führte. In Maxwell Bay (King George Island, KGI) verdreifachte sich die jährliche Sedimentakkumulationsrate innerhalb des letzten Jahrhunderts. Dies veränderte die Lebensbedingungen für benthische Filtrierer, wie die antarktische Muschel *Laternula elliptica*.

Im Vergleich zu anderen Muschelarten weisen die Gewebe von *L. elliptica* hohe Fe- und Mn-Gehalte auf, die rund um die Antarktis stark variieren.

Frühere Studien machen dafür einen (unterschiedlich) starken Eintrag lithogenen Materials verantwortlich. Für beide Elemente wurde daraus eine potentielle Eignung als Proxy für einen verstärkten Eintrag an lithogenem Material abgeleitet, sofern sich der Eintrag glazigener Gesteinspartikel direkt in der Fe- und Mn-Assimilation bzw. in der Elementeinlagerung in der Muschelschale wiederspiegelt.

In dieser Dissertation wird die Metallassimilation und -einlagerung in die Kalziumkarbonatschale in *L. elliptica* diskutiert. Insbesondere beurteilt die vorliegende Arbeit, ob Fe und Mn als Proxies für den Sedimenteintrag durch Schmelzwässer in die Potter Cove (KGI) geeignet sind.

Laternula elliptica assimiliert bioverfügbares Fe und Mn aus verschiedenen gelösten und partikulären Quellen (z.B. planktonischen und benthischen Mikroalgen, detritischen und mineralischen Partikeln, Meerwasser, Porenwasser). Das heißt, dass die Aufnahmewege bekannt sein müssen, um einen direkten Zusammenhang zwischen den potentiellen Proxies (Fe und Mn Konzentrationen in der Schale von *L. elliptica*) und den sich änderndem Umwelteinfluss (Fe- und Mn-Eintrag durch Schmelzwasser in die Potter Cove) nachweisen zu können.

Dazu wurde zunächst die Zusammensetzung der aufgenommenen Partikel im Sipho, auf den Kiemen und im Verdauungstrakte von *L. elliptica* qualitativ analysiert (Kapitel 2). Mineralische Partikel waren meist kleiner als 5 µm Durchmesser, jedoch am weitaus häufigsten. Sichtbare organische Partikel waren deutlich seltener aber größer (10 – 250 µm) und wurden von Diatomeen dominiert. Dies verweist in Kombination mit früheren Studien auf feinen, organischen Detritus und in geringerem Ausmaß benthische Diatomeen als Hauptnahrungsquellen für *L. elliptica* in Potter Cove. Die Größenunterschiede zwischen organischen und mineralischen Partikeln resultieren auf Grund einer aktiven Partikelselektion und dem Ausscheiden unerwünschter Partikel als Pseudo-Facies. Diese physiologische Steuerung der Partikelaufnahme beeinflusst

letztendlich auch die Assimilation von Fe und Mn und kann dadurch den Einsatz von Fe und Mn als Proxies verkomplizieren.

Eisen- und Mn-Konzentrationen in *L. elliptica* (Hämolymphe, Gewebe) wurden mit Konzentrationen in Porenwasser- und Meerwasserproben sowie Fe- und Mn- Gehalten in Sedimenten der Potter Cove verglichen, um die Bedeutung geochemischer Quellen abschätzen zu können (Kapitel 3). Hälterungsexperimente unter niedrigen Fe-Konzentrationen resultierten in einer raschen Senkung der hohen Fe-Hämolymph-Konzentrationen und verdeutlichen eine starke Abhängigkeit der Fe-Hämolymph-Konzentrationen von externen Fe-Konzentrationen.

Weitere Untersuchungen zeigten, dass durchschnittlich nur 30% der gesamten Fe-Hämolymph-Konzentration zellulär – in Hämozyten – gebunden war. Die Meerwasser Fe-Konzentrationen ($0.01 - 0.76$ µmol L^{-1} Fe) waren zu gering, um die hohen Fe-Hämolymph-Konzentrationen ($5.6 - 458$ µmol L^{-1} Fe) erklären zu können. Vielmehr erscheint Porenwasser, aufgrund ähnlich hoher Fe-Konzentrationen in Hämolymph- und Porenwasserproben ($1.4 - 192$ µmol L^{-1} Fe; Sedimentoberfläche bis 5 cm Sedimenttiefe), die bedeutendste Fe-Quelle für *L. elliptica* in der Potter Cove zu sein. Die Mn-Hämolymph-Konzentrationen ($0.1 - 4.0$ µmol L^{-1} Mn) waren deutlich niedriger als die Konzentrationen im Porenwasser ($0.8 - 60$ µmol L^{-1} Mn), jedoch deutlich höher als im Meerwasser ($0.01 - 0.09$ µmol L^{-1} Mn). Der Einfluss von lithogenen, partikulärem Fe und Mn erscheint weniger bedeutend, da zwischen zwei Standorten unterschiedlichen Eintrags glazigenen Materials keine signifikanten Unterschiede in Fe- und Mn-Konzentrationen in Hämolymphe und Geweben gefunden wurde. Folglich dürfte die Sedimentgeochemie und daraus resultierenden Unterschiede der gelösten Fe- und Mn-Konzentrationen im Porenwasser für die hohe Variabilität der Fe- und Mn-Konzentrationen in *L. elliptica* verantwortlich sein. Da die Sedimentdiagenese und die resultierenden Konzentrationen an gelöstem Fe und Mn im Porenwasser durch unterschiedliche Faktoren (u.a. Gehalt an organischem Material, Sauerstoffeindringtiefe, Remineralisationsrate, Bioturbation) gesteuert werden, ist eine Abhängigkeit der Metallaufnahme durch *L. elliptica* vom lithogenen, partikulären Materialeintrag äußerst unwahrscheinlich.

Darüber hinaus wurden/werden auch die Fe-Isotopenverhältnisse der Hämolymphe und potentieller Fe-Quellen (Sediment, Porenwasser) analysiert, um die Abhängigkeit der Fe-Hämolymph-Konzentrationen vom Porenwasser zu untermauern. Stabile Fe-Isotope können jedoch nur als Proxy für die Herkunft des assimilierten Fe eingesetzt werden, wenn physiologische Fraktionierungsprozesse im Zuge der Aufnahme, der Speicherung oder des Transports in *L. elliptica* bekannt sind oder ausgeschlossen werden können.

5

Diese Arbeit präsentiert die erste Charakterisierung der Fe-Isotopensignatur (δ^{56}Fe) in Muschelhämolymphe (Kapitel 4).

Vor der Analyse der Spurenmetallgehalte im Chondrophor von *L. elliptica* wurde dessen mineralogische Zusammensetzung hinsichtlich der Kalziumkarbonat-Polymorphe untersucht (Kapitel 5), da die Spurenmetalleinlagerung polymorphspezifisch ist. Diese Studie belegt erstmals die Koexistenz dreier Kalziumkarbonat-Polymorphe (Aragonit, Kalzit, Vaterit) in einem marinen, kalzifizierenden Organismus. Jährliche Wachstumsringe verliefen durch verschiedene Polymorphe. Dies deutet auf eine simultane Mineralisation hin. Auf Grund der polymorphabhängigen Spurenmetalleinlagerung in die Karbonatmatrix (nachgewiesen für Sr und Mg) wird die Anwendung eingelagerter Spurenmetalle als Umweltproxies verkompliziert. Zusätzliche mineralogische Analysen werden daher notwendig, um eine mineralogische Fraktionierung der Spurenmetalle ausschließen zu können. Deshalb wurden die Spurenmetallkonzentrationen nur in Chondrophoren mit rein aragonitischen Probenoberflächen analysiert (Kapitel 6). Die Konzentrationen der Elemente B, Ba, Mg, und Sr waren einer starken Saisonalität unterworfen. Ausgeprägte Konzentrationsmaxima von B, Mg und Sr koinzidierten mit den Konzentrationsminima von Ba in den winterlichen Wachstumslagen. Während der ersten Lebensjahre sanken die Fe- und Mn-Konzentrationen stark ab (analog zu einer früheren Studie) und unterschritten die Bestimmungsgrenzen. Alle fünf Schalen (gleicher Standort, ähnliches Alter) zeigten unterschiedliche Veränderungen der Elementkonzentrationen, welche nicht systematisch durch Umweltveränderungen (z.B. Temperatur, Salzgehalt, Sedimenteintrag, Nahrungsverfügbarkeit) erklärt werden konnten. Vielmehr deuten die Ergebnisse auf eine stark physiologische Kontrolle der Spurenmetalleinlagerung – vor allem durch die Stoffwechsel- und/oder Wachstumsrate - hin.

Insgesamt schränken mehrere Faktoren die Verwendung von Fe und Mn als Proxies für einen verstärkten Eintrag an lithogenem Material durch Schmelzwässer ein:
(i) Die verstärkte Assimilation von Fe und Mn in Gewebe und Hämolymphe von *L. elliptica* auf Grund höherer Einträge lithogenen Materials konnte in dieser Studie nicht belegt werden. Es ist sehr wahrscheinlich, dass Porenwasser die Hauptquelle für Fe und Mn darstellt.
(ii) Die Koexistenz von bis zu drei Kalziumkarbonat-Polymorphen erfordert zusätzliche mineralogische Analysen des Chondrophors, um Effekte der polymorphabhängigen Elementeinlagerung ausschließen zu können.
(iii) Eisen- und Mn-Gehalte sind im Chondrophor von *L. elliptica* zu niedrig, um in ausreichend räumlicher und zeitlicher Auflösung der Wachstumsschichten mittels hochauflösender Massenspektrometrie quantifiziert zu werden.
(iv) Der ausgeprägte physiologische Einfluss auf die Elementeinlagerung in die Schalenmatrix überprägt potentielle Umwelteinflüsse.

1 Introduction

1.1 Consequences of global climate change at the Antarctic Peninsula

Global climate change and its consequences vary in nature and strength among different areas around the world (summarized in IPCC, 2007; Solomon et al., 2007; Bates et al., 2008) as e.g. among Antarctic regions (e.g. Turner et al., 2005; Steig et al., 2009; Maksym et al., 2012; Stammerjohn et al., 2012). The Western Antarctic Peninsula (WAP) experienced a strong rise in air temperature, decreasing period of sea ice cover, and glacial retreat during the last decades (Rignot and Thomas, 2002; Vaughan et al., 2003; Braun and Hock, 2004; Cook et al., 2005; Turner et al., 2005; Vaughan, 2006; Stammerjohn et al., 2008; Steig et al. 2009; Rueckamp et al., 2011; Maksym et al., 2012; Stammerjohn et al., 2012). From 1951 till 2000 the near surface air temperature (annual mean) rose by +0.53 (±0.43)°C per decade at Faraday/Vernadsky station, located on the WAP (Turner et al., 2005). On King-George-Island (KGI; Fig. 1.1a,b) a weaker annual warming trend (+0.35 ±0.46°C per decade; 1969-2000) was observed at Bellingshausen (Fig. 1.1b), with strong temperature rises in Austral summer (+0.30 ±0.20°C per decade) and in Austral winter (+0.58 ±0.97°C per decade). As a result of rising air temperatures glaciers melt which in turn leads to an increasing release of freshwater and lithogenic material into coastal waters (Vaughan, 2006; Dominguez and Eraso, 2007; Meredith et al., 2010). For example, a tripling of sediment accumulation rates in Maxwell Bay (KGI; Fig. 1.1b,c) was observed during the last century (Monien et al., 2011).
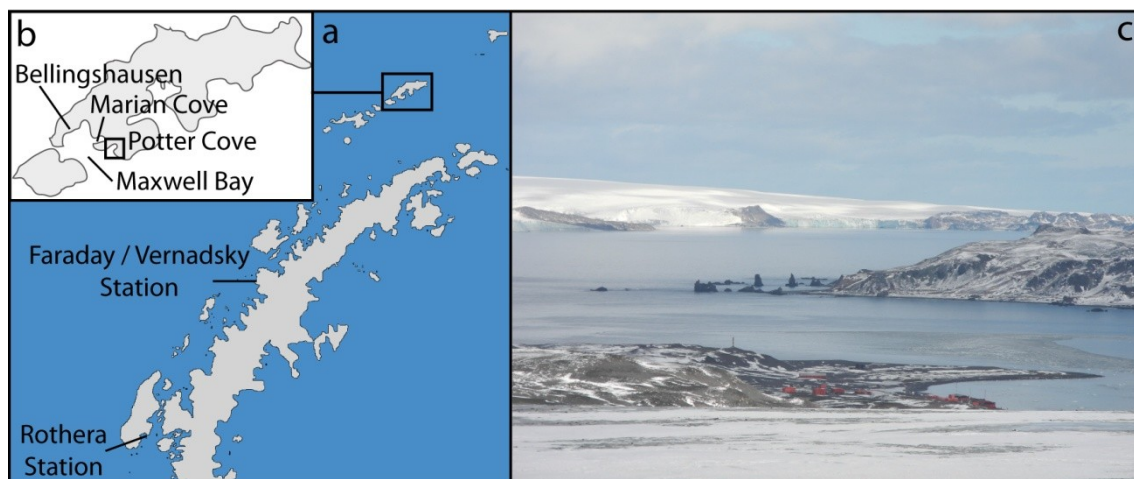
Figure 1.1: a) Map of the Antarctic Peninsula (King George Island highlighted); b) Map of King George Island; c) View to Nelson Island, overlooking Carlini Station* and Dallmann Laboratory, Potter Cove, and Maxwell Bay.

* The former Argentinean scientific Antarctic station Jubany was renamed into Scientific Base Dr. Alejandro Carlini on March 5th, 2012. Both names occur within this thesis depending on the date of submitting or publishing.

This intensified input of freshwater including suspended inorganic particles and rising sea surface temperatures affect the physical (e.g. sea ice duration, ice scouring, salinity, stratification, turbidity) and chemical environment of benthic and pelagic communities in Potter Cove (KGI; Fig. 1.1c, 1.2) and other locations along the WAP (e.g. Peck et al., 1999; Dierssen et al., 2002; Schloss and Ferreyra, 2002; Peck, 2005; Smale and Barnes, 2008; Montes-Hugo et al., 2009; Zacher et al., 2009; Philipp et al., 2011; Piquet et al., 2011; Harper et al., 2012; Schloss et al., 2012; Smith et al., 2012; Steinberg et al., 2012; reviewed in Murphy et al., 2013; Quartino et al., 2013). For example, higher amounts of inorganic suspended particulate matter in the water column attenuate light for phytoplankton photosynthesis (Schloss et al., 2002). Schloss et al. (2012) reported decreasing concentrations of *chlorophyll a* in Potter Cove, caused by a decrease in phytoplankton biomass and/or changes in species composition. In succession, lower phytoplankton concentrations strongly diluted by lithogenic sediment particles influence the physiology and ecology of benthic filter feeders like ascidians (e.g. Kowalke, 1999; Tatián et al., 2004, 2008; Torre et al., 2012) and the Antarctic soft shell clam *Laternula elliptica* (Schloss et al., 1999; Tatián et al., 2008; Brey et al., 2011; Philipp et al., 2011; Husmann et al., 2012) and affect, therefore, the whole food web of the cove. For instance, the decrease in maximum attainable size for *L. elliptica* (from 100 mm to 83 mm between 1961/62 – 2009/10) is likely related to higher metabolic costs, due to higher energy expenses for feeding (i.e. increased rejection of lithogenic particles as pseudofeces and lower filtration rate) and decreasing oxygen saturation of seawater with increasing water temperature (Brey et al., 2011).

Figure 1.2: Potter Cove

On the other hand the authors related the increasing annual growth rate of *L. elliptica* to a longer growth season triggered by increasing temperature. Husmann et al. (2012) found a faster accumulation of oxidative waste products in nervous tissues of *L. elliptica* exposed to intensified environmental stressors (e.g. higher sedimentation, intensified iceberg scouring). These stressors are expected to affect population structures, because older

individuals of *L. elliptica* are more sensitive to increasing environmental stress (Philipp et al., 2011).

Such dominant physiological secondary effects, caused by changes of the pelagic system which effects on pelagic-benthic coupling, complicate the determination of systematic responses of the benthic fauna to environmental changes.

1.2 Are biological archives suitable to document consequences of climate change in coastal Antarctic regions?

Regional changes in climate and meteorology are already well documented (e.g. Turner et al., 2005; Steig et al., 2009; Maksym et al., 2012; Stammerjohn et al., 2012), although direct meteorological observations in Antarctic regions are young and time records are relative short (e.g. Bellingshausen, KGI: 1969 – present; Turner et al., 2005) and a dense network of observatories is lacking. If we need to reconstruct climate change on a longer time scale, climate archives such as e.g. sediment cores, ice cores, snow, and biogenic carbonates are analyzed for their e.g. element composition and stable isotope ratios. These proxies reflect for example changes in water or air temperature, pH-value of the surrounding sea water, sedimentation rate, or freshwater input. In this context sediment cores are widely used to reconstruct the environmental history of any given location, also at the Antarctic Peninsula (e.g. Pudsey, 2000; Domack et al., 2001; Yoon et al., 2002; Santos et al., 2005; Heroy et al., 2008; Michalchuk et al., 2009; Milliken et al., 2009; Monien et al., 2011). Such climate reconstructions provide basic information to biologists, because time records of recent changes are rare and short. Sediments are, however, subjected to bioturbation by the benthic macrofauna (e.g. Pudsey, 2000; Diaz, 2004; reviewed in Turekian and Bacon, 2003; reviewed in Teal et al., 2008) or ice scouring (Jacobs, 1989; Brown et al., 2004 and references therein; Smale and Barnes, 2008) and to re-suspension of the sediment surface, induced by storm events, internal waves, tides, and currents (e.g. Berkman et al., 1986; Syvitski, 1989; Jacobs, 1989; Isla et al., 2006; Zajaczkowski and Wlodarska-Kowalczuk, 2007; Stastna and Lamb, 2008; Martins et al., 2012; van Haren and Gostiaux, 2012). These effects affect the stratigraphy of the sediments and probably restrict their suitability for high timely resolved climate reconstructions. Further, sediment cores may reflect changes in biocenosis and food webs or ecology and physiology only to a limited extend, because organisms likely react different to environmental changes. Therefore a biogenic environmental archive like the biogenic carbonate of bivalve shells may fill this gap.

1.3 Formation of bivalve shells and implications on the usability as environmental archives

The outside of the bivalve carbonate shell is covered by the periostracum (an organic layer), which is secreted by mantle cells (Fig. 1.3a). Inside the shell, the inner shell surface (site of shell formation) and the outer surface of the mantle tissue enclose an extrapallial space, filled with (inner/outer) extrapallial fluid (EPF). Specialized epithelial cells of the mantle tissue secret organic macro molecules, which mediate the mineralization of the calcium carbonate shell (e.g. mineral type, crystal orientation, and microarchitecture). These molecules are particularly acidic proteins, glycoproteins, β chitin, and hydrophobic silk protein and largely constitute the later organic shell matrix (e.g. Crenshaw, 1972; Lowenstam, 1981; Falini et al., 1996; Addadi et al., 2006; Nudelman et al., 2007; Jacob et al., 2008; Jackson et al., 2010). Although the main components of the shell matrix are identified, the mechanisms of shell formation are not fully understood and are described by several models (e.g. Bevelander and Nakahara, 1969; Schaeffer et al., 1997; Fig. 1.3b). Both explanations agree on the assumption that the organic matrix forms first and mediates the carbonate crystallization. Chitin forms the structure of organic compartments, which dictates the later orientation of $CaCO_3$ crystals (Addadi et al., 2006). The compartments are prefilled with silk gel to keep the three-dimensional structure and avoid an uncontrolled crystallization of the amorphous calcium carbonate (ACC; which act as precursor for the later calcium carbonate polymorph; Wehrmeister et al., 2011), until ACC is in contact with already formed crystals or a nucleation site (Addadi et al., 2006). This agrees with the idea of epitaxial crystal growth on active sites located on the surface of organic compounds (e.g. highly structured carboxylate surface formed by proteins rich in aspartic acid) and it further implies a nucleation of each aragonite crystal from one nucleation site (e.g. Falini et al., 1996; Addadi et al., 2006). Similarly, Bevelander and Nakahara (1969) proposed aragonite crystallization within the organic compartments by heteroepitaxial nucleation (Fig. 1.3b, left side). Aragonite crystals first grow longitudinally until they reach the opposite organic interlamellar sheet followed by lateral growth (Addadi et al., 2006). Acidic proteins are assumed to be incorporated into the crystals (Addadi and Weiner, 1989), whereas silk proteins are pushed forward during crystal growth (due to the hydrophobic properties) and are encased between crystals and chitin layers or adjacent crystals (Addadi et al., 2006). In contrast to this/these model(s), Schaeffer et al. (1997) suggested that aragonitic stacks of several single crystals are nucleated at once and coherent crystal growth propagates through holes in the organic interlamellar sheets ("mineral bridges") from one compartment to the next (Fig. 1.3b, right side). Furthermore, the role of the EPF and the mechanism of ion transport (Ca^{2+}, CO_3^{2-}, trace metals) during calcification remain

controversial. Several authors interpret the EPF as bulk solution, which further provides molecules and ions to the mineralization site. For example, organic macromolecules are secreted by epithelial cells into the EPF and form the organic matrix by self-assembly (e.g. Bevelander and Nakahara, 1969; reviewed in Samata, 2004; Addadi et al., 2006; Ma et al., 2007; Jackson et al., 2010). Similar assumptions were made for the transport of Ca^{2+} and CO_3^{2-} to the calcification site. Aquatic mollusks build their carbonates largely from ambient dissolved organic carbon and CO_2 from seawater diffusing through the mantle into the EPF and to a lesser extend from respired CO_2 (reviewed in McConnaughey and Gillikin, 2008). The authors considered an ion transport (Ca^{2+}, HCO_3^-) by leakage of ambient seawater into the EPF around the periostracum and/or between mantel cells (compare Fig. 1.3a) explaining similar chemical signatures of seawater and inner EPF. Seawater provides most of the Ca^{2+} supply for shell formation at low energy expense (no ion pumping; Carre et al., 2006). However, this process does not increase the $CaCO_3$ saturation above ambient levels. This is provided by an active ion transport (especially protons) catalyzed by Ca^{2+}-ATPase (Klein, 1996b; Gillikin et al., 2005; McConnaughey and Gillikin, 2008). The exchange of Ca^{2+} (pumped into the EPF) and 2 H^+ (pumped out of the EPF) raise the pH of the EPF and CO_2 and HCO_3^- are transferred to CO_3^{2-} within the alkaline EPF.
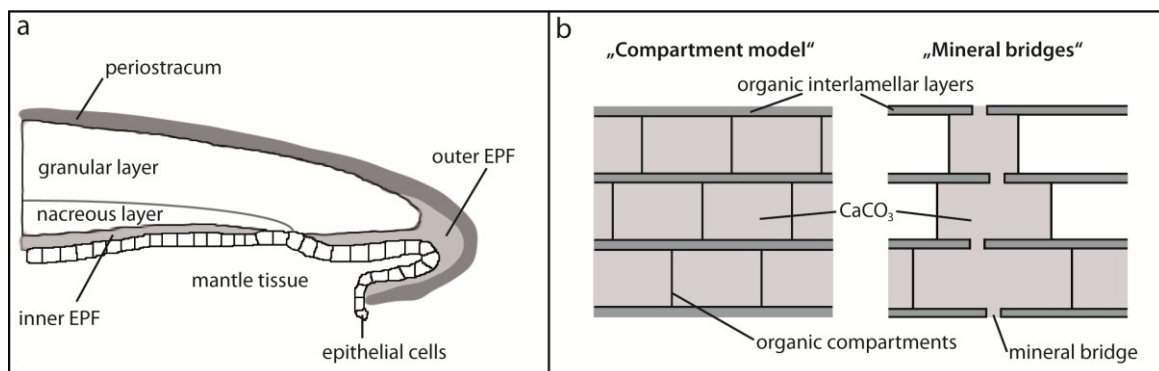
Figure 1.3: a) Schematic cross section of a bivalve shell with attached mantle tissue (modified after Vander Putten et al., 2000 and Jacob et al., 2008; adapted to Laternula elliptica after Sato-Okoshi and Okoshi, 2008); b) Schematic overview of the "compartment model" (Bevelander and Nakahara, 1969) and the "mineral bridge model" (Schaeffer et al., 1997) of nacre formation (modified after Jacob et al., 2008).

Alternatively, Weiss (2010) proposed a calcification model which excludes a direct involvement of the EPF. Instead, epithelial cells of the mantle (covered by a chitin-like membrane) are pinned to the inner shell surface due to cellular mechanical forces and regulate the formation of new shell material. Similarly to the previous model, the authors assume a $Ca^{2+}/2\ H^+$-exchange to avoid local acidification at the mineralization site and balance chemical gradients over the chitin-like membrane.

Overall, both models include an active ion transport to the site of shell formation, whereas Carre et al. (2006) proposed a passive Ca^{2+}-transport through ion channels to cover the high demand in Ca^{2+} and H^+ is evacuated by proton channels. Nevertheless, other ions (e.g. Sr^{2+}) are discriminated during transportation to the calcification site or during the shell calcification by e.g. metabolic activity and crystal growth rate (Klein et al., 1996b; Gillikin et al., 2005; Carre et al., 2006). In case of Ca^{2+}-channels, the selectivity against Sr^{2+} depends on the electrochemical potential induced by the crystallization and on the density of Ca^{2+}-channels on the mantle epithelia (Carre et al., 2006). Physiological or vital effects alter the trace metal incorporation into biogenic carbonates, which differs from the metal incorporation into organic precipitated $CaCO_3$ (Epstein et al., 1951; Urey et al., 1951). Thus, the suitability of incorporated elements and isotopes as proxies for environmental parameters needs to be verified for each single species, because the applicability of many environmental proxies was deduced from other calcifying taxa (in particular foraminifera and corals) to bivalves (e.g. B; McCoy et al., 2011). This is of particular importance, since expressed genes related to initiation and regulation of shell calcification vary already considerable among mollusks (bivalve vs. gastropod; Jackson et al., 2010). Thus, trace metal incorporation during calcification and trace metal signatures may be difficult or even impossible to compare among different taxa (e.g. mollusks vs. foraminifera, corals).

However, bivalve carbonate shells were already proposed as environmental archives based on the incorporation of trace elements (e.g. B, Ba, Fe, Mn, Mg, Sr) and/or stable isotopes (e.g. $\delta^{11}B$, $\delta^{18}O$), which can be used as proxies for environmental changes. The $\delta^{18}O$ composition of biogenic marine carbonates is a function of the $\delta^{18}O$ ratio and the temperature of the seawater during formation (e.g. McCrea, 1950; Urey et al., 1951; Epstein et al., 1953; Shackleton, 1967, Grossman and Ku, 1986). In coastal Antarctic waters the input of melt water, which is depleted in $\delta^{18}O$ (Craig, 1961; Lorius et al., 1985), causes fluctuations in the $\delta^{18}O$ ratio of the seawater (e.g. Lorius et al., 1985; Langebroek et al., 2010 and references therein). Hence, the $\delta^{18}O$ signature of bivalve carbonate shells represents a proxy for water temperature (e.g. Barrera et al., 1994; Goodwin et al., 2001; Schoene et al., 2004a, b; Batenburg et al., 2011) or melt water/fresh water input in coastal areas (Barrera et al., 1994; Miura et al., 1998; Tada et al., 2006; Strauss et al., 2012). In several bivalve species the incorporation of the trace metals Mg and Sr into the shell correlates to water temperature and both metals are, thus, discussed as temperature proxies (Klein et al., 1996a; Lazareth et al. 2003; Immenhauser et al., 2005; Wanamaker et al. 2008). Background levels of Ba/Ca are proposed to reflect ratios of dissolved Ba/Ca

in the water column (Gillikin et al., 2008; Barats et al., 2009), whereas distinct Ba/Ca peaks in the carbonate shells of different species may relate to phytoplankton blooms (Stecher et al., 1996; Vander Putten et al., 2000; Lazareth et al., 2003; Barats et al., 2007; Gillikin et al., 2008 and references therein; Thebault et al., 2009). Additionally, Mn in bivalve carbonate shells was suggested as a marker for phytoplankton blooms as well (Vander Putten et al., 2000; Lazareth et al., 2003; Langlet et al., 2007), whereas other authors related higher incorporation of Mn into the shell to higher concentrations of dissolved Mn concentrations in the water column and/or stronger Mn release into the water column due to changing sediment redox conditions (Freitas et al. 2006; Barats et al., 2008). Further, the incorporation of B into marine carbonates and its δ^{11}B ratio are strongly controlled by pH of the seawater and probably can, therefore, be used as proxy for changes in pH (e.g. Hemming and Hanson, 1992; Sanyal et al., 2000; McCoy et al., 2011).

Nevertheless, there is no consensus on applicable elemental proxies in bivalve shells in the literature, because in many species environmental factors have only minor influences on trace metal incorporation into the shell and biological effects (e.g. vital effects, metabolic activity of the mantle, lifetime respiration mass, crystal growth rate) are dominating (e.g. Klein et al., 1996b; Gillikin et al., 2005; Carre et al., 2006; Dick et al., 2007; Heinemann et al., 2008; Heinemann et al., 2011; Schoene et al., 2011). In other words, potential environmental signals are readily overprinted by ecophysiological processes over animal lifetime. Thus, the suitability of bivalve shells as environmental archive has to be verified and calibrated for each element and each species.

1.4 The Antarctic softshell clam *Laternula elliptica*

Laternula elliptica (King and Broderip, 1832; Fig. 1.4a*)* is a benthic key species of circum Antarctic distribution. High abundances, mostly up to 80 individuals m^{-2}, were found in coastal areas of KGI (Ahn, 1993; Urban and Mercuri, 1998; Philipp et al., 2011). The clam is a sessile benthic filter feeder and plays an important role in biodeposition and sedimentation processes of organic and lithogenic particulate matter (Ahn, 1993; reviewed in Gili et al., 2001) through ingestion of water and particles out of the bottom water layer. Several authors, therefore, held the soft tissues of *L. elliptica* suitable as biomonitors for natural metal enrichment and man-made metal contaminations in Antarctic waters and sediments (e.g. Ahn et al., 1996, 2001; Lohan et al., 2001; Curtosi et al., 2010). Indeed, baseline Fe and Mn concentrations in tissues differ considerably among sites around Antarctica, and were up to 10-times higher in adults from KGI (Marian Cove, Potter Cove) than from Adelaide Island (Rothera Station; Fig. 1.1a) and Terra Nova Bay (Ahn et al., 1996; Nigro et al., 1997; Lohan et al., 2001; Curtosi et al., 2011; Husmann et al. 2012).

Figure 1.4: a) *Laternula elliptica* (whole animal); b) cut through the shell and the chondrophore (red arrow); c) seasonal growth layers.

The highest tissue concentrations of Fe and Mn in *L. elliptica* were found within the active volcanic environment of Deception Island (Deheyn et al., 2005). Several authors proposed a metal assimilation into bivalve tissues via the ingestion of particulate matter (including lithogenic material; e.g. Abele et al., 2008; Curtosi et al., 2010; Husmann et al., 2012) even though lithogenic particles are also excreted as pseudofeces in a large extend (a conglomerate of particles and mucus; Ahn, 1993; Kowalke, 1998). Ahn et al. (1996) and Abele et al. (2008) related Mn and Fe tissue concentrations to glacial runoff and input of lithogenic sediment into Marian and Potter Cove. Husmann et al. (2012) held the increasing sediment input caused by an intensified melt water discharge at KGI responsible for the higher accumulation of Fe in soft tissues of *L. elliptica* from KGI compared to individuals collected at Rothera Point (Adelaide Island). Bivalves also assimilate dissolved metals from inhaled water (Rainbow, 2002; Griscom and Fisher, 2004) and free metal ions are most easily absorbed and readily bioavailable to marine organisms (e.g. Fisher et al., 1996; Bjerregaard and Depledge, 1994). Consequently, Rainbow (1990) described seawater, bottom water, and sediment pore water as important alternative sources of bioavailable metals for burrowing bivalves. In sediment pore water and bottom water dissolved Fe and Mn concentrations are particularly dependent on the geochemical environment of the sediment, namely e.g. the content of organic matter, stage of diagenesis, oxygen penetration depth, remineralization rate, bioirrigation, and flux across the benthic boundary (e.g. Froelich et al., 1979; Berner, 1981; Canfield et al., 1993, Elrod et al., 2004; Sachs et al., 2009; Severmann et al., 2010) and not exclusively on the mass accumulation rate. Therefore, the alternative sources (seawater, bottom water, pore water) need to be excluded as important sources for the Fe and Mn assimilation in *L. elliptica* to support the assumption that metal accumulation in *L. elliptica* increases due to increasing climate driven input of lithogenic Fe and Mn. Additionally, the ingestion of lithogenic particulate matter remains to be verified as the origin of high Fe and

Mn concentrations in tissues of *L. elliptica*, before both metals can potentially be used as proxies for changing input of lithogenic debris into the water.

Bivalve tissues are, however, more important for biomonitoring, but less suitable as archive, since they reflect the lifetime integrated metal assimilation, excretion, and storage (Phillips, 1976; Rainbow, 1990) without any temporal resolution.

The calcium carbonate shell of *L. elliptica* represents a possible alternative. It is reported as aragonitic (Barrera et al., 1994; Tada et al., 2006) and consists of seasonal layers (Fig. 1.4b,c) over a lifetime of ≥ 36 years (Philipp et al., 2005). Brey and Mackensen (1997) validated an annual formation of the growth bands by stable isotope analysis (δ^{18}O and δ^{13}C) and found light-colored growth bands formed during summer and dark growth bands formed during winter (Fig. 1.4c). The shell of *L. elliptica*, therefore, features several characteristics which favor the use as an environmental archive. A first promising application of the shell of *L. elliptica* as climate archive was provided by Brey et al. (2011), who analyzed decadal variability in shell growth through the measurement of annual growth increments. The result was a master chronology over 49 years, which exhibits a clear relationship between El Nino Southern Oscillation (ENSO) and *L. elliptica* growth. Apparently surface air temperature and/or indirect effects of climate change (e.g. heterotrophy, food web structure) affect bivalve growth stronger than sea surface temperature. Hence, this method and the coupling of *L. elliptica* growth to ENSO likely support the climate reconstruction of earlier periods at the WAP. With reference to trace metal concentrations as environmental proxies Dick et al. (2007) analyzed concentrations of Al, Fe, Mn, Cu, Pb, and U in the chondrophore of *L. elliptica* by means of laser ablation - inductively coupled plasma – mass spectrometer (LA-ICP-MS). This first approach was performed through single spot ablation analysis (200 µm in diameter). This provided an annual resolution of the first twelve growth bands. Afterwards up to four growth bands were averaged, due to decreasing increment width with increasing age. The authors found a relationship between decreasing respiration mass and the drop of metal concentrations during the first eight years of lifetime. It remains unclear, which influence is responsible for the variability in trace metal concentrations of the older growth layers, but a clear relation to an environmental force needs to be verified, to use the shell of *L. elliptica* as high timely resolved environmental archive.

1.5 Objectives of the thesis

This thesis aims to investigate the general applicability of *L. elliptica* as environmental archive for the documentation of biogeochemical changes in Antarctic coastal waters due to global climate change. More explicitly, this work should verify whether Fe and Mn concentrations in tissues and in the growth bands of the shell of *L. elliptica* reflect the melt water driven sediment input into coastal waters and can, therefore, be used as proxies for the intensity of glacial melting, as proposed by other authors (Abele et al., 2008; Curtosi et al., 2010; Husmann et al., 2012). Therefore the aims of this thesis are:

i) to define assimilation pathways of Fe and Mn into *L. elliptica*. It is essential to verify if particulate Fe and Mn is the predominant environmental source. The uptake of dissolved Fe and Mn from seawater and pore water need to be excluded as additional or alternative sources (chapter II – chapter IV).

To this end a comparison of metal concentrations of environmental sources (sediment, seawater, pore water) and in bivalve hemolymph ("blood") and tissues (gill, digestive gland, mantle) is accomplished, to define transport pathways of metals from the site of assimilation to the sites of excretion or storage (tissues and shell). Therefore, tissues from animals collected at stations of high and low input of lithogenic particulate matter are analyzed to reveal the most dominating source for Fe and Mn (chapter III). Further indication for the environmental Fe source and assimilation pathway into *L. elliptica* should be provided by the comparison of Fe isotopic ratios (δ^{56}Fe) of the bivalve hemolymph, sediment, and sediment pore water (chapter IV).

ii) to optimize the LA-ICP-MS setup for the ablation of continuous transects along the chondrophore in order to analyze isotopes at high spatial and temporal (seasonal) resolution. Before, a mineralogical fractionation or a strong physiological control on trace metal incorporation during calcification must be ruled out (chapter V, VI).

iii) to compare the variability of trace metal contents in the carbonate shell matrix of the bivalve to meteorological and biological time records, as well as to physiological parameters (e.g. growth rate, age), in order to separate environmental signals from the effects of animal lifetime metabolism on metal accretion (chapter VI).

Only if a clear, reproducible relation between the incorporation of Fe and Mn into the shell matrix and an environmental force (e.g. sediment load of the water column) is verified, both elements can be used as proxies for glacial retreat and lithogenic debris discharge into the water column. Under such pre-conditions, the shell of *L. elliptica* would provide a suitable highly time resolved archive of environmental change.

2 Particle ingestion

of the Antarctic clam Laternula elliptica in Potter Cove, King George Island

Harald Poigner[1], Marcelo Hernando[2], Dorothee Wilhelms-Dick[1], Doris Abele[1]

[1]Alfred Wegener Institute Helmholtz Centre for Polar and Marine Research,
27570 Bremerhaven, Germany
[2]Comisión Nacional de Energía Atómica, Departamento Radiomicrobiología,
B1650KNA Buenos Aires, Argentina

Abstract

Filter feeders in shallow coastal environments receive particles from many different sources including planktonic and benthic microalgae, as well as detritic and inorganic particulate matter. Food web models for coastal communities benefit from direct observations of particle flux from the water column to the benthos through the benthic filter feeders, including the description of ingested and rejected particulate matter. We analyzed the ingested particulate matter of *Laternula elliptica* from Potter Cove (King George Island, Western Antarctic Peninsula). Particle composition of material retrieved from siphon, gills, and digestive tract was qualitatively analyzed on smear slides in March 2010. Lithogenic particles rarely exceeded 5 µm diameter. Visible organic particles were bigger (10 – 250 µm) and consisted mainly of diatoms, especially *Ceratoneis spp.* and *Pleurosigma spp.*. Nevertheless they appeared strongly diluted by lithogenic material. Comparisons with existing literature suggest suspended organic matter mainly of detritic origin and benthic diatoms as major food source for *L. elliptica* in Potter Cove.

2.1 Introduction

Laternula elliptica plays an important role in biodeposition and sedimentation processes of particulate matter, organic as well as lithogenic material (Ahn, 1993). The bivalves ingest water and particles from the bottom water layer through its inhalant siphon. Particles are filtrated via gills and transported to the digestive tract or excreted as mucous fecal pellets (pseudofeces).

Sinking phytoplankton, especially diatoms, are assumed to be the primary food source for *L. elliptica* in Potter Cove and the neighboring Marian Cove. Ahn et al. (2003) reported a positive correlation between chlorophyll concentrations and bivalve tissue mass, with high increases in mass after phytoplankton blooms. Contrary, under conditions of limited food availability in winter especially muscle tissues and digestive gland lost mass considerable (Ahn et al., 2003), when *L. elliptica* is reported to remain active albeit at reduced metabolic rate in Maxwell Bay (Ahn and Shim, 1998). Contrary, at Adelaide Island (Rothera Station, Fig. 2.1a) *L. elliptica* did not feed for 4 months during winter, and siphons reappeared with rising chlorophyll concentrations at the end of September (Brockington, 2001). The somatic dry mass (musculature, ctenidia, and digestive tissue) remained constant throughout the winter at Adelaide Island (Rothera). These works indicate the importance of the seasonal availability of food sources on the ecology of *L. elliptica*. Further, a combined gut content and δ^{15}N-analysis in the Ross Sea showed a strong dependence between the available food sources and ingested particles (Norkko et al., 2007). The nutrition shifted from high amounts of detritus in areas with permanent ice cover to freshly produced algal material in ice free waters. These results highlight the broad omnivorous feeding spectrum of *L. elliptica*.

At King George Island *L. elliptica*'s feeding behavior, physiology, and biochemistry have been investigated mostly under laboratory conditions (e.g. Ahn, 1993; Kowalke, 1998; Tatian et al., 2008) or by the use of biochemical markers, e.g. δ^{13}C and fatty acids (Corbisier et al., 2004; Graeve et al., 2008), whereas direct observations of the ingested material were only done by Ahn et al. (1993) for Marian Cove. This lack of more recent investigations was the motivation to take a closer look at the nutrition of *L. elliptica* at Potter Cove during summer 2010.
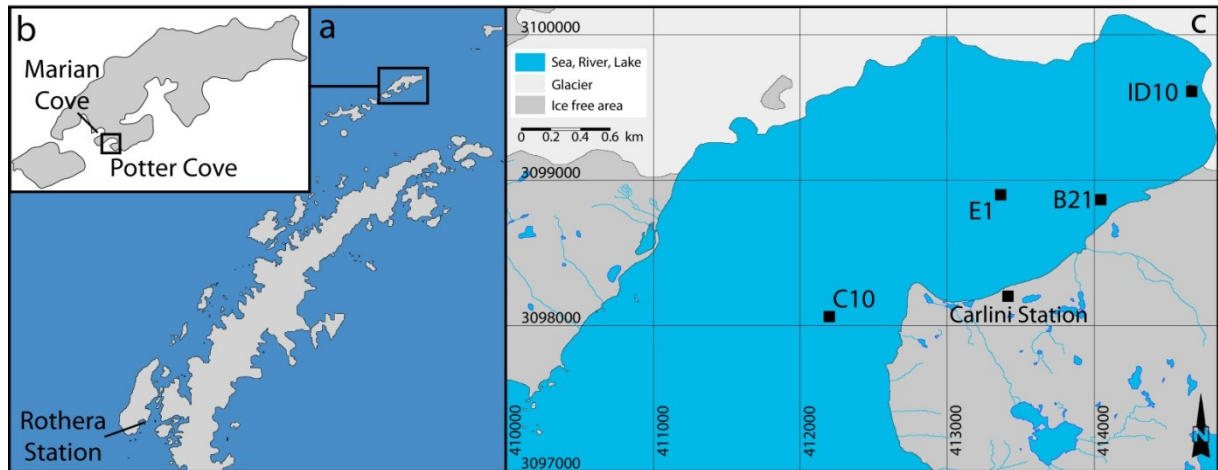
Figure 2.1: a) Map of the Antarctic Peninsula (King George Island highlighted), b) Map of King George Island, c) Map of Potter Cove including the sampling stations.

2.2 Material and methods

The particulate matter accumulated in siphons (15 samples), digestive tracts (5 samples), and on gills (12 samples) was collected from animals of three stations in Potter Cove in March 2010 (Fig. 1c) and smeared on object slides. Station C10 is located in the outer Potter Cove close to Maxwell Bay and B21 is situated next to melt water inlets of the southern shoreline. Station ID10 is close to the glacier front and has been ice-free since Austral summer 2002/03. This location was colonized later, and only animals younger than 5 years were found.

The nature of particulate and organic matter of samples (Fig. 2) was qualitatively determined by means of an Axioplan light microscope (Carl Zeiss AG, Göttingen, Germany) equipped with a 20x and 40x objective. Diatoms sampled in *L. elliptica* were compared with plankton samples taken at station E1 (Fig. 1; 62.232°S; 58.667°W) in January and February 2010. Diatom taxa were identified on the basis of the silicified frustules using an inverted microscope (DM2500, Leica, Microsystems, Wetzlar, Germany).

2.3 Results and discussion

Irrespective of the analyzed organ, samples consisted mainly of inorganic particles smaller than 5 µm in diameter. In the digestive tract and elsewhere organic particles (e.g. diatoms) were strongly diluted by these fine lithogenic material. Similarly, Ahn (1993) found only a small percentage of organic carbon (1.6 – 5.2%) in feces and pseudofeces of *L. elliptica* from Marian Cove (field and experimental investigations). Mineral particles, such as quartz, feldspar, and mica, were the major constituents of these fecal pellets in Ahn's investigation.
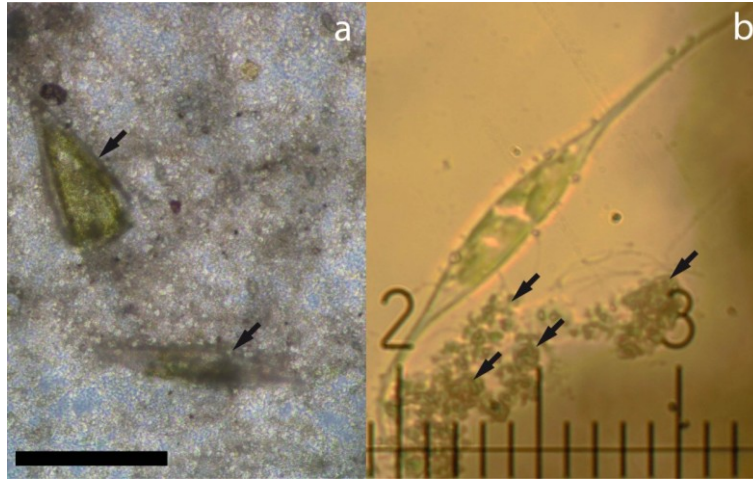
Figure 2.2: a) Example of a smear slide sample containing two diatoms (black arrows) and mainly fine grained material (< 2.5 µm diameter), the black bar approximates 50 µm; b) sample containing an exemplar of *Ceratoneis spp.* and fine grained material (black arrows), 0.1 units of the reticle equals 5 µm.

In our samples the number of inorganic particles > 5 µm as well as the maximum diameter decreased between siphon and gill in most samples. This indicates that bigger particles were rejected with the exhalant water flow. This discrimination of inorganic particles against organic particles indicates an active selection process of food particles by the bivalve, even if particle size cannot be the only selective criterion. Due to increased sizes of organic particles compared to inorganic the particle's surface charge might also influence this process. Ahn (1993) already proposed selection of phytoplankton, deduced from elevated chlorophyll a concentrations in feces of *L. elliptica* compared to seston and pseudofeces. Also Kowalke (1998) suggested an active particle sorting and formation of mucus-coated pseudo feces by cilia bands of *L. elliptica*. In his experiments the size dependent decrease of the particle concentration in the aquarium water was measured to calculate the filtration efficiency of *L. elliptica*. Particle uptake efficiency increased with increasing particle size from 50% for particles of 1.8 µm diameter to 80% for particles ≥ 3.0 µm. Particle diameters below 1.8 µm were not investigated. These findings contrast our results, since particle sizes > 5 µm were rarely found in the digestive tract material in-situ.

By contrast, the organic particles identified in our samples were always of bigger size and reached up to 250 µm length and 15 – 40 µm in diameter (Tab. 2.1). Benthic (epipelic) diatoms dominated the organic fraction and were enriched in the digestive tract compared to siphon and gill derived material. *Ceratoneis spp.* and *Pleurosigma spp.* were the most abundant species and usually benthic, except *C. closterium* which remains planktonic for a certain time after resuspension (Round et al., 1990). Cells of *Pseudogomphonema spp.*, *Cocconeis spp.*, and *Fragilariopsis spp.* were less abundant. *Fragilariopsis* includes planktonic, benthic, and ice-associated species and occurs in high abundances in

Antarctic waters (Hasle and Medlin, 1990). *Cocconeis spp*. and *Pseudogomphonema spp*. are epiphytic species, usually occurring on the subtidal macroalgaes (e.g. *Desmarestia mensiesii*; Ahn et al., 1997; Klöser, 1998). Nevertheless, especially after strong wind events both species were also found in the water column at Marian Cove (Kang et al., 2002).

Table 2.1: Results of the qualitative analyses of particulate matter derived from different tissues (S = siphon, G = gill, DT = digestive tract). The presence of different organic particles is expressed by '+' or its maximum length (or length range).

sample	organ	org. particles [Length in µm]			
		diatoms	makroalgae	nematodes	zooplankton
C101	S	+	75		
C101	G	25	50	+	
C102	S	+	+		
C102	G	+	+		
C102	DT	35	>25		
C103	S	50			
C104	S	+	+		
C105	S	25 - 125	25	+	
C105	G	40 - 125			
B211	S	30 - 150			
B211	G	125			
B212	S	30 - 150			
B212	G				
B213	S	60 - 150			
B213	G	125	250		
B214	S	125		+	
B214	G	40 - 50			
B215	S	25 - 125			
B215	G	30 - 80			
ID101	S	25 - 125			
ID101	G	12.5 - 110		+	+
ID101	DT	25 - 150		+	
ID102	S	12.5 - 150			
ID102	G	20 - 150		+	
ID103	S	12.5 - 150			
ID103	G				
ID103	DT	40 - 125			
ID104	S	20 - 125	125		
ID105	S	50 - 150			
ID105	G	125			
ID105	DT	50 - 150			

The dominance of benthic diatom species in the gut content of *L. elliptica* is consistent with the results of Ahn et al. (1993), although some of the taxa differed. *Cocconeis spp.*, *Licmophora spp.*, and *Trachyneis spp.* were abundant in the sediment and water column as well as in *L. elliptica* (Ahn et al., 1993). Benthic diatoms are an important primary producer and suggested to represent an important food source for the benthos in Antarctic coastal waters (Kang et al., 2002; Tatian et al., 2004). In a few samples also nematodes, zooplankton (1 sample), and pieces of macroalgae were found (Tab. 2.1). Uptake of macroalgal fragments was restricted to the animals from station C10 in the outer Potter Cove where kelp forests of red algae are located (Kloeser et al., 1996; Quartino and Boraso de Zaixso, 2008). Ferreyra et al. (2003) proposed a transport of macroalgal fragments to the inner cove by water currents. However, except two fragments (Tab. 1) no macroalgal fragments were found in the animals sampled in the inner cove (B21, ID10). Thus, based on this small dataset, macroalgal fragments seem to be less important for the nutrition of *L. elliptica* within the inner Potter Cove at the end of summer. Further, Norkko et al. (2007) assumed red algal detritus to form part of the *L. elliptica`s* diet at Tethys Bay (Ross Sea). In form of fine grained detritus (instead of fragments) this can be also assumed for Potter Cove, since macroalgal biomass has been one main energy source for benthic secondary production there (Quartino and Boraso de Zaixso, 2008). Corbisier et al. (2004) and Graeve et al. (2008) reported close relation between biochemical signatures (δ^{13}C, fatty acids) of *L. elliptica* and suspended particulate matter (SPM) and zooplankton.

The SPM signature was mainly determined by degraded material (detritus) with only small contributions of phytoplankton, whereas the copepods signature may reflect uptake of fecal pellets (Graeve et al., 2008). Fatty acids typical for highly degraded organic matter from surface sediments were found only in small amounts. The signature in *L. elliptica* remained constant throughout the year without any seasonal variations (Graeve et al., 2008). In keeping with this observation, Norkko et al. (2007) described detritus as constant food source in *L. elliptica* which compensates seasonal fluctuations in primary production. Taking into account the published and our own results we suggest fine grained detritus (< 5 µm; not distinguishable from fine grained sediment under the light microscope) and benthic diatoms to be the major nutritional sources for *L. elliptica* in Potter Cove. Ahn et al. (1997) proposed that wind driven resuspension of the sediment surface makes benthic diatoms available for benthic suspension feeders like *L. elliptica*. The same applies for the fine grained detritus and lithogenic material. In agreement with the generally low phytoplankton biomass (Schloss et al., 2002) pelagic diatoms seem to play a less important role in the nutrition of *L. elliptica* in Potter Cove.

Acknowledgements

We would like to thank the divers and the crew of the Argentinean Antarctic Station Carlini (former Jubany) for their logistic help and Stefanie Meyer (AWI) for her support during expedition preparations. This work was supported by the German Research Foundation (DFG) under grant AB 124/11-1 in the framework of priority program 1158 – Antarctic Research and is associated to the IMCOAST project.

3 Influence of the pore water geochemistry on Fe and Mn assimilation in *Laternula elliptica* at King George Island (Antarctica)

Harald Poigner[1], Patrick Monien[2], Donata Monien[2], Michael Kriews[1], Hans-Jürgen Brumsack[2], Dorothee Wilhelms-Dick[3], and Doris Abele[1]

[1]Alfred Wegener Institute Helmholtz Centre for Polar and Marine Research, Am Handelshafen 12, 27570 Bremerhaven, Germany

[2] Carl von Ossietzky University Oldenburg, Institute for Chemistry and Biology of the Marine Environment (ICBM), Carl-von-Ossietzky-Str. 9-11, P.O. Box 2503, 26111 Oldenburg, Germany

[3]University of Bremen, Geoscience Department, Klagenfurter Straße, 28359 Bremen, Germany

Abstract

Fe and Mn tissue concentrations in *Laternula elliptica* vary by more than one order of magnitude around the Antarctic continent. The rapid decline of high initial Fe concentrations in hemolymph at low experimental Fe concentrations indicates an environmental control of high Fe hemolymph concentrations. To determine the environmental influence on element assimilation in the bivalve, Fe and Mn contents of the hemolymph and tissues of *L. elliptica* were compared to sediment, pore water, and seawater concentrations in Potter Cove (King George Island, Antarctic Peninsula). Seawater Fe concentrations were too low to explain high Fe concentrations in the hemolymph. Also no significant differences in hemolymph and tissue concentrations were found between two sites of high and lower input of lithogenic debris. Based on similarly high Fe concentrations in the hemolymph and pore water samples from selected sampling sites in the Cove we conclude that pore water is the main Fe source for *L. elliptica*. Manganese concentrations in hemolymph showed a discrimination against pore water concentrations. Differences in the geochemical environment of the sediment and resulting concentrations of dissolved Fe and Mn in pore water at different sampling sites seem to be responsible for the high variability of Fe and Mn contents in tissues of *L. elliptica*.

3.1 Introduction

Baseline Fe and Mn contents in the tissues of the circum Antarctic clam *Laternula elliptica (King and Broderip, 1832)* differ considerably among sites around Antarctica. This led scientists to search for the environmental sources of both metals to explain local differences. At King George Island (KGI; South Shetland archipelago, western Antarctic Peninsula (WAP)) several authors related relatively high contents of both metals in bivalve tissues to a high input of lithogenic debris transported by melt water streams into the coastal areas (e.g. Abele et al., 2008; Curtosi et al., 2010; Husmann et al., 2012). Recently, Monien et al. (2011) reported a tripling of sediment accumulation rates in Maxwell Bay (KGI) during the last century, with the highest increase during the decade 1990-2000. The increased input of lithogenic debris coincides with intensified melt water discharge from retreating land glaciers on the Antarctic Peninsula as a consequence of the strong rise in air temperature in the WAP region during the last decades (Rignot and Thomas, 2002; Vaughan et al., 2003; Braun and Hock, 2004; Cook et al., 2005; Turner et al., 2005; Vaughan, 2006; Dominguez and Eraso, 2007; Steig et al., 2009; Rueckamp et al., 2011). Husmann et al. (2012) proposed the intensified sediment and melt water input at KGI to be responsible for the higher Fe accumulations in *L. elliptica* from KGI compared to individuals collected at Rothera Point (Adelaide Island). The origin of high tissue Fe levels in *L. elliptica* from ingestion of lithogenic debris still remains to be verified.

Like other benthic deposit feeders, *L. elliptica* ingests particles and water from the benthic boundary layer. Trace metals are assimilated from both sources (Rainbow, 2002; Griscom and Fisher, 2004). The proportion of metal assimilation from the particulate and dissolved phase depends on the bioavailability of the metal in each fraction and on the physiological characteristics of the species (e.g. pH-conditions in the gut) (e.g. Wang and Fisher, 1999; Rainbow and Wang, 2001; Griscom and Fisher, 2004). Large amounts of lithogenic sediment particles are ingested together with the nutrition. However, the assimilation efficiencies (AE) of metals are generally higher for organic matter compared to inorganic matter, because organic particles are processed more intensely in the gut, due to their nutritional value (e.g. Willows, 1992; Decho and Luoma, 1996; Gagnon and Fisher, 1997; Lee and Luoma, 1998; Griscom and Fisher, 2004). Free metal ions are most easily absorbed and readily bioavailable to marine organisms (e.g. Fisher et al., 1996; Bjerregaard and Depledge, 1994).

Concentrations of Fe and Mn usually do not exceed low nanomolar levels in oxic ocean waters (e.g. Landing and Bruland, 1987; Bruland and Lohan, 2004; Middag et al., 2012), but bivalves accumulate trace metals even when exposed to low concentrations (Rainbow, 1990). The same author, however, described sediment pore water as an alternative source of bioavailable metals for burrowing bivalves. Pore waters in the

suboxic sediment zone (preferentially termed as manganous and ferruginous zones; Canfield and Thamdrup, 2009) generally show high concentrations of dissolved Mn(II) and Fe(II) due to the dissimilatory reduction of manganese oxides and iron(hydr)oxides during early diagenesis (e.g. Froelich et al., 1979; Berner, 1981; Lovley and Phillips, 1988; Rutgers Van Der Loeff et al., 1990; Canfield et al., 1993). Dissolved Fe(II) and Mn(II) diffuse into the benthic boundary layer or into the overlying water layers due to concentration gradients between pore water and seawater and in dependence of the oxygen penetration depth (e.g. Lynn and Bonatti, 1965; Yeats et al., 1979; Sundby and Silverberg, 1985; Laës et al., 2007; Pakhornova et al., 2007; Kowalski et al., 2012).

In the present study we investigate the influence of metal concentrations in sediment pore water on the metal assimilation in *L. elliptica* in Potter Cove (King George Island, Antarctica). To this end we compared Fe and Mn concentrations in bivalve hemolymph ("blood") and tissues (gills, digestive gland, and mantle) to sediment, sediment pore water and seawater concentrations in the vicinity of the animal sampling sites. In an experimental approach, Fe concentrations in the hemolymph were monitored *in vivo* during 14 days of exposure to low Fe conditions to assess whether Fe levels in bivalve "blood" indeed reflect the environmental Fe concentrations or are controlled physiologically. This study provides the first chemical characterization of the hemolymph of *L. elliptica* with respect to metals as well as the origin of Mn and Fe.

3.2 Material and Methods

3.2.1 Sample collection and experimental treatment

Individuals of the Antarctic soft shell clam *Laternula elliptica* were collected by scuba divers at seven stations in Potter Cove on King George Island (KGI; Fig. 3.1; Tab. 3.1) between January and March 2010. Five stations (B; Fig. 3.1c; Tab. 3.1) located next to the discharge area of melt water streams were chosen pseudo randomly on a UTM-grid (100 m grid point distance). One station was positioned in a newly ice free area (ID) and one in the outlet of Potter Cove to Maxwell Bay (C). Schloss and Ferreyra (2002) reported a decreasing concentration of terrigenous material in the water column with increasing distance to the discharge area. Consequently, station B is defined as highly impacted by sediment input compared to both other stations (C, ID).

At all stations only bivalves with a shell length > 7.0 cm were collected, except for station ID, where only smaller individuals < 6.4 cm were found. The age of 37 individual shells was determined according to Brey et al. (2011). Modifications include the use of epoxy-metal (liquid metal, Toolcraft, Conrad Electronic SE, Germany) as embedment and carbon carbide grinding paper (Buehler-Met[®]II, Buehler, USA) in steps of P1000, P2500 and

P4000 grades. Annual growth rings were counted under a stereomicroscope (SZX12, Olympus, Japan).
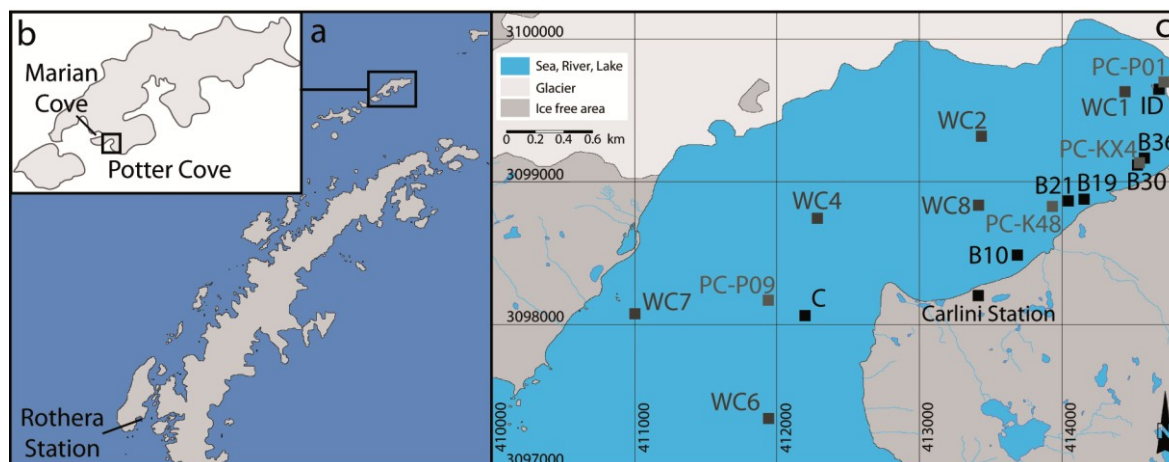
Figure 3.1: a) Map of the Antarctic Peninsula (King George Island highlighted); b) Map of King George Island; c) Map of Potter Cove including the sampling stations (B, C, ID: stations for bivalve sampling; PC-K48, PC-KX4, PC-P01, PC-P09: sediment cores; WC: sea water samples; UTM grid: zone Z21E; WGS84).

Hemolymph and tissues (digestive gland (DG), gill, and mantle) were sampled from all replicates of each station within 12 hours after collection. Individuals used in withdrawal experiments were acclimatized in natural seawater at 1°C at least for one week. 50% of the water was renewed every two days to ensure good water quality. Three replicates (EH1 - EH3; one animal per aquarium) of *L. elliptica* were kept in 0.5 µm-filtrated seawater (WFMB0.5-93/4 cartridge filter, Wolftechnik Filtersysteme GmbH, Germany) over a period of 14 days. A second treatment group of three individuals (EH4 – EH6) were exposed to 0.5 µm-filtrated seawater spiked with 10 µmol L^{-1} Fe; dissolved as a Fe:EDTA complex. The Fe-EDTA solution was prepared by dissolving 100 µmol EDTA (≥ 99%, Sigma-Aldrich, Steinheim, Germany) in 100 mL of 18.2 MΩ water. After cooling, 100 µmol Fe (Ammoniumiron(II)sulfatehexahydrate, ≥ 98%, Sigma-Aldrich, Germany) were added and diluted with 0.5 µm filtrated seawater to the final volume (10 L). Water of each aquarium and hemolymph of each bivalve were sampled at the days 0, 5, 10, and 14. The water temperatures ranged between -0.5°C and 2°C.

Hemolymph (fluid and hemocyte cells) was taken of the posterior adductor muscle by using a G26x1 needle (Sterican®, B. Braun Melsungen AG, Germany) and a 1 mL or 10 mL syringe (Omnifix®, B. Braun Melsungen AG, Germany). Subsamples were centrifuged with 400 *g* (a force that did not lyse cellular material) for 15 min at 2°C (Centrifuge 5403, Eppendorf AG, German) to remove hemocytes from suspension to determine the Fe content of the hemolymph fluid. Afterwards original samples and centrifuged sub-samples were acidified with 20 µL nitric acid (≥ 69%, TraceSelect®, Sigma Aldrich, Germany) per 1 mL sample and stored and transported at 4°C in safe-lock-tubes

27

(Eppendorf AG, Germany). Tissues (DG, gill) were sampled using ceramic scissors and rinsed carefully with 18.2 MΩ water in order to remove seawater and sediment. This ensures that the body tissue metal concentrations represented only assimilated metals. Cleaned tissues were stored at -80°C and lyophilized.

Table 3.1: Overview of all stations and sample types, including UTM coordinates (Zone Z21E; WGS84), sampling depth and date. The locations of sediment and pore water samples are assigned to corresponding bivalve sampling stations. Dates and replicates of multiple sampling of one station are denoted by '/'. Stations B10 – B36 are pooled to station B.

Stations - Bivalves (replicates)	Easting [UTM]	Northing [UTM]	Water depth [m]	Date
B10 (5)	413656	3098497	10	2010-01-26
B19 (5)	414115	3098868	5	2010-01-29
B21 (5)	414045	3098875	5	2010-03-18
B30 (5)	414492	3099119	10	2010-02-18
B36 (5)	414494	3099156	20	2010-01-21
C (5)	412204	3098059	25	2010-03-05
ID (5/ 5)	414714	3099635	20	2010-02-22/ 2010-03-12
Stations - Pore water/ (corresponding station)	Easting [UTM]	Northing [UTM]	Water depth [m]	Date
PC-K48 (B)	413906	3098827	12	2010-03-01
PC-KX4 (B)	414493	3099121	10	2010-02-18
PC-P01 (ID)	414712	3099674	30	2010-12-28
PC-P09 (C)	411900	3098200	55	2011-02-10
Stations - Seawater	Easting [UTM]	Northing [UTM]	Water depth [m]	Date
WC1	414400	3099600	5/ 30	2010-12-23/ 2010-12-30/ 2011-01-07/ 2011-01-15/ 2011-01-21/ 2011-01-31/ 2011-02-06/ 2011-02-14
WC2	413400	3099300	5/ 30	
WC4	412240	3098743	5/ 30	
WC6	411900	3097400	5/ 30	
WC7	411000	3098100	5/ 30	
WC8	413383	3098844	5/ 30	

3.2.2 Element analysis

All lab ware exposed to samples and standards was cleaned by soaking in >10% (v/v) HNO_3 (subboiled, 65%, Merck, Germany) for a minimum of 24 h, and rinsed subsequently with 18.2 MΩ water. PTFE vessels were cleaned with 10 mL >30% HNO_3 and heated at 160°C for 2 h under recirculation and also rinsed with 18.2 MΩ water prior to use. Before hydrolysis lyophilized tissues were powdered using an agate mortar and pestle and

weighed into PTFE vessels (mainly 50 – 100 mg). Hemolymph (1 – 2 mL) was transferred to PTFE pots and sample vials were rinsed with 1 M bidistilled HNO_3 to ensure that the whole sample was transferred into the PTFE vessels.

First, 5 mL of HNO_3 (65%, subboiled) and 1 mL of H_2O_2 (30%, Suprapur®, Merck, Germany) were added. Due to strong outgassing samples were kept at room temperature until out gassing ceased. Finally, 1 mL of HF (40%, Suprapur®, Merck, Germany) was added and vessels were heated under recirculation for 1 h at 60°C, 1 h at 100°C, and 8 h at 160°C. After cooling, 5 mL of 18.2 MΩ water were added and evaporated at 160°C to a residual volume of approx. 1 mL. Samples were filled up with 1 M nitric acid (65%, bidistilled) to a final volume of 10 mL (hemolymph) or 50 mL (tissues) and transferred to polypropylene (PP) tubes.

Element concentrations of Ca, Fe, K, Mg, Mn, Na, and Sr were analyzed by means of inductively coupled plasma - optical emission spectroscopy (ICP-OES; Iris Intrepid, Thermo Fisher Scientific Inc., Waltham, USA). Additionally, Mn concentrations below the lowest calibration standard of the ICP-OES measurements (0.01 mg L^{-1} Mn) were analyzed by inductively coupled plasma – mass spectrometry (ICP-MS; Perkin Elmer/Sciex, Elan6000, Massachusetts, USA). Iron background concentrations of the aquarium waters during the experiment were determined after tenfold-dilution with 1 M bidistilled nitric acid by ICP-MS. The ICP-multi-element calibration standard IV (CertiPURE®, Merck, Germany; used for ICP-OES), multi-element calibration standard 2 and 3 (Perkin Elmer, USA; used for ICP-MS), and rhodium(III)chloride solution (Merck, Germany) as internal standard were used for calibration of the ICP-OES and ICP-MS system. All element concentrations analyzed in this study are available at Pangaea® (doi:10.1594/PANGAEA.776600).

3.2.3 Standard reference material

The standard reference materials IAEA-A13 (freeze dried animal blood; International Atomic Energy Agency, Vienna, Austria) and IAEA407 (fish homogenate; International Atomic Energy Agency, Vienna, Austria) were hydrolyzed during each digestion procedure to assure constant digestion quality (Tab. 3.2). Lyophilized animal blood (IAEA-A13) was chosen due to the lack of matrix matched reference material, although matrix discrepancies between samples (liquid, no hemoglobin) and reference material (lyophilized, hemoglobin) exist. Additional hydrolysis and analyses were done at the Institute of Soil Science of Temperate Ecosystems (University of Göttingen) for both reference materials and at the Institute for Chemistry and Biology of the Marine Environment (University of Oldenburg) for IAEA407 to prove the accuracy of our digestion procedure.

Concentrations were similar between institutes and ranged within the 95% confidence interval (95%CI; Tab. 3.2) for most elements. For all elements precision ranged between 3.5% and 5.9% except for K (12.9%) in IAEA-A13 and between 5.2% and 8.9% in IAEA407.

Table 3.2: Results of the certified reference materials IAEA-A13 and IAEA407 analyzed at two/three different laboratories (SD = standard deviation, 95% CI = 95% confidence interval, b.d.l. = values below detection limit, n.d. = not determined). All certified values are recommended values.

| Reference Material | Element | Reference Material | | Alfred Wegener Institute | | | University of Göttingen (N = 8) | | University of Oldenburg (N = 1) |
		Recommended Value [mg kg^{-1}]	95% CI	N	Found concentration [mg kg^{-1}]	SD [mg kg^{-1}]	Found concentration [mg kg^{-1}]	SD [mg kg^{-1}]	Found concentration [mg kg^{-1}]
IAEA-A13	Ca	286	226 - 332	32	265	16	275	15	n.d.
	Fe	2400	2200 - 2500	34	2230	110	2110	73	n.d.
	K	2500	2100 - 2700	33	2040	260	2100	30	n.d.
	Na	12600	11600 - 13500	28	11070	390	10760	90	n.d.
IAEA 407	Ca	27000	25700 - 28300	13	26200	1700	26100	2160	25650
	Fe	146	143 - 149	12	132	12	129	10	b.d.l.
	K	13100	12200 - 14000	14	11000	710	11700	290	11500
	Mn	3.52	3.44 - 3.60	3	3.76	0.28	3.88	1.44	b.d.l.
	Sr	130	125 - 135	14	136	7	n.d.	n.d.	122

Table 3.3: Replicate analyses of ASW reference material (N = 17; Atlantic Seawater, OSIL, UK) and Cass-5 (N=7; NRCC, Canada) using ICP-OES. Measured and certified values are reported as average concentration ± standard deviation. Accuracy and precision of the measured ASW samples are displayed. "[a]" Solution containing 71.6 µmol L^{-1} Fe and 72.8 µmol L^{-1} Mn was added to ASW. "[b]" Solution containing 0.895 µmol L^{-1} Fe and 0.910 µmol L^{-1} Mn was added to CASS-5.

Element	ASW certified [µmol L^{-1}]	ASW measured [µmol L^{-1}]	Accuracy [%]	Precision [%]	CASS-5 certified [µmol L^{-1}]	CASS-5 measured [µmol L^{-1}]	Accuracy [%]	Precision [%]
Fe	71.6[a]	71.1 ± 0.6	-0.7	0.9	0.898 ± 0.001[b]	0.865 ± 0.022	-3.7	2.5
Mn	72.8[a]	72.8 ± 1.1	-0.02	1.5	0.915 ± 0.002[b]	0.925 ± 0.015	1.2	1.6

3.2.4 Pore water analysis

Two sediment push cores (PC-K48, PC-KX4) and two sediment gravity cores (PC-P01, PC-P09) were retrieved close to the bivalve sampling stations in Potter Cove (KGI) during austral summers 2009/2010 and 2010/2011 (Fig. 3.1c). All cores were taken by the Argentine Diving Division using a push corers and a gravity corer system (UWITEC, Austria). Immediately after coring sediments were transported to the Dallmann laboratory at the Argentine Carlini Station and directly sampled for pore water in 1 cm to 2 cm resolution (1 cm between 0-5 cm and 2 cm between 7-15 cm core depth) using 18.2 MΩ water-washed rhizons (0.15 µm mean pore size, Rhizosphere Research Products, The Netherlands) that were inserted simultaneously into the core liner through pre-drilled holes. Pore waters were then collected for up to 60 min under vacuum in 12 mL syringes. An aliquot of each pore water sample was transferred to 5 mL polypropylene tubes (conditioned with 2% (v/v) subboiled HNO_3 conc.), acidified with nitric acid (≥ 69%, TraceSelect®, Sigma Aldrich, Germany) to pH < 2, stored at 4°C and transported to the home lab laboratory at the ICBM (Oldenburg, Germany) for trace element analyses.

Fe and Mn were determined at 2-fold dilution by ICP-OES (iCAP 6000, Thermo Scientific, Germany). In case of low Fe and Mn concentrations (< 0.9 µmol L^{-1} Fe and < 0.5 µmol L^{-1} Mn) further analyses on 10-fold diluted sample aliquots were performed with an Element 2 ICP-MS (Thermo Scientific, Bremen, Germany) to validate the results obtained by ICP-OES. In order to guarantee precision and accuracy of the methods carefully selected international reference materials were measured, namely Atlantic Seawater (ASW, Osil, UK) spiked with single-element standard solutions (Alfa Aesar, U.S.) and CASS-5 (NRCC, Canada). Precisions and accuracies for Fe (ICP-OES) and Mn (ICP-OES) are given in table 3.3.

3.2.5 Statistical analysis

Since stations B10 – B36 are representing the discharge area of meltwater streams all five substations were pooled to one station B, now represented by 25 bivalves. Element tissue concentrations were normalized to bivalve shell volume to enable the comparison of sampling sites with non-overlapping animal size ranges. Since the shell does not grow exclusively along the anterior-posterior axis, the volume of an ellipsoid calculated from shell length, height, and width (Equation 3.1) was chosen as a more conservative approximation. The ellipsoid proxy was also favored over shell weight, because sediment particles were frequently enclosed between the shell layers in the siphon area of the shell (compare Harper et al., 2012), which would have biased shell weight as a normalization proxy.

$$V_{Shell} = \frac{4}{3} \times \pi \times \frac{length_{Shell}}{2} \times \frac{height_{Shell}}{2} \times width_{Shell} \qquad (3.1)$$

Descriptive statistics were computed by Origin 8.5.1 (OriginLab Corporation, USA). In order to identify and diminish outliers the Q-test after Dean and Dixon (1951) for N < 10 was applied. Differences in means were tested on significance between stations by the nonparametric Kruskal-Wallis-test (using R 2.12.1; R Development Core Team, 2010) and Nemenyi-test (computed manually). Equality of variances was tested by the Levene's test implemented in the lawstat package (Noguchi et al., 2009). An alpha level of 5% was chosen as statistically significant.

3.3 Results

Animals from stations B and C were older than 13 years (N=28), whereas animals collected at ID reached a maximum age of only five years (N=9). The lack of older individuals at station ID indicates a colonization of the southern side of the island (close to station ID; Fig. 3.1) during the Austral summer 2004/05. The island was covered by the Fourcade Glacier until 2002/03 and the results from station ID provide first evidence that benthic colonization around the rocky island commenced only after the glacial retreat. As maturation in *L. elliptica* sets in at around 8 years (Dick et al., 2007), animals collected at station ID with a maximum age of 5 years are referred to as juveniles.

3.3.1 Iron withdrawal experiments

Iron concentrations of the aquarium water during the experiment are given in figure 3.2. Figure 3.3a shows hemolymph Fe concentrations over time with regression lines for the Fe-withdrawal experiment where bivalves were kept in filtrated seawater. Only two replicates are shown since a third replicate was excluded because the measured hemolymph Fe concentrations were inconsistent over time.

In the experiment where bivalves were kept in Fe spiked filtrated seawater (10 µmol L^{-1} Fe; Fig. 3.3b), replicate EH4 showed increasing blood Fe concentration between day 0 (58.7 µmol L^{-1}) and day 5 (64.4 µmol L^{-1}), with concentrations declining consistently after day 5. In all other replicates of both treatments the Fe concentration decreased continuously and rapidly over time. We expect, therefore, the initial Fe concentration of EH4 to be higher than the Fe concentrations of the following samples (day 5, 10, and 14) and assume the value of day 0 as non credible result.
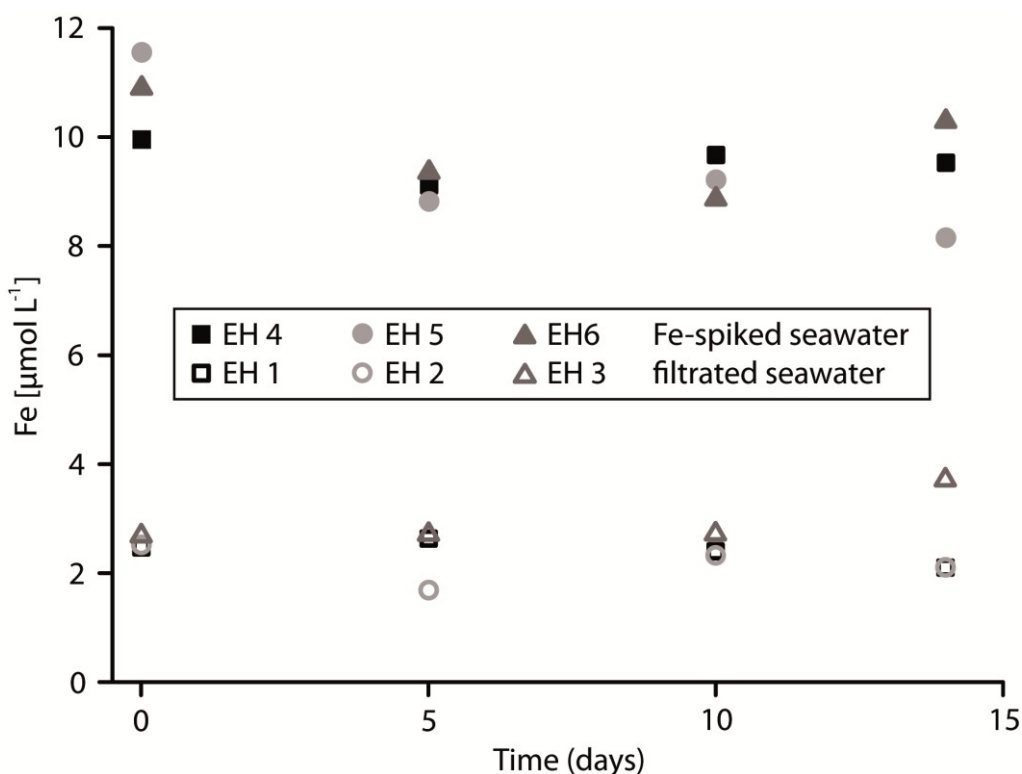
Figure 3.2: Background Fe concentrations in the aquarium water during the 14 day Fe withdrawal experiment with *L. elliptica*. Replicates EH1 – EH3 were kept in filtrated seawater and replicates EH4 – EH6 in Fe spiked seawater.

The slopes of the regression lines of the experimental setup (a) (replicates kept in filtrated seawater; Fig. 3.3a) decline more steeply (slopes: -6.9 (EH2) and -2.8 (EH3)) than for the regression lines of the experimental setup (b) (replicates kept in iron spiked seawater, Fig. 3.3b, EH4 – EH6: slopes: -0.9 to -1.8). Steeper slopes are also found in bivalves with higher initial Fe hemolymph concentrations. The half-time values of EH2 and EH3 (8 days, 13 days) were lower than for replicates EH4 to EH6, which ranged from 19 to 31.5 days (half-time value of EH4 was calculated without day 0). The adjusted determination coefficient (R^2) exceeds 0.91 for all replicates (EH4 was calculated without day 0). Iron contamination during sampling can be excluded due to this highly linear regression.

Thus in both treatments the Fe concentration declined strongly over time.

3.3.2 Element concentrations of hemolymph, pore water, and seawater samples

The mean concentrations of Ca, Na, and Sr in hemolymph were similar to mean concentrations in pore water and seawater (Tab. 3.4; means over all stations). The mean K concentration in hemolymph samples (11.2 mmol L^{-1}) was marginally higher than the maximum pore water and seawater concentrations (10.7 mmol L^{-1}).

Hemolymph Fe concentrations of bivalves from different sampling locations (B, C, ID) are shown in figure 3.4. Significant differences in mean hemolymph Fe concentrations were only found between Station B (169 ± 51 µmol L^{-1}) and station ID (36 ± 13 µmol L^{-1}). Iron

concentrations at station C (141 ± 108 µmol L^{-1}) were similar to both other stations. Centrifuged hemolymph samples contained 71% ± 10% (N=29, across stations) of the total Fe concentration in hemolymph (data are not shown in the tables), which means that approximately 30% of total Fe in hemolymph is bound in cells.
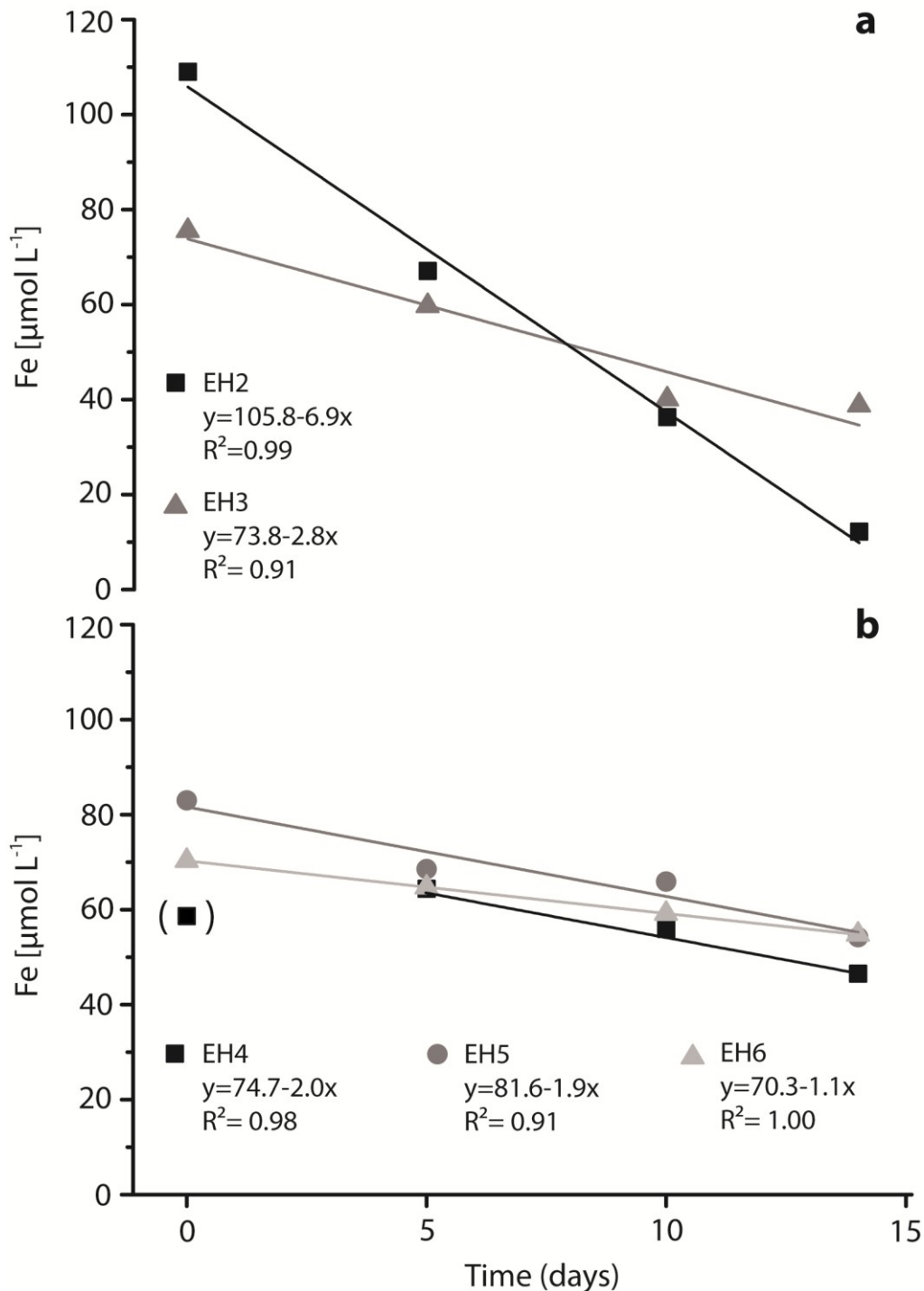
Figure 3.3: Hemolymph Fe concentrations in bivalve hemolymph during a 14 day withdrawal experiment in a) filtrated seawater and b) filtrated seawater spiked with 10 µmol L^{-1} Fe. Equations and adjusted R^2 are given for the linear regression lines. Day 0 of EH4 was not considered for linear regression.

Table 3.4: Mean and range of Ca, Fe, K, Mn, Na, and Sr concentrations in bivalve hemolymph (stations B, C, and ID), pore water (cmbsf = cm below seafloor), and seawater.

Element	Hemolymph		Pore water (0 - 5 cmbsf)		Sea water (5 & 30 m water depth)	
	Mean	Range	Mean	Range	Mean	Range
Ca [mmol L^{-1}]	10.6	8.9 - 11.7	10.6	10.1 - 11.4	10.4	9.0 - 10.8
K [mmol L^{-1}]	11.2	8.9 - 12.6	10.3	9.7 - 10.7	10.3	8.8 - 10.7
Na [mmol L^{-1}]	429	347 - 465	460	444 - 476	452	413 - 470
Sr [µmol L^{-1}]	93	79.5 - 104	90	88.7 - 92.5	91	79 - 94
Fe [µmol L^{-1}]	134	5.6 - 458	84	1.4 - 192	0.11	0.01 - 0.76
Mn [µmol L^{-1}]	< 0.4	0.1 - 4.0	18.8	0.8 - 60	0.02	0.01 - 0.09
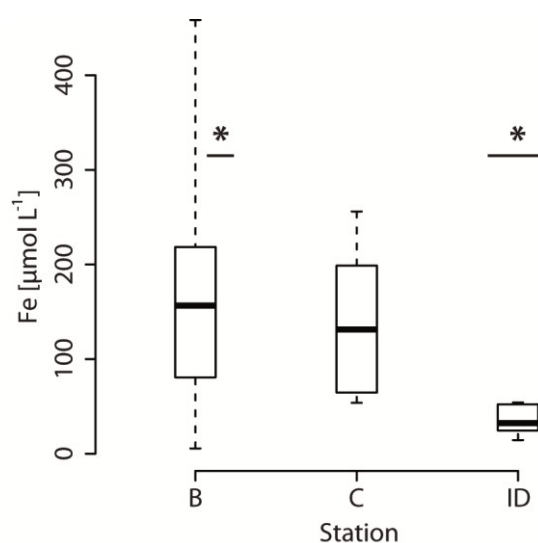
Figure 3.4: Fe concentrations in bivalve hemolymph (N= 22(B)/ 5(C)/ 8(ID)). Boxplot whiskers represent the range. '*' denotes significant differences between stations B and ID at an alpha level of 5%.

In contrast to Fe, Mn concentrations were below the ICP-MS detection limit (< 0.1 µmol L^{-1}) in most hemolymph samples. At station B the maximum Mn concentration was 3.9 µmol L^{-1}, and thus similar to station ID (4.0 µmol L^{-1}) and higher than at station C (2.4 µmol L^{-1}). Fe and Mn concentrations in hemolymph were considerably higher than in seawater. Average concentrations in seawater were 0.11 µmol L^{-1} Fe and 0.02 µmol L^{-1} Mn between 5 and 30 m water depth with maximum concentrations of 0.76 µmol L^{-1} Fe and 0.09 µmol L^{-1} Mn.

Contrary, pore water Fe and Mn concentrations were distinctly higher than in seawater and similar as in bivalve hemolymph. Pore water profiles down to 11 cm below seafloor (cmbsf) are shown in figure 3.5. Cores PC-K48 and PC-KX4 are located in the vicinity of station B. Cores PC-P09 and PC-P01 are located close to the bivalve reference stations C and ID (Fig. 3.1c), respectively. At stations PC-K48 and PC-KX4 Fe and Mn concentrations changed similarly with depth and peaked in 5 cm (PC-K48; 167 µmol L^{-1} Fe, 32 µmol L^{-1} Mn) and 7 cm below seafloor (PC-KX4; 176 µmol L^{-1} Fe, 40 µmol L^{-1} Mn). Only within the first 3 cmbsf Fe and Mn concentrations increased faster

at site PC-K48 compared to PC-KX4. At Station PC-P01, close, to the glacier the highest maximum concentrations (202 µmol L^{-1} Fe in 9 cmbsf, 82 µmol L^{-1} Mn in 11 cmbsf) were found for both elements, with the strongest increase between 1 cm and 3 cm depth. Compared to the other cores, core PC-P09 had the lowest peak Fe and Mn concentrations (99 µmol L^{-1} Fe in 2 cmbsf, 4.8 µmol L^{-1} Mn in 11 cmbsf).

Fe concentrations were between 2.6 (PC-P01) and 17.6 (PC-P09) times higher than Mn concentrations. Cores sampled close to station B showed similar Fe/Mn-ratios of 3.8 (PC-K48) and 5.2 (PC-KX4). In comparison, the Fe/Mn ratio in hemolymph averaged over all stations was 660.
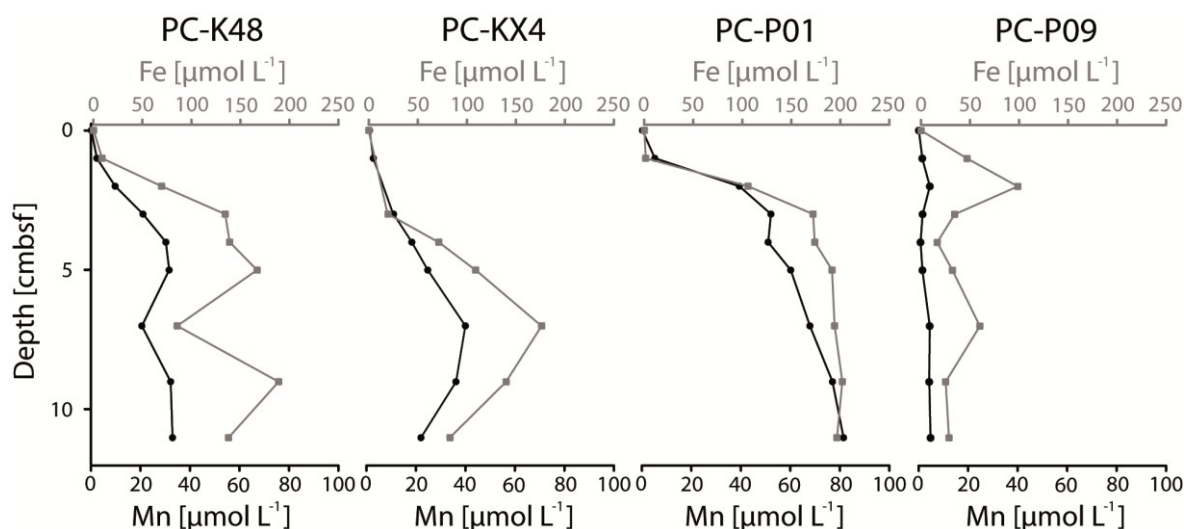
Figure 3.5: Pore water profiles of Fe and Mn down to 11 cm below seafloor (cmbsf) of four stations related to the sampling sites of *L. elliptica* (PC-K48, PC-KX4 correspond to animals collected at stations B, PC-P01 to station ID, and PC-P09 to animals collected at station C).

3.3.3 Tissue element analysis (Fe, Mn)

Manganese contents in DG and mantle tissue ranged mostly between the detection limit (defined as 3 times the single standard deviation, SD) and the lowest calibration standard and are therefore not shown in figure 3.6.

Differences in Fe and Mn contents between station B and the two reference stations (C, ID) were tested after normalization to shell volume according to equation (3.1) to account for size and age effects (e.g. individual life times, metabolic rates). Iron and Mn contents in gills did not differ significantly between stations B and C and B and ID (Fig. 6a,b). Manganese contents differed significantly between stations C and ID. Especially station B underlies a high variation with respect to both elements. Iron was higher concentrated in the digestive gland of animals collected at station ID with mean contents differing

significantly between stations C and ID (Fig. 3.6c). Mantle tissue concentrations for Fe did not differ significantly between all three stations (Fig. 3.6d).
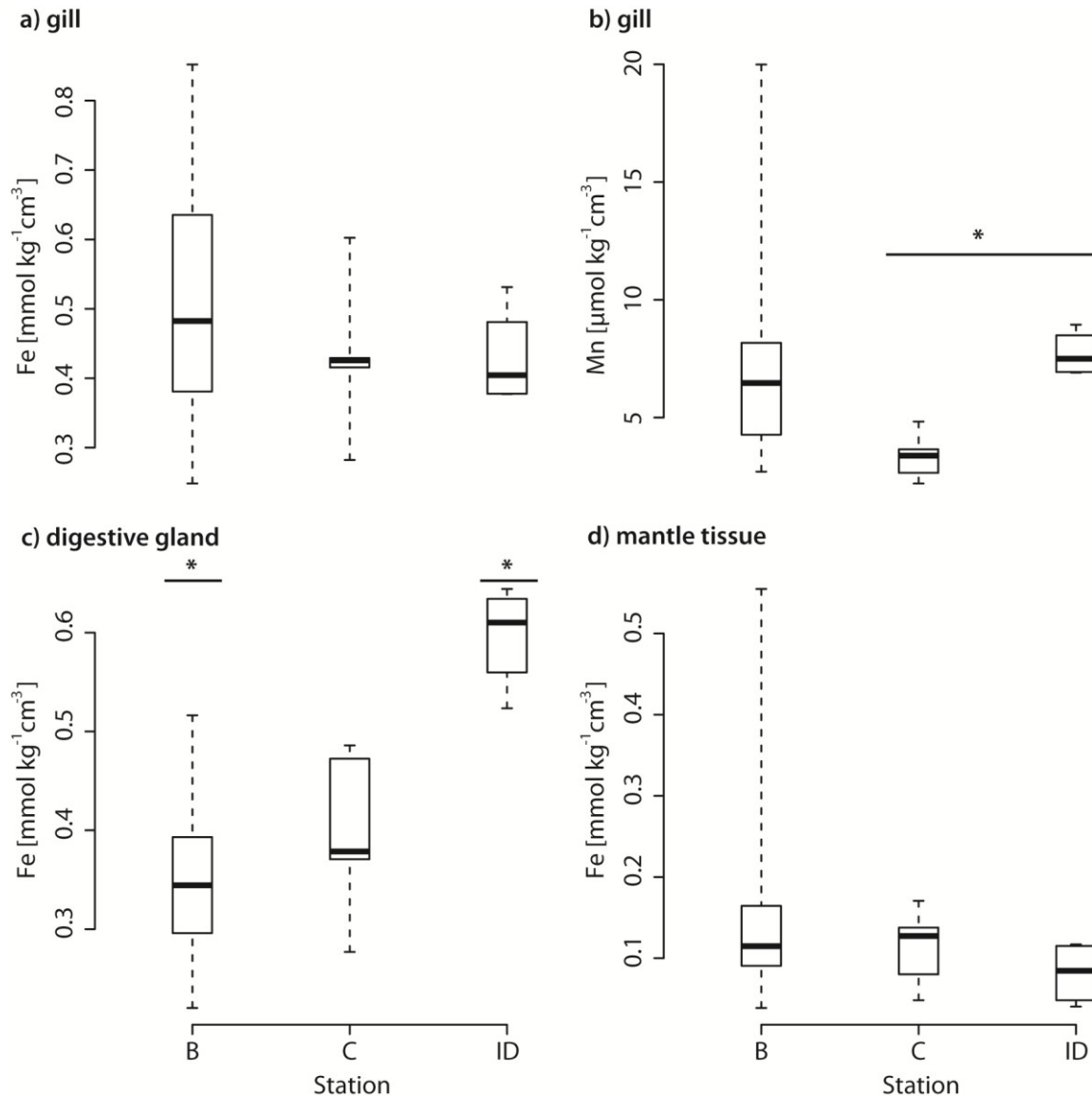
Figure 3.6: Shell volume normalized Fe and Mn tissue concentrations: a) Fe contents in gills; b) Mn contents in gills; c) Fe contents in digestive gland; d) Fe contents in mantle tissues. Mn contents in DG and mantle tissue are between the detection limit and lowest calibration standard and are therefore not shown. Tissue sample sizes (N) were 25 (B), 5 (C) and 4 (ID) for all elements, except for Fe contents in mantle tissues at station B (N=19). Boxplot whiskers represent the range. '*' denotes significant differences between two stations at an alpha level of 5%.

3.3.4 Iron and manganese content in sediment cores

The Fe sediment content ranged from 5.5% (PC-P09) to 6.3% (PC-P01) with an average of 5.8% across all stations and the Mn content was between 0.10% and 0.11% in sediments of Potter Cove (Tab. 3.5).

Table 3.5: Fe and Mn content sediment cores retrieved at four stations in Potter Cove.

Sample	Fe [%]	Mn [%]
PC-K48	5.8	0.10
PC-KX4	5.7	0.10
PC-P01	6.3	0.11
PC-P09	5.5	0.10
Mean	5.8	0.10

3.4 Discussion

3.4.1 Does sediment input from glacial erosion increase metal concentrations in *L. elliptica*?

Several authors proposed an assimilation of metals into bivalve tissues via the ingestion of particulate matter (including lithogenic material; e.g. Abele et al., 2008; Curtosi et al., 2010; Husmann et al., 2012). Indeed, *L. elliptica* permanently ingests lithogenic particles. The greater part, however, is excreted as pseudofeces (a conglomerate of particles and mucus; Ahn, 1993; Kowalke, 1998). Iron (~5.8%) and Mn (~0.1%) contents in sediments from Potter Cove are high compared to metal concentrations in the bivalve tissues (Tab. 5 and 6), but the extent of metal assimilation from the ingested sediment depends on the bioavailability of each element. This is usually described by the assimilation efficiency (AE) for a given animal under specified conditions.

Assimilation efficiencies are defined as the fraction of a metal in ingested particles, including sediment, which is physiologically assimilated across the gut lining into the tissues of an animal during one complete digestive cycle (e.g. Reinfelder et al., 1997; Griscom and Fisher, 2004). Assimilation efficiencies are generally higher for particles of higher nutritional value (compare chapter 1; Willows, 1992; Decho and Luoma, 1996; Lee and Luoma, 1998; Griscom and Fisher, 2004). Assimilation efficiencies are known for some intensively studied bivalves as *Macoma balthica*, *Mercenaria mercenaria*, or *Mytilus edulis* (e.g. Luoma et al., 1992; Wang and Fisher, 1996; Wang et al., 1996; Reinfelder et al., 1997, Thomas and Bendell-Young, 1998; Griscom et al., 2000) but Fe and Mn were hardly considered in these studies. For example, the facultative deposit feeding clam *M. balthica* showed AEs of sediments between 1% (Cr) and 42% (Zn). Assimilation efficiencies of Ag, Cd, and Co from anoxic sediments (9 - 16%) were two-fold lower than

from oxic sediments (Griscom et al., 2000). Similar investigations for *L. elliptica* are lacking. Further, iron nano-particles (and other small metalrich particles) can be assimilated over the gills by phagocytic pinocysts (e.g. George et al., 1976; Kadar et al., 2010).

Nevertheless, assimilation of lithogenic Fe may be restricted to the exchangeable Fe fraction (adsorbed Fe), because the pH-value in the DG of *L. elliptica* range between 5.8 and 6.5 (Poigner, unpublished). Several studies (e.g. Fisher and Teyssie, 1986; Wang and Fisher, 1996; Gagnon and Fisher, 1997; Griscom et al., 2000) used sea water (pH 5 – 5.5) for desorption of sediment bound [adsorbed] metals (Ag, Am, Cd, Cr, Co, Se, and Zn) to mimic pH conditions in bivalves' guts (pH 5 – 6). Griscom et al. (2000) found a consistency (for Ag, Cd, Co, and Se) between the fraction dissolved in sea water (pH 5, 3 hrs) and AEs for *Mytilus edulis* and *Macoma balthica*. Harvey and Luoma (1985) assumed amorphous and crystalline Fe-oxides as unavailable in the digestive environment of *Macoma balthica*. In comparison, Poulton and Canfield (2005) performed an inorganic sequential Fe extraction procedure to analyze different Fe fractions of sediments. Adsorbed Fe was released by a weak treatment with $MgCl_2$ (1 M, pH 7, 2 hrs), whereas the next fraction – carbonate bound Fe – was dissolved through a sodium acetate treatment (pH 4.5, 24 hrs, room temperature/ 50°C). Other minerals required even lower pH values and more aggressive chemical treatments to hydrolyze bound Fe. Therefore the DG pH-value appears to be too high to enable the digestion of lithogenic bound Fe and therefore the assimilation of lithogenic bound Fe by *L. elliptica* is most probably restricted. This is in line with Turner and Olsen (2000) who found that the release of bioavailable Fe may be overestimated through the use of chemical reagents compared to the natural gastro-intestinal fluid (in their study: of the plaice *Pleuronectes platessa*).

The significantly lower Fe concentrations in hemolymph and significantly higher normalized Fe concentrations in DG of juveniles from station ID may relate to physiological factors compared to adults. Similar was already reported for the shells of *L. elliptica,* where Fe incorporation decreases strongly during the first years of lifetime in relation to lifetime mass specific respiration (Dick et al., 2007). Since neither the normalized Fe and Mn tissue contents nor the Fe hemolymph concentrations in *L. elliptica* differed significantly between the adults of station B (highest input of lithogenic debris) and station C (outer Potter Cove), no influence of higher amounts of lithogenic suspended matter on metal concentrations in adult *L. elliptica* was found in Potter Cove.

3.4.2 What determines the Fe concentrations in the hemolymph of *L. elliptica*?

Bivalves are basically iso-osmotic to the surrounding water, which is shown for *L. elliptica* in chapter 3.3.1. This means that the concentrations of major seawater ions (e.g. Na^+, Cl^-, SO_4^{2-}) in the hemolymph should reflect the environmental concentrations as long as the clams' siphons (or shells of a mussel) remain open (e.g. Robertson, 1949, 1953; Shumway, 1977; Willmer et al., 2000).

In the hemolymph of *L. elliptica*, the major ion concentrations (Ca, K, Na, Sr; see Tab. 3.4) did not differ from either seawater or pore water concentrations, and can, therefore, not be used to determine the origin of hemolymph ions (pore vs. sea water).

Contrary, in situ Fe hemolymph concentrations in *L. elliptica* from Potter Cove were in the same order of magnitude as sediment pore water and several orders of magnitude above sea water concentration.

Experimental exposure of *L. elliptica* to low concentrations of dissolved Fe (filtrated seawater; spiked with 10 µmol L^{-1} Fe) indicated a strong dependence of hemolymph Fe concentrations on the levels of dissolved Fe in the incubation water. In both treatments the Fe hemolymph concentrations decreased rapidly within days, but in Fe-spiked filtrated seawater the Fe hemolymph concentrations decreased slower than in filtrated seawater. Thus Fe equilibration between environmental (sea)water and hemolymph appears to be a passive process which depends mainly on the amount of bioavailable Fe in the surrounding medium. Therefore, Fe hemolymph concentrations presented in figure 3.4 were not normalized to shell volume. These results also support a passive Fe assimilation by *L. elliptica* (without any ion pumping) probably explainable by the free ion model (reviewed in Simkiss and Mason, 1983 and Rainbow, 1990). Metal ions cross the epithelial layers at sites of high permeability (e.g. gills), enter the blood and are subsequently bound to proteins for further storage, distribution or excretion (reviewed in Simkiss and Mason, 1983 and Rainbow, 1990; Kadar et al., 2010). In this concept of passive assimilation, the hemolymph is regarded as the organ of first storage. If Fe is not securely bound to Fe binding proteins it can be cytotoxic to mollusks (reviewed in Simkiss and Mason, 1983; Gonzalez et al., 2010; Gonzalez and Puntarulo; 2011), although Fe is an essential trace metal for many physiologically important biomolecules (e.g. cytochromes, metabolic enzymes, oxidases) (reviewed in Simkiss and Mason, 1983 and Rainbow, 1990).

Hemocyte cells of *L. elliptica* express the Fe storage protein ferritin in large quantities (Husmann et al., in prep.) and can, therefore, detoxify dissolved Fe taken up over the gills. Our results showed, however, that around 30% of the total Fe content in hemolymph of *L. elliptica* is bound in hemocyte cells. This cellular Fe storage is further indicated by the maximum total Fe concentration which exceeds the maximum Fe pore water concentration by a factor of 2 (Tab. 3.4). Approximately 70% of the total Fe content in

hemolymph is contained in the extracellular compartment of the hemolymphatic fluid and mainly depends on the environmental concentration of dissolved Fe in the closest environment of the bivalves. As this concentration was more than 500fold higher than the concentration in seawater we exclude seawater as an important Fe (and also Mn) source for *L. elliptica*. In oxic seawater inorganic, dissolved Fe(II) immediately oxidizes to the more stable oxidation state Fe(III), which underlies strong hydrolysis and precipitates as Fe(oxyhydr)oxides (e.g. Ahrland, 1975; Millero et al., 1995; Waite, 2001). Compared to Fe the kinetic oxidation of dissolved Mn^{2+} is relatively slow and Mn remains primarily as free Mn^{2+} and $MnCl^+$ in the water column (Roitz et al., 2002). The analogy of high hemolymph and porewater Fe concentrations on the one hand and the withdrawal experiments on the other hand suggest an uptake of dissolved Fe mainly from pore water.

Several geochemical studies have already demonstrated a diffusion of dissolved Fe and Mn from pore water into the benthic boundary layer and overlying water, if no precipitation occurs within the oxic sediment layer (e.g. Elderfield, 1976; Sundby and Silverberg, 1981; 1985; Slomp et al., 1997; Dellwig et al., 2007; Beck et al., 2008; Severmann et al., 2010; Kowalski et al., 2012). Bottom water has been reported as a third source of dissolved metals for the deposit feeding clam *Macoma balthica*, besides seawater and pore water (Griscom and Fisher, 2004 and references therein).

In this study we present a first approach to describe the possible Fe uptake routes for *L. elliptica* in Potter Cove (Fig. 3.7). In Potter Cove, however, the bottom water concentrations (0 cmbsf; Fig. 3.4) were similarly low as in seawater and much lower than in pore water or hemolymph. Nevertheless, the transfer of dissolved metals through the benthic boundary is intensified through bioturbation (Elrod et al., 2004; Severmann et al., 2010) or physical irrigation/hydraulic gradients: e.g. tides, currents, and waves (Falter and Sansone, 2000; Dellwig et al., 2007; Beck et al., 2008), or icebergs. The burrowing activities of *Laternula elliptica* can be assumed to reach down to a sediment depth of 25 cm (total length of shell and siphon) and dissolved metals released through bioturbate activity can subsequently be inhaled by the bivalve. In this case differences in Fe concentrations within the first centimeters of sediment depth would be responsible for the Fe uptake by *L. elliptica* and the variability within station B. At station ID lowest Fe hemolymph concentrations corresponded to the highest Fe pore water concentrations of core PC-P01. This may result from a higher exchange of hemolymph Fe due to a stronger respiratory dilution by the overlying seawater in intensely respiring young and small bivalves. Iron(oxyhydr)oxide nano particles, precipitated after the leakage of pore water into the bottom water, may be assimilated through phagocytic pinocysts by *L. elliptica* and transferred into its hemolymph, as it was shown for $Fe(OH)_3$ particles in *Mytilus edulis* (George et al., 1976).
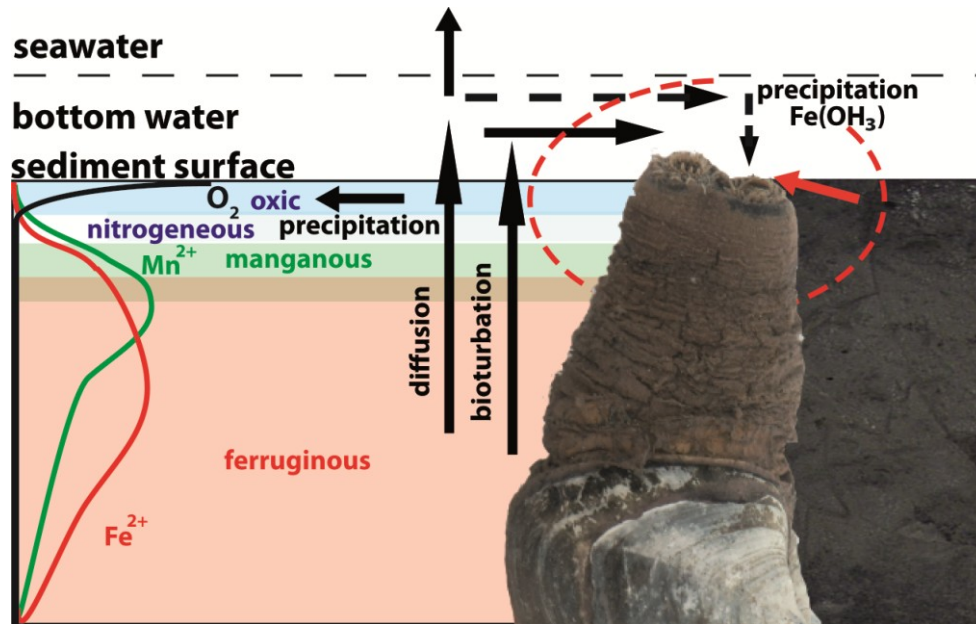
Figure 3.7: Possible Fe and Mn uptake pathways for *L. elliptica* in Potter Cove related to diagenetic processes in the upper sediment layers. Chemical zonation of the diagenetic series after Froelich et al. (1979) and Canfield and Thamdrup (2009).

Alternatively to the uptake via the siphon, an uptake of pore water via the foot seems possible. The two marine gastropods *Busycon carica* and *Hemifusus tuba* take surrounding seawater (containing dissolved metals) into the foot, when it expands (Mangum, 1979; Depledge and Phillips, 1986). There the water subsequently mixes with hemolymph, which is concentrated again (containing assimilated metals) before it returns to the gill or mantle tissue, when the animal retracts it foot into the shell again. Since *L. elliptica* is not able to inflate its foot, pore water may leak into the bivalve cavity passively, when the foot is extended out of the shell during burrowing.

Despite the complexity of possible uptake pathways pore water appears to be the main source of Fe for *L. elliptica* in Potter Cove (Fig. 3.7).

3.4.3 Discrimination of Mn in *L. elliptica*?

Maximum Mn pore water concentrations were considerably higher than seawater concentrations in Potter Cove. Although we expected Mn to be assimilated from pore water to the same extent as Fe, the Fe/Mn ratio was up to 20 in pore water compared to an average ratio of 600 in the hemolymph. Thus, we can show a strong discrimination of Mn between pore water and bivalve hemolymph. But we are not able to offer a sufficient explanation within this study, if Mn is discriminated during assimilation or underlies a faster excretion.

3.4.4 Variations of metal contents in tissues of *L. elliptica* around Antarctica

Tissue concentrations (gills, DG, and mantle; not normalized) of Fe and Mn in adult animals from station B and C are in the same order of magnitude as reported earlier for adult individuals from KGI (Tab. 3.6). Lower tissue concentrations (Fe, Mn) at station ID can be explained by a lower net accumulation due to shorter lifetime of the juveniles. Adult individuals from KGI (Marian Cove, Potter Cove) have Fe and Mn tissue concentrations up to 10-times higher than animals from Adelaide Island (Rothera Station) and Terra Nova Bay (Ahn et al., 1996; Nigro et al., 1997; Lohan et al., 2001; Curtosi et al., 2011; Husmann et al. 2012; this study). The lacking normalization of metal concentrations is probably responsible for the variations in mean concentrations among different KGI studies (Tab. 3.6), although sizes (shell length) of adults were similar (except for juvenile groups). Philipp et al. (2008) showed a high inter-individual variability in the shell length-age relationship. An age range between 10 and 36 years was, for instance, observed for individuals with a constant shell length of 76 mm (therefore we normalized on shell volume, compare chapter 3.2.4). Consequently, the lifetime integrated accumulation can vary greatly across homogenous size (shell length) classes in one and the same and between different sampling sites. This effect, however, cannot explain significant differences to other non-active volcanic sites, because juveniles from station ID in Potter Cove had distinctly higher Fe concentrations in DG and gills than adults from Rothera Island and Terra Nova Bay.

The highest accumulation of Fe in mantle tissues of *L. elliptica* found at Deception Island (9200 mg kg^{-1} dw Fe) relates to the high loads of dissolved metals to the benthic environment provided by volcanic geothermal activity (Deheyn et al., 2005). Elements released by geothermal sources diffuse ("non-point source") through the marine sediment and elevate seawater concentrations (Elderfield, 1972; Rey et al., 1995). Dissolved Fe and Mn seawater concentrations at Deception Island (3.2 µmol L^{-1} Fe [one value]; 0.5 – 2.3 µmol L^{-1} Mn; Elderfield, 1972) are considerable higher than seawater concentrations in Potter Cove, but lower than pore water concentrations in Potter Cove (Tab. 3.4). With reference to the metal bioavailability pore water and geothermal waters appear as similar sources, since both sources supply metals in the dissolved state. According to the chapters before we assume that the sediment pore water is the most important source of high Fe concentrations in *L. elliptica* in Potter Cove and around KGI.

Although pore water data (Fe, Mn) of other stations around the Antarctic Peninsula (e.g. Rothera Station, Palmer Station) are lacking, we hold differences in the geochemical environment of the sediments (including pore water) responsible for this variations in metal accumulation in *L. elliptica* around Antarctica. Especially, since no effect of sedimentation of lithogenic particles (station B: melt water inlets vs. C) on the Fe hemolymph and tissue concentrations was found within this study.

Table 3.6: Mean concentrations ± 95% confidence intervals [mg kg^{-1} dry weight] of Fe and Mn in tissues (DG = digestive gland, MAN = mantle tissue) of *L. elliptica* for all three stations. Sample sizes were 25 for station B and 5 for each of station C and ID, except mantle tissue samples of station B (N = 19). Results of this study are compared with tissue concentrations of previous studies (mean ± SD).

Location	Fe			Mn			Shell length [mm]	Source
	DG [mg kg^{-1} dw]	Gill [mg kg^{-1} dw]	MAN [mg kg^{-1} dw]	DG [mg kg^{-1} dw]	Gill [mg kg^{-1} dw]	MAN [mg kg^{-1} dw]		
B	1444 ± 154	2060 ± 305	764 ± 315		29 ± 8.3		73.2 - 90.7	this study
C	1864 ± 668	2006 ± 678	549 ± 385		15 ± 2.6		85.0 - 101.8	this study
ID	981 ± 404	639 ± 233	119 ± 58		11 ± 3.4		56.9 - 63.8	this study
Deception Island			9200 ± 2200			700 ± 400	-	Deheyn, 2005
Maxwell Bay (KGI)	2000 ± 720	2000 ± 650		18.6 ± 7.5	44.7 ± 16.3		72 - 95	Ahn et al., 1996
Potter Cove (KGI)	1660 ± 653	1360 ± 360	572 ± 484	9.2 ± 6.6	11.4 ± 3.2	7.4 ± 3.8	76 ± 8 mm	Husmann et al., 2012
Potter Cove (KGI)	1150 ± 310	350 ± 64	377 ± 102	11.9 ± 3.8	7.1 ± 0.8	5.9 ± 1.4	43 ± 6 mm	Husmann et al., 2012
Potter Cove (KGI)	1070 ± 50			4.1 ± 0.4			> 70	Curtosi et al., 2010
Rothera Point	422 ± 19	371 ± 25	98.5 ± 7.7	3.3 ± 0.07	4.2 ± 0.15	1.42 ± 0.04	59.2 - 83.5	Lohan et al., 2001
Terra Nova Bay	145 ± 58	178 ± 56		4.5 ± 0.4	5.1 ± 0.7		-	Nigro et al., 1997

3.5 Conclusions and outlook

Several studies assumed high input of lithogenic sediment to be causal of high metal concentrations in *L. elliptica* tissues. In our study no significant differences in Fe and Mn shell volume normalized tissue concentrations and hemolymph concentrations were, however, found between two sites of high and lower influence of lithogenic suspended particulate matter. Fe withdrawal experiments indicated environmental control of hemolymph Fe concentrations which were comparable to concentrations in pore water. Therefore we deduced a strong influence of pore water Fe concentrations on Fe assimilation into *L. elliptica*. The amount of hemolymph Fe that is most probably bound to Fe binding ferritin within the hemocyte cells amounts to 30% of overall hemolymph concentration. These 30% would then be responsible for the Fe uptake into the tissues. Contrary, Mn concentrations in hemolymph were as low as in the pore water of the first two centimeters below the seafloor. Deeper in the sediment, Mn pore water concentrations exceeded hemolymph concentrations several times. It remains unclear,

whether Mn is regulated actively by *L. elliptica* or whether Mn is less assimilated or faster excreted compared to Fe. From the geochemical view an explanation is difficult. For instance, several factors such as organic matter content of the sediment, remineralization rate, oxygen penetration depth, and bioirrigation affect the flux of dissolved Fe and Mn across the benthic boundary layer into the overlying water as well as the predominating pore water concentrations (e.g. Elrod et al., 2004; Sachs et al., 2009; Severmann et al., 2010). Consequently, differences in the geochemical environment of the sediment (including pore water) appear responsible for variations in background concentrations, like they were found for *L. elliptica* around the Antarctic continent. Fe and Mn pore water data are lacking for other sites, where metal accumulation was investigated in *L. elliptica*. Therefore, analysis of Fe and Mn concentrations in pore water of areas with lower Fe accumulation in *L. elliptica* tissues are desirable to complete the puzzle.

4 Stable Fe isotopes (δ^{56}Fe) in the hemolymph of the clam *Laternula elliptica* as indicator for sources of assimilated Fe

Harald Poigner[1], Dorothee Wilhelms-Dick[1], Doris Abele[1], Michael Staubwasser[2], and Susann Henkel[2]

[1]Alfred Wegener Institute Helmholtz Centre for Polar and Marine Research,
 27570 Bremerhaven, Germany
[2]University of Cologne, Institute for Geology and Mineralogy, 50937 Cologne, Germany

4.1 Introduction

Benthic deposit feeders ingest particles and water from the benthic boundary layer and assimilate trace metals from seawater, bottom water, pore water, and organic and lithogenic particles (Rainbow, 2002; Griscom and Fisher, 2004). Dominating assimilation pathways and bioavailable metal sources are, however, difficult to verify. In the circum Antarctic clam *Laternula elliptica (King and Broderip, 1832)* Fe tissue concentrations vary considerably around Antarctica (Ahn et al., 1996; Nigro et al., 1997; Lohan et al. 2001; Deheyn et al., 2005; Curtosi et al., 2010; Husmann et al., 2012; Poigner et al., under review). Highest concentrations were found in animals at Deception Island, where hydrothermal waters provide high loads of dissolved Fe to the environment (Rey et al., 1995; Deheyn et al., 2005). At King George Island (KGI) the predominating Fe source for the assimilation into *L. elliptica* remains unclear and is discussed controversially. Several authors propose lithogenic sediment particles as source for high Fe tissue concentrations in *L. elliptica* (e.g. Abele et al., 2008; Curtosi et al., 2010; Husmann et al., 2012). Alternatively, Poigner et al. (under review) assume dissolved Fe of the sediment pore water as predominating Fe source for *L. elliptica* in Potter Cove, based on similarly high Fe concentrations in hemolymph (blood) and pore water. Elevated concentrations of dissolved Fe occur in pore waters (within the ferruginous sediment zone) due to the release of Fe(II) by dissimilatory reduction (DIR) of iron(hydr)oxides during early diagenesis (e.g. Froelich et al., 1979; Berner, 1981; Lovley and Phillips, 1988; Rutgers Van Der Loeff et al., 1990; Canfield et al., 1993). Iron concentrations of bivalve hemolymph should reflect elevated environmental concentrations of dissolved Fe, since metals cross the epithelial layers at sites of high permeability (e.g. gills) relatively indiscriminated and enter the hemolymph (Simkiss and Mason, 1983; Rainbow, 1990; Kadar et al., 2010). The hemolymph is not only regarded as the organ of first storage, it is further of particular importance for the metal transport from assimilation sites (e.g. intestinal tract, gills) to sites of excretion (Simkiss and Mason, 1983; Rainbow, 1990; Kadar et al., 2010). Therefore, Fe concentrations as well as Fe isotope signatures of the assimilation source should be reflected by the fingerprint of the hemolymph. The stable isotopic Fe signature may be suitable as tracer for predominating, bioavailable Fe sources for *L. elliptica*, since Fe isotopes are emerging as a tracer for biogeochemical Fe cycling in aquatic environments (reviewed in Anbar and Rouxel, 2007; Johnson et al., 2008).

Stable Fe isotopes occur in the following relative abundances: ^{54}Fe: 5.84%, ^{56}Fe: 91.76%, ^{57}Fe: 2.12%, and ^{58}Fe: 0.28% (e.g. Beard and Johnson, 1999 and references therein). Iron isotopic compositions are commonly expressed as ^{56}Fe/^{54}Fe and ^{57}Fe/^{54}Fe ratios, whereas the δ notation is widely used to demonstrate isotopic shifts of samples against a standard

material (e.g. Belshaw et al., 2000). The δ^{56}Fe value [‰] (Equation 4.1) relates the ^{56}Fe/^{54}Fe ratio of a sample relative to the ^{56}Fe/^{54}Fe ratio of the standard reference material IRMM-014 (e.g. Beard et al., 2003a; Anbar and Rouxel, 2007).

$$\delta^{56}Fe \ [‰] = \left(\frac{\left(^{56}Fe/\, ^{54}Fe \right)_{Sample}}{\left(^{56}Fe/\, ^{54}Fe \right)_{IRMM-014}} - 1 \right) \times 1000 \qquad (4.1)$$

Shifts in δ^{56}Fe values result from mass dependent biotic and abiotic processes, which fractionate among lighter and heavier Fe isotopes (e.g. Beard et al., 2003a). For instance, in sediments lighter Fe isotopes are preferentially released through the DIR (Beard et al., 1999; Icopini et al., 2004; Crosby et al., 2007), resulting in lower δ^{56}Fe values in pore waters, whereas pore waters strongly influenced by sulfide formation are characterized by higher δ^{56}Fe (Severmann et al., 2006; Staubwasser et al., 2006). Other biogeochemical redox processes (e.g. abiotic Fe(II) oxidation; Bullen et al., 2001) and sorption of aqueous Fe(II) on Fe(III)-hydroxides (Balci et al., 2006) exert a fractionation of Fe isotopes as well. As a consequence the δ^{56}Fe signatures of pore water range between +0.5‰ and -4.0‰ (e.g. Bergquist and Boyle, 2006; Severmann et al., 2006; Homoky et al., 2009; Severmann et al., 2010). The isotopic signatures of sediment Fe and pore water Fe are expected to differ, since light isotopes are preferentially subject to dissolution. Therefore, heavier Fe isotopes become enriched in the residual sediment fraction. Contrary, freshly derived lithogenic material is relatively unfractionated and shows δ^{56}Fe values of ~0‰ (Beard et al., 2003a,b).

Hence, the comparison of isotopic Fe signatures among environmental Fe sources, in particular sediment and pore water, and bivalve hemolymph may provide evidence of the predominating Fe source for *L. elliptica* in Potter Cove.

Here, for the first time, δ^{56}Fe of the hemolymph of the Antarctic clam *L. elliptica* are reported and discussed based on known Fe fractionation patterns in subsurface sediments.

4.2 Material and methods

Individuals of the Antarctic soft shell clam *Laternula elliptica* and sediment cores for pore water extraction were collected at two stations in Potter Cove on King George Island (Fig. 4.1) between February and March 2012. Potter Cove is covered by the UTM grid zone Z21E (WGS84) and STA04 is located at 0414281 E and 3098994 N (water depth: 12 m) and STA11 at 0414715 E and 3099516 N (water depth: 9 m). The bivalves as well as the core at site STA11 were taken by scuba divers, whereas the sediment core at site STA04 was gained using an UWITEC coring device.
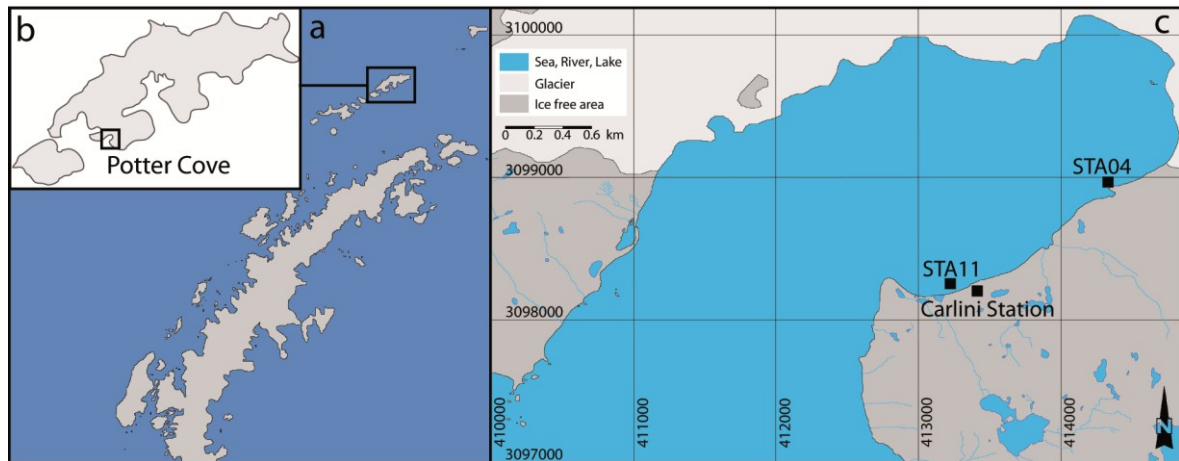
Figure 4.1: a) Map of the Antarctic Peninsula (King George Island highlighted); b) Map of King George Island; c) Map of Potter Cove including the sampling stations (UTM grid: zone Z21E; WGS84).

Pore water was extracted immediately after retrieving the cores using rhizons with a mean pore size of 0.15 µm (Seeberg-Elverfeldt et al., 2005; Dickens et al., 2007). Aliquots of pore water were taken for SO_4^{2-} and dissolved iron (Fe^{2+}) analyses. For photometrical analysis of Fe^{2+}, 1 mL sample aliquots were transferred into cuvettes pre-filled with a 50 µl Ferrospectral solution. At high Fe^{2+} concentrations (> 1 mg L^{-1}), sample aliquots were preserved with 10 µL of 1% ascorbic acid and subsequently diluted with oxygen-free artificial seawater. Analyses of Fe^{2+} were performed using a CECIL CE2021 photometer at wavelengths of 565 nm. Sulfate measurements were performed onshore by suppressed ion chromatography at a 1:50 dilution with 18MΩ-water on a Metrohm IC Net 2.3. Seawater provided by the International Association for the Physical Sciences of the Oceans (IAPSO) was used in each run either for preparation of the calibration standards or as a quality control.

Hemolymph (fluid and hemocyte cells) was taken of the posterior adductor muscle by using a G26x1 needle (Sterican®, B. Braun Melsungen AG, Germany) and a 1 mL syringe (Omnifix®, B. Braun Melsungen AG, Germany) within 12 hours after collecting. Samples were acidified with 100 µL nitric acid (65%, Suprapur®, Merck, Germany) per 1.5 mL sample and stored or transported at 4°C.

Prior to hydrolysis all beakers (PTFE, PFA) were cleaned with acetone, 3 M HCl (p.a. grade) at 120°C (> 6 h), 7.5 M HNO_3 (p.a. grade) at 120°C (> 6 h), and deionized water at 100°C (> 6 h). All other vials and tubes (PP, PE) were cleaned with 3% alkaline detergent (24h) and 3 M HCl (3 days; p.a. grade) at room temperature. Additionally, PP vials were left in 7.5 M HNO_3 (p.a. grade) for less than 6h. After the cleaning procedure beakers and vials were rinsed with deionized water first and finally with 18.2 MΩ-water.

Hemolymph (1 – 1.5 mL) was transferred to PTFE beakers and sample vials were rinsed with 1 M bidistilled HNO_3 to ensure the complete transfer of the sample. First, 5 mL of HNO_3 (65%, subboiled) and 1 mL of H_2O_2 (30%, Suprapur®, Merck, Germany) were added. Samples were kept at room temperature for 4 h to avoid strong out gassing. Vessels were heated under recirculation for 1 h at 60°C, 1 h at 120°C, and 8 h at 160°C and thereafter evaporated at 160°C. After cooling, the residuals were dissolved in 5 mL 6 M HCl, evaporated at 90°C, and again dissolved in 6 M hydrochloric acid.

Subsequently Fe was enriched by anion-exchange chromatography after Schoenberg and von Blanckenburg (2005) using BioRad AG® 1-X8, 100-200 mesh resin in a 7.5 mL Spectrum® PP column.

The Fe-containing fraction was evaporated at 90°C and subsequently redissolved in 1 mL 0.3M HNO_3 (dest.). Sample splits of 100 µL were diluted to a final volume of 5 mL with 0.3M HNO_3 (dest.) in order to determine Fe concentrations using Inductively Coupled Plasma - Optical Emission Spectroscopy (ICP-OES; Spectro Arcos, SPECTRO Analytical Instruments GmbH). Afterwards, the original purified Fe samples were diluted to a final concentration of 1 mg L^{-1} Fe for final Fe isotope analyses by Multiple Collector - ICP - Mass Spectrometry (MC-ICP-MS, ThermoFinnigan Neptune). Iron isotope ratios were measured following the protocol of Schoenberg and von Blanckenburg (2005) using the sample standard bracketing method (e.g. Belshaw et al., 2000; Weyer and Schwieters, 2003). All δ^{56}Fe [‰] data are relative to the IRMM-14 standard reference material. JM standard reference material (inhouse-standard) was measured (N=8) in between the samples to verify the analytical method and revealed a precision of 4.1% and an accuracy of +2.4% (average δ^{56}Fe of 0.43 ± 0.02‰, given value: 0.42 ± 0.05‰).

The elution of Fe and Zn overlaps chromatography and Zn is not completely removed during anion-exchange chromatography (Schoenberg and von Blanckenburg, 2005). However, matrix effects during MC-ICP-MS analyses due to high concentrations of Zn in the hemolymph samples (compare Poigner, 2012) could be excluded by measuring Fe standard solutions (Certipur®, Merck, stock solution 1000 ppm) spiked with different Zn concentrations. The results for δ^{56}Fe between Zn-spiked standards (1 and 2 mg L^{-1} Zn) did not differ significantly (p-value: 0.153). Iron isotope data of measured hemolymph samples, JM standard reference material, and Zn-spiked Fe standard solution are plotted as δ^{57}Fe versus δ^{56}Fe in figure 4.2 to check the instrumental mass discrimination (White et al., 2000; Schoenberg and von Blanckenburg, 2005). The least-square regression through all samples features a slope of 1.49 ± 0.01 (adj. R^2=0.997) similar to the theoretical mass dependent fractionation line (δ^{57}Fe ≈ 1.5 × δ^{56}Fe).
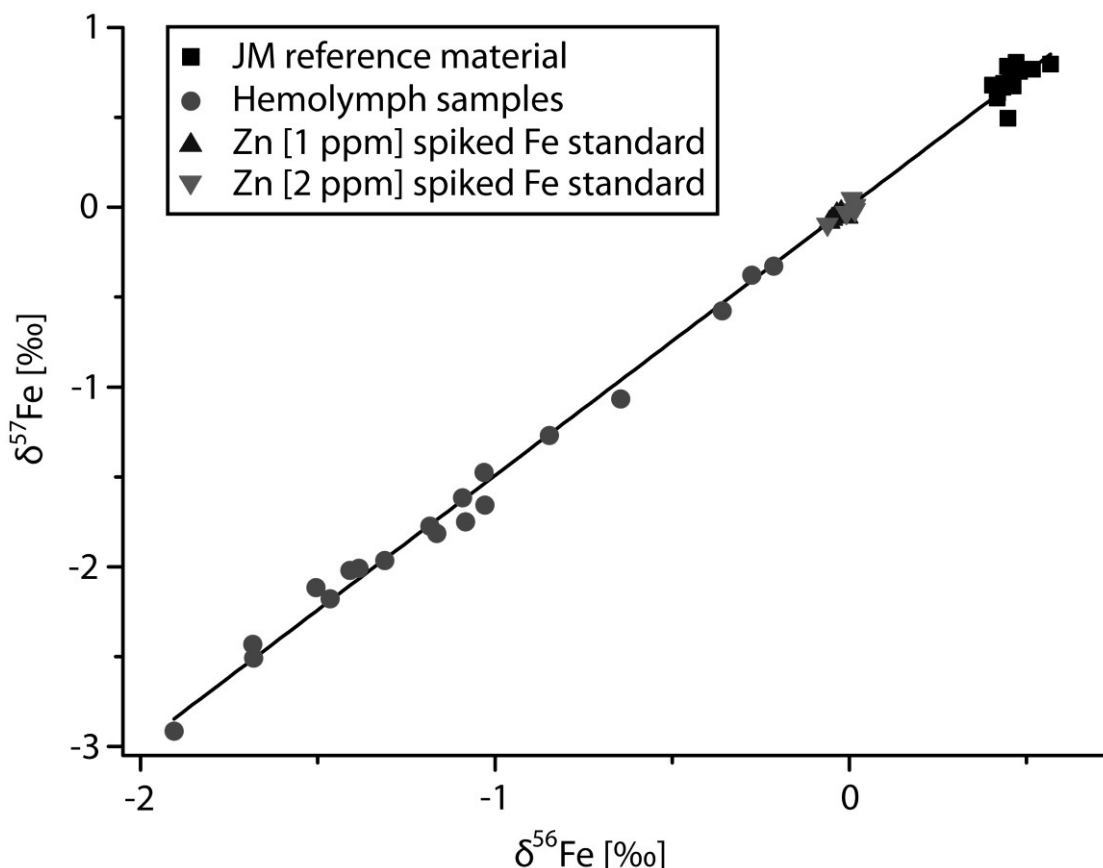
Figure 4.2: Fe isotope data as δ^{57}Fe versus δ^{56}Fe of hemolymph samples of *L. elliptica* (solid circles), JM reference material (solid squares), and Zn-spiked Fe-standards (solid triangles). The regression line was determined by the least square method.

Descriptive statistics were computed by Origin 8.5.1 (OriginLab Corporation, USA). Differences in means were tested on significance between stations by the Welch-test and the two sample t-test (using R 2.12.1; R Development Core Team, 2010). Normal distribution and homogeneity of variances were tested by the Shapiro-Wilk-test and Bartlett's test. An alpha level of 5 % was chosen as statistically significant.

4.3 Results

At station STA04 hemolymph Fe concentrations (32 - 131 µmol L^{-1} Fe) were within the range of pore water Fe concentrations of the first 5 cm below seafloor (5 – 120 µmol L^{-1} Fe; Fig. 4.3). Station STA11 showed Fe pore water concentrations between 10 and 45 µmol L^{-1} Fe within the first 5 cm of sediment depth (Fig. 4.3), and Fe concentrations in hemolymph ranged between 28 to 186 µmol L^{-1}. Mean (±95% confidence interval) Fe concentrations in hemolymph reached 72 ± 20 µmol L^{-1} (STA04, N=10) and 89 ± 46 µmol L^{-1} (STA11, N=9) and did not differ significantly (p-value = 0.462).

In bivalve hemolymph the δ^{56}Fe values ranged between -0.27‰ and -1.68‰ at STA11 and between -0.21‰ and -1.91‰ at STA04. Means did not deviate significantly (p-value = 0.508) between both stations (STA04: -1.19 ± 0.34‰, STA11: -1.04 ± 0.39‰). Further, at both stations the SO_4^{2-} concentrations decreased only slowly from the sediment-water interface downwards and remaind in sediment depths greater than 10 cm relatively high (Fig. 4.3).
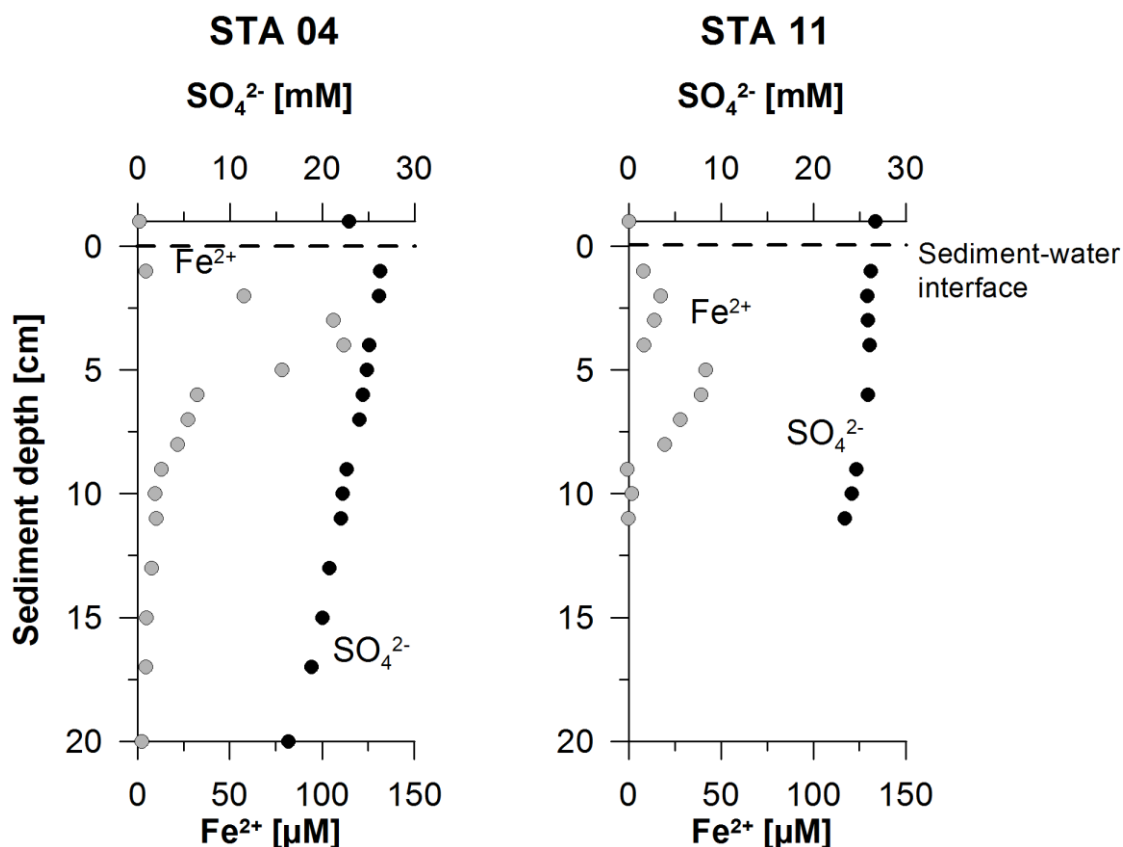
Figure 4.3: Pore water profiles of Fe^{2+} and SO_4^{2-} of STA04 and STA11.

4.4 Discussion

Stable Fe isotope signatures (δ^{56}Fe) of bivalve hemolymph are within the range of reported δ^{56}Fe values of pore waters (+0.5‰ - -4.0‰; Bergquist and Boyle, 2006; Severmann et al., 2006; Homoky et al., 2009; Severmann et al., 2010) and do not differ between the two stations. Poigner et al. (under review) suggested that the main Fe source for *L. elliptica* is pore water, which is supported by the comparatively low δ^{56}Fe values measured in bivalve hemolymph within this study. In this case, hemolymph is likely affected by the range of δ^{56}Fe in the pore water within the uppermost 5 cm of the sediment, the sediment environment close to the siphon. Other possible explanations for the heterogeneous δ^{56}Fe hemolymph values are (i) inter-individual differences in Fe

assimilation from sources with different δ^{56}Fe signatures resulting in a mixed δ^{56}Fe hemolymph signature and (ii) fractionation of Fe isotopes related to transport and storage processes within the bivalve. These two options are discussed in the following.

(i) As benthic deposit feeder *L. elliptica* ingests organic and sediment particles. The gut content can vary widely among sites and season (Norkko et al., 2007). In Potter Cove mainly lithogenic particles and fine detritus (organic and inorganic – visually indistinguishable) dominated within the gut and digestive gland of *L. elliptica* (compare chapter 2). Diatoms (mainly benthic forms) and other organic particles occurred to a lesser extent. These particulate Fe sources as well as inhaled dissolved Fe sources (pore water, bottom water) differ in abundance, Fe concentration, bioavailability, and especially Fe isotope signature and so might the δ^{56}Fe signature of ingested phytoplankton and sediment or inhaled water mix:

The Fe isotope composition of lithogenic particles transported into the ocean remains relatively unfractionated (Beard et al., 2003a,b; Beard and Johnson, 2004) and oxic shelf sediments show average crustal δ^{56}Fe signature (~0.1‰; Severmann et al., 2008; Fehr et al., 2010). During diagenesis the δ^{56}Fe signature of sediment can be altered to 0.5 to 3‰ through microbiological and abiotic processes (Beard et al., 1999; Brantley et al., 2004; Icopini et al., 2004; Johnson et al., 2005; Walczyk and von Blanckenburg, 2005 and references therein; Crosby et al., 2007). Microbes preferentially reduce iron particles containing light Fe isotopes and therefore the residual sediment becomes relatively enriched in heavy isotopes (Staubwasser et al., 2006). Consequently, the δ^{56}Fe signatures in both, the residual sediment and the pore water are affected by the redox zonation and vary with sediment depth (Severmann et al., 2006; Staubwasser et al., 2006). Depending on the depth and the extend of the redox boundary (i.e. the ferruginous zone) dissolved Fe diffuses out of the sediment, escapes with the pore water into the water column due to bioirrigation/bioturbation, or precipitates (preferentially light Fe isotopes) as iron-oxyhydroxides (Severmann et al., 2006; Staubwasser et al., 2006; Severmann et al., 2010). In consequence the amount of precipitated, light Fe isotopes determines the δ^{56}Fe value of benthic Fe flux, which can be enriched in light isotopes (-1.6‰ to -3.8‰; Severmann et al., 2006; Severmann et al., 2010). This sensitivity to a variety of environmental processes is responsible for the aforementioned range of δ^{56}Fe values in pore waters and a trend towards lighter isotopes closer to the sediment surface (Staubwasser et al., 2006).

This trend can also be expected for the two stations in Potter Cove, since high dissolved Fe and SO_4^{2-} concentrations in the pore water indicate that sulfide formation may occur in

sediment depths deeper than 10 cm and, therefore, does not affect the pore water δ^{56}Fe signature close to the siphon. The presence of high SO_4^{2-} concentrations down to 20 cm depth shows that the investigated individuals of *L. elliptica* were sited above the sulphidic zone. Further, the pore water profiles of both stations, STA04 and STA11, in Potter Cove reveal an increase in dissolved Fe concentrations at 1 to 2.5 cm below the seafloor. This implies that only a thin oxic layer separates the ferruginous zone from the benthic boundary, which eases diffusion into the bottom water. The close distance to the siphon of the bivalve supports the inhalation of diffusively transported Fe and Fe rich pore water released through bioturbation.

Stable Fe isotope signatures of potential organic food sources (e.g. diatoms, macro algae, detritus) for bivalves are lacking for Antarctica. As an example, marine plankton from the Amazon shelf shows δ^{56}Fe values between -0.05 and -0.39‰ (mean: -0.24‰; Bergquist and Boyle, 2006).

In consequence, the wide spectrum of ingested (organic and lithogenic) particles (compare Ahn, 1993; Norkko et al., 2007) and inhaled water result in a "mixed" δ^{56}Fe fingerprint.

(ii) Light isotopes are preferentially assimilated from dietary sources (e.g. humans: Walczyk and von Blanckenburg, 2002; Walczyk and von Blanckenburg, 2005; mammals: Hotz et al., 2011; plants: Guelke and von Blanckenburg, 2007; Kiczka et al., 2010) and lighter Fe isotopes become enriched with increasing trophic levels (Zhu et al., 2002). Thus, humans show the lightest Fe isotope signature among all investigated organisms (δ^{56}Fe values in human blood ranged between -1.6 and -3.0‰; Walczyk and von Blanckenburg, 2002; Hotz et al., 2012). Isotope fractionation during physiological processes related to Fe-assimilation, Fe-transport, and Fe-storage was intensively investigated with reference to humans (e.g. Walczyk and von Blanckenburg, 2002; Krayenbuehl et al., 2005; Walczyk and von Blanckenburg, 2005; Hotz et al., 2012; Hotz and Walczyk, 2013). Therefore we assume, that the hemolymph of *L. elliptica* should show a heavier Fe isotope signature compared to humans.

The Fe isotopic composition of the human blood, however, vary among individuals due to differences in Fe metabolism (Walczyk and von Blanckenburg, 2002; Ohno et al., 2004; Walczyk and von Blanckenburg, 2005; Hotz et al., 2011, 2012). Further, heavier Fe isotope signatures were found in ferritin-rich human organs (Walczyk and von Blanckenburg, 2002, 2005; Hotz et al., 2011, 2012), whereas red blood cells* are enriched in lighter isotopes (Hotz et al., 2011). The authors, therefore, suggested a strong effect of the Fe storage protein ferritin on Fe isotope fractionation, which also affects the isotopic

signature of blood Fe (Hotz et al., 2012). Moreover, humans need months or years to restore the original isotopic composition of their blood, due to low Fe turnover (Hotz et al., 2012).

In *L. elliptica* several tissues (digestive gland, gill, foot) and also hemocyte cells express the Fe storage protein ferritin in large quantities (Husmann, 2013). On average 30% of total Fe within the hemolymph* are bound in hemocyte cells (Poigner et al., under review) and digestive gland and gills show higher Fe concentrations (Husmann et al., 2012; Poigner, 2012) compared to tissues of lower ferritin expression (e.g. siphon, mantle; liver was not investigated; Husmann et al., 2012; Poigner, 2012; Husmann, 2013). Thus, a physiological influence on the δ^{56}Fe hemolymph signature appears to be likely. On the other hand, the Fe turnover is much faster in *L. elliptica*, since Poigner et al. (under review) found a drop of Fe concentrations in the hemolymph of ~50% within 15 days as soon as an environmental Fe source was lacking. If hemolymphmatic Fe exhibits very high turnover rates and "new" Fe is subsequently assimilated from the environment, the accelerated Fe flow would probably reduce the sensitivity of the hemolymph Fe signature to mass dependent fractionation related to the transfer of Fe into tissues and cells (but not any fractionation during assimilation!).

Another physiological alteration of the isotope signature within a bivalve was observed for Ca in *Mytilus edulis* (Heinemann et al., 2008). Briefly, the extrapallial fluid (compartment of shell formation; $\delta^{44/40}$Ca= -0.01‰) was isotopically heavier than the Ca source, the ambient seawater ($\delta^{44/40}$Ca= -0.32‰), due to a favored incorporation of lighter Ca isotopes into the bivalve carbonate shell ($\delta^{44/40}$Ca= -1.09‰ to -1.33‰). If a similar Fe isotope fractionation during physiological processes (assimilation, transport, storage) is present within the bivalve, the δ^{56}Fe signature of the environmental Fe source would be altered.

* The white-transparent hemolymph of the bivalve *L. elliptica* is free of hemoglobin.

4.5 Conclusions and outlook

In our study we showed that the δ^{56}Fe signatures (-0.21‰ to -1.91‰) of *L. elliptica* is within the general range of pore water samples (+0.5‰ to -4.0‰). The clam assimilates Fe from several Fe sources with varying δ^{56}Fe values and therefore it is presumable that the hemolymph shows a "mixed" δ^{56}Fe signature, which is isotopically lighter (or at least similar) compared to the predominating Fe dietary source (based on the favored assimilation of lighter Fe isotopes along the food chain). As a next step, the δ^{56}Fe hemolymph data will be compared to Fe isotope data of pore water of the investigated stations to achieve further evidence for the origin of high Fe concentrations in *L. elliptica* and the usability of stable Fe isotopes as tracers for bioavailable Fe sources.

5 Coexistence of three calcium carbonate polymorphs in the shell of the Antarctic clam *Laternula elliptica*

Gernot Nehrke[1], Harald Poigner[1], Dorothee Wilhelms-Dick[2], Thomas Brey[1], and Doris Abele[1]

[1]Alfred Wegener Institute Helmholt Centre for Polar and Marine Research, Am Handelshafen 12, 27570, Bremerhaven, Germany

[2] Geoscience Department, University of Bremen, Klagenfurter Str., 28359, Bremen, Germany

Abstract

We analyzed shell cuts of five individuals of the Antarctic bivalve *Laternula elliptica* from three locations along the Antarctic Peninsula by means of Confocal Raman Microscopy (CRM) as well as Electron Microprobe (EMP). The shell of *L. elliptica* has been previously described as being composed of aragonite exclusively. Now, CRM mapping reveals that three polymorphs of calcium carbonate – aragonite, calcite, and vaterite – are present in the chondrophore region of the examined individuals. Annual shell growth layers continue through aragonite and vaterite, suggesting simultaneous mineralization of both polymorphs. Spatially congruent EMP scans showed that the calcium carbonate polymorph affects the distribution of magnesium and strontium within the chondrophore. This is, to our knowledge, the first report of the coexistence of these three calcium carbonate polymorphs within the mineralized structures of a marine calcifying organism. Particularly the presence of vaterite is unexpected, but shows striking similarities to some fish otoliths. The strong effect of the calcium carbonate polymorph on trace element incorporation restricts the suitability of magnesium and strontium based proxies for the chondrophore area of *L. elliptica*.

5.1 Introduction

Many organisms produce mineralized calcium carbonate ($CaCO_3$) structures, ranging from small platelets formed by coccolithophorides to the shells of mollusks and skeletons of reef forming corals.

Calcite and aragonite represent the main mineral phases among these marine biogenic $CaCO_3$ (Lowenstam and Weiner, 1989; Watabe, 1974). Only in a few cases the polymorphs vaterite and amorphous calcium carbonate (ACC) have been found (e.g. Beniash et al., 1997; Lowenstam and Abbott, 1975; Watabe, 1974). Moreover, most marine biogenic $CaCO_3$ structures consist of just one mineral polymorph, albeit some marine organisms produce aragonite and calcite [see, e.g. Carter, 1980].

During the last decades interest in understanding biomineralization processes leading to the formation of biogenic structures of $CaCO_3$ is growing for several reasons: (i) The extent to which elements like e.g. magnesium (Mg) or strontium (Sr) substitute Ca in biogenic $CaCO_3$ depends on their concentration in the surrounding water and is species dependent. However, the incorporation of some elements also correlates to the environmental conditions, e.g., salinity or temperature (Dissard et al., 2010; Nürnberg et al., 1996), during formation. I.e., such elements can serve as proxies in climate reconstruction. (ii) "Ocean acidification" (OA), i.e., the deceasing ocean pH caused by increasing atmospheric CO_2 concentrations, leads to lower saturation levels with respect to the different $CaCO_3$ phases. Apparently, some marine calcifying organisms may be restricted in their ability to calcify at such lowered saturation levels (e.g. Langer et al., 2009, 2011) which in turn could affect marine ecosystem functioning and the global carbon cycle (Caldeira and Wickett, 2003; Hoegh-Guldberg et al., 2007). (iii) Biogenic carbonates show unique properties that make them interesting for possible industrial applications (e.g. Estroff and Hamilton, 2001).

These investigations demonstrated that biogenic $CaCO_3$ represent complex composites of one or more mineral phases and organic molecules. This complexity is visible at the macroscopic level and manifests down to sub-micrometric structures which are only revealed by micro analytical techniques (e.g. Cuif et al., 2011, 2012). Understanding to what extent and how organisms can control the formation of these structures, the major aim of biomineralization research, requires identifying the mineral and organic phases and their spatial organization. During the last decades, advances in micro-/nano-analytical techniques such as Atomic Force Microscopy (AFM), synchrotron based micro X-Ray Diffraction (XRD) and Confocal Raman Microscopy (CRM) facilitated the analysis of biogenic minerals distinctly (Nehrke and Nouet, 2011).

One interesting finding was that in some cases during the biomineralization process a less stable $CaCO_3$ precursor such as amorphous calcium carbonate (ACC) is precipitated

initially which subsequently (partially) transforms into a more stable polymorph, e.g. into calcite during sea urchin larval spicule growth (Beniash et al., 1997) or into vaterite and aragonite during pearl formation (Soldati et al., 2008). Jacob et al. (2008) state that (page 5401): "Freshwater and marine cultured pearls form via identical processes to the shells of bivalves and can therefore serve as models for biomineralization of bivalve shells in general." Spann and coworkers (Spann et al., 2010) found that vaterite can occur in the usually fully aragonitic shells of the freshwater bivalve *Corbicula fluminea*. Frenzel and Harper (2011) demonstrated that the two polymorphs within *Corbicula fluminea* show distinct differences in the incorporation of elements like e.g. Mg and Sr. This polymorph dependent uptake is well known for $CaCO_3$, but challenges the use of proxies based on different element/Ca ratios like Mg/Ca and Sr/Ca if a biogenic carbonate is comprised of different polymorphs.

In the present study we investigated the shell of the clam *Laternula elliptica*, a prominent Antarctic bivalve that is present in coastal shallow water soft sediments throughout the Southern Ocean (Ahn, 1993; Ahn et al., 2003; Ralph and Maxwell, 1977; Urban and Mercuri, 1998). Owing to its wide distribution, large shell (up to >100 mm length) and an age of ≤ 40 years (Philipp et al., 2005), *L. elliptica* is a potentially valuable bioarchive. The shell shows a distinct pattern of annual growth increments in the chondrophore (Brey et al., 2011), enabling intraannual resolution analysis of morphological, mineralogical and chemical features. Brey et al. (2011) showed that annual shell growth of *L. elliptica* is an indicator of the warming trend at the Antarctic Peninsula over the last 50 years ("Distinct changes in shell growth pattern include a near doubling of specific growth rate, a 25% decrease in maximum size, and a shift in individual energy expenditure from production to respiration." page 542). Previous studies on *L. elliptica* shell biogeochemistry, e.g., oxygen stable isotope ratios $\delta^{18}O$ (Brey and Mackensen, 1997; Tada et al., 2006), trace element concentrations (Dick et al., 2007) and effects of ocean acidification (Cummings et al., 2011) all presumed (explicitly or implicitly) that the shell of *L. elliptica* is completely comprised of aragonite.

In the present study we used CRM mapping to confirm aragonite as exclusive $CaCO_3$ polymorph throughout the shell of *L. elliptica* and Electron Microprobe (EMP) mapping of Mg and Sr to test its usability as proxy archive.

5.2 Materials and methods

5.2.1 Sample preparation

Three *L. elliptica* (Fig. 5.1a) were collected in Potter Cove, King George Island (62° 14' S, 58° 40' W, 10 to 20 m water depth) in January 2010 by scuba diving, and one further specimen each at Collins Harbor, King George Island (62° 11' S, 58° 51' W) in 1993, and at Rothera Station, Adelaide Island (67° 34' S, 68° 08' W) in 2000. One clam sampled in Potter Cove was the major object of our analysis, whereas the other four shells served for confirmation of our findings.

Air-dried shells were cut through the chondrophore (Fig. 5.1b) with a diamond saw (Buehler, Isomet Low Speed Saw). Saw blade and samples were water cooled during cutting. One half of the chondrophore was embedded in resin (Araldite2020®, Huntsman International LLC., USA) and hardened under five bar pressure and 60°C for 16 h. The chondrophore surface of both halves was ground using waterproof silicon carbide paper in the qualities of P1200, P2400, P4000 (Struers, Denmark). Finally, the sample surface was polished (Fig. 5.1c, 5.2a) with a 3 mm diamond suspension (Dia Duo, Struers, Denmark) and with a 0.3 mm Al_2O_3 emulsion (Struers, Denmark) using an automated polishing machine (Logitech PM2A, Logitech, Great Britain).
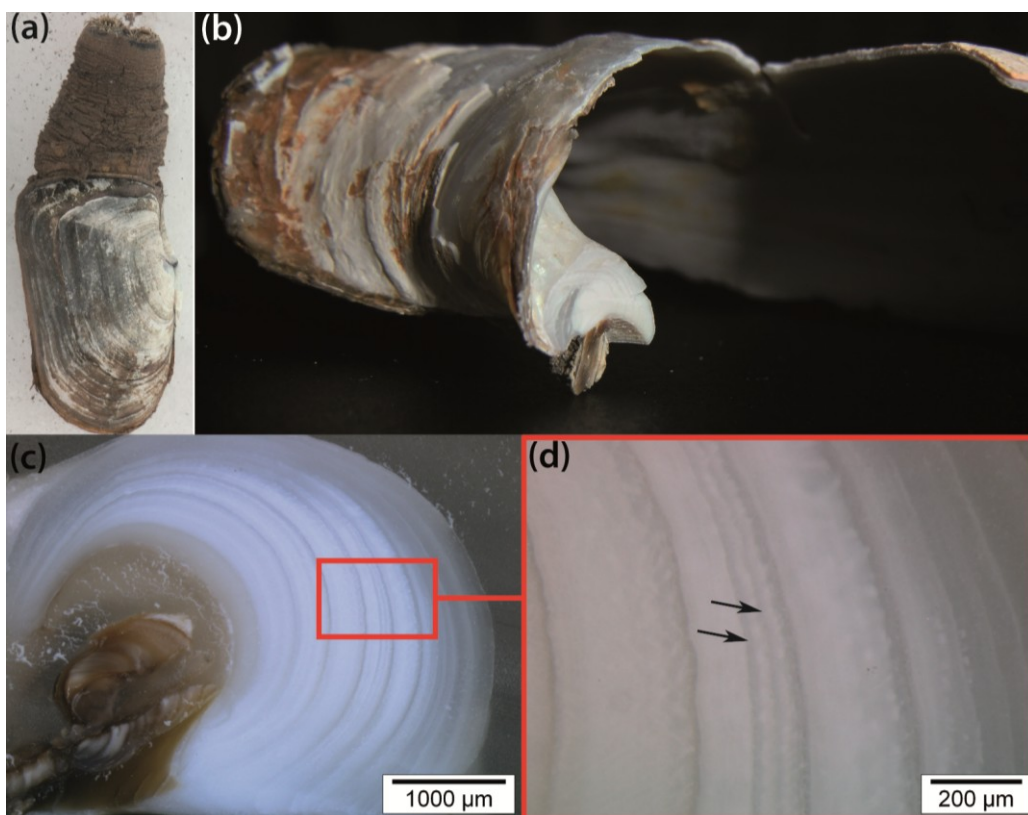
Figure 5.1: a) *Laternula elliptica*; b) cut through the shell and the chondrophore; c) chondrophore including visible seasonal growth layers; d) seasonal growth layers. The annual formation of the growth bands were validated by stable isotope analysis ($\delta^{18}O$ and $\delta^{13}C$) earlier (Brey and Mackensen, 1997). Major dark bands were deposited during winter. However, a secondary pattern can occur too (see black arrows).

59

5.2.2 Micro analysis

Mineralogical phase identification (mapping) was performed on a WITec alpha 300 R (WITec GmbH, Ulm, Germany) confocal Raman microscope (CRM), equipped with a diode laser (excitation wavelength 512 nm) and a 20x objective (Zeiss EC Epiplan, Oberkochen, Germany). Raman signals were detected by a high throughput spectrometer (UHTS300, WITec, Ulm, Germany) including a DV401 CCD detector and a grating of 600 grooves mm^{-1} at 500 nm blaze.

The 6000 x 2000 μm large area scan was performed on a motorized scan table. Spectra were acquired every 10 μm with an integration time of 0.2 s per spectrum. All measurements were conducted at room temperature. WITecProject software (version 2.04, WITec GmbH, Ulm, Germany) was used for spectral analysis and imaging processing. The peak positions given are determined using the "Multipeak Fitting 2" routine of IGOR Pro (version 6.11, WaveMetrics, Inc. USA).

The spatial distributions of Ca, magnesium (Mg) and strontium (Sr) were analyzed by means of Electron Probe Microanalysis (EPM) at the Institute of Geosciences of the Christian Albrechts University Kiel (Germany) using a JXA 8900 R Electron Probe Microanalyzer (JEOL Ltd., Japan). Parameter settings were: 15.0 kV accelerating potential, 50.2 nA probe current, 5 μm probe diameter and a dwell time of 120.0 ms.

5.3 Results and discussion

Confocal Raman microscope analysis identified three different polymorphs of $CaCO_3$ within the chondrophore area of the *L. elliptica* shells, mainly aragonite, but also calcite and vaterite (Fig. 5.2b). The Raman spectra of the different polymorphs (Fig. 5.3) showed the typical vibration modes ν1 (1085 cm^{-1} calcite and aragonite) and ν4 (711 cm^{-1} calcite and 705 cm^{-1} aragonite) for CO_3 in a crystal lattice (Behrens et al., 1995). Further peaks of the lattice modes were located at 155 cm^{-1} (aragonite and calcite), 282 cm^{-1} (calcite), and at   206 cm^{-1} (aragonite). Vaterite was identified by the two doublets of the vibration modes ν1 (1075 cm^{-1}, 1090 cm^{-1}) and ν4 (740 cm^{-1}, 750 cm^{-1}). Raman lattice peaks of all three $CaCO_3$ polymorphs are very specific. Lattice mode frequencies of vaterite showed strong peaks at 105 cm^{-1}, 114 cm^{-1}, 267 cm^{-1}, and 300 cm^{-1}. The spectra were compared to in-house reference material and agree very well with the data reported by Behrens et al. (1995). The reference materials have been natural calcite and aragonite from Spain and vaterite precipitated as described in Nehrke and Van Cappellen (2006) (all verified by XRD analysis).
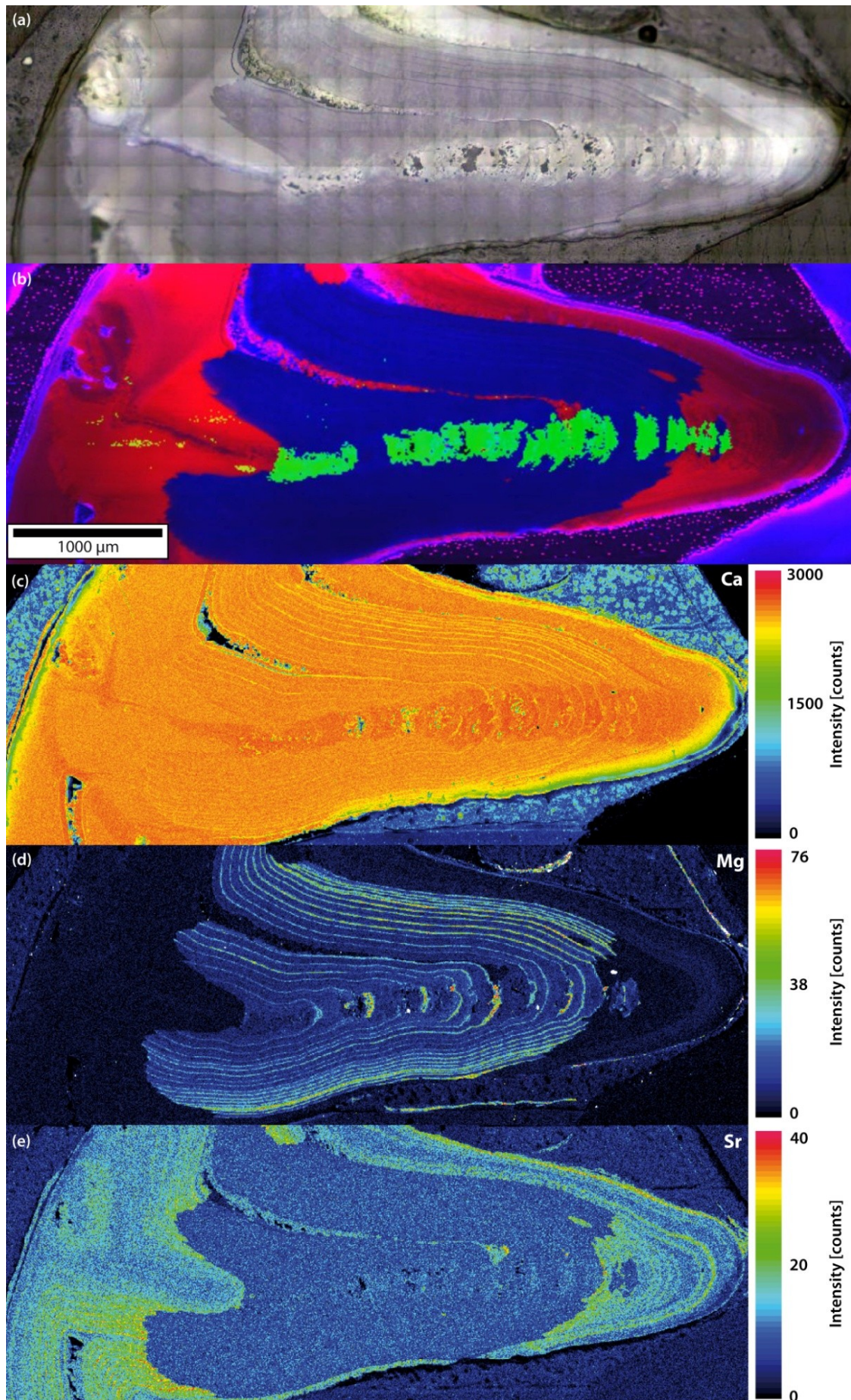
Previous page:

Figure 5.2: a) Reflected light microscopy image of the investigated chondrophore; b) Distribution of aragonite (red), calcite (green), and vaterite (blue) measured by CRM. Element distributions of c) calcium, d) magnesium, and e) strontium within the chondrophore area of *L. elliptica* as measured by EMP.
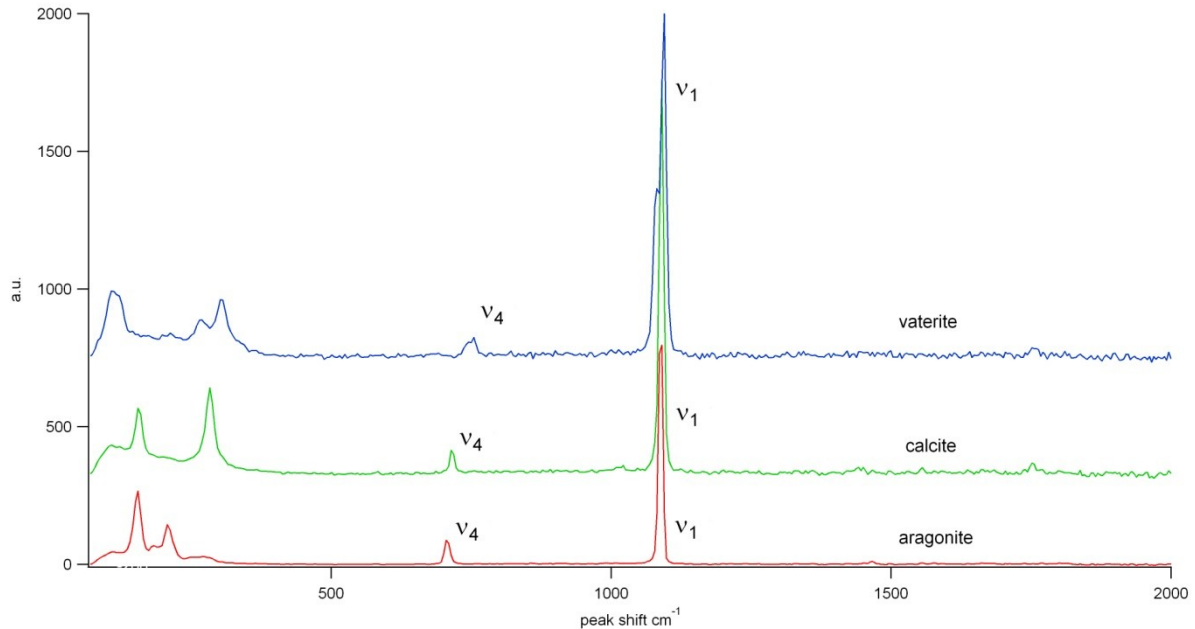
Figure 5.3: Raman spectra of the three $CaCO_3$ polymporphs aragonite, calcite, and vaterite.

Figure 5.2b shows the spatial distribution of the three polymorphs within the chondrophore area. While aragonite (red) is present in the outer areas, vaterite (blue) dominates the inner area of the section plane shown. Calcite (green) is present in the innermost part and is surrounded by vaterite and aragonite. Annual growth layers are clearly visible within the areas comprised of aragonite and vaterite, suggesting simultaneous mineralization of both polymorphs. Raman point measurements on a further chondrophore that was not embedded and polished confirmed the presence of the three polymorphs, i.e. sample preparation did not cause the formation of vaterite and/or calcite.

After CRM analysis, an additional 1 mm of the sample surface was abraded to determine the mineral composition in deeper layers of the chondrophore. The new section plane (data not shown) showed a slightly larger aragonitic area at the expense of the calcite area. Extent and location of vaterite did not change. All five specimens examined contained the three polymorphs in the chondrophore area, albeit with varying spatial pattern and share of each polymorph.

Even though all five examined individuals of *L. elliptica* from two distant sampling sites along the Antarctic Peninsula (Potter Cove, Marian Cove on KGI and at Adelaide Island) show the presence of different $CaCO_3$ polymorphs in the chondrophore area, at present our observation should not be generalized without further testing.

The phenomenon seems, however, to be at least frequent across different *L. elliptica* populations. To evaluate whether or not the presence of different $CaCO_3$ polymorphs affects trace element distribution in the shell, we scanned Ca, Mg and Sr by means of EMP across the same area previously mapped by CRM (Fig. 5.2c – 5.2e). To estimate absolute concentrations in the different polymorphs a set of single point measurements were performed, two single point measurements in the aragonitic area (between seasonal growth layers) and ten measurements in the vateritic area (six measurements between seasonal growth layers and within winter growth bands). As major constituent of $CaCO_3$, Ca shows a nearly homogenous distribution throughout all three polymorphs. Only layers deposited during winter are characterized by a depletion in Ca concentration (Fig. 5.2c). Ca concentrations ranged from 35.0 weight% to 37.3 weight% in winter layers (vaterite: Va_{winter}) and from 37.1 weight% to 42.1 weight% in summer layers (aragonite: Ar_{summer}; vaterite: Va_{summer}). Magnesium concentrations are distinctly higher in the calcite/vaterite area, particularly in the layers deposited during winter (Va_{winter}: 6160 – 11,000 ppm >>> Va_{summer}: 1000 –1630 ppm), while aragonitic structures show Mg concentrations close to the detection limit (Ar_{summer}: 96 – 110 ppm) (Fig. 5.2d). Sr shows just the opposite distribution, it is distinctly enriched in the aragonitic regions (Ar_{summer}: 1840 – 2280 ppm > Va_{summer}: 180 – 650 ppm / Va_{winter}: 340 – 550 ppm), particularly in the winter layers (Fig. 5.2e). The polymorph dependent element incorporation is well known from inorganic data and is related to the difference in cation size and crystal structure (e.g. Finch and Allison, 2007).

Our finding of three $CaCO_3$ polymorphs in the chondrophore area of *L. elliptica* contradicts the present view that the whole shell is aragonitic (e.g. Tada et al., 2006; Cummings et al., 2011). Previous studies, however, may have been hampered by methodical limits. The chondrophore constitutes a relatively small part of the entire shell, and thus vaterite and/or calcite may not be detectable by XRD within a mainly aragonitic sample. Vaterite is quite rare in natural environments due to its relatively low stability under Earth's surface conditions, under which it normally transforms into aragonite or calcite within hours to days (e.g. Nehrke and Van Cappellen, 2006). However, it is well documented that unstable polymorphs of $CaCO_3$ (especially vaterite and ACC) can be present in biogenic $CaCO_3$ (Beniash et al., 1997; Weiss et al., 2002; Wehrmeister et al., 2011). In such complex biogenic composites their transformation is probably inhibited by e.g. divalent

cations and/or organic macromolecules (e.g. Aizenberg et al., 1996; Loste et al., 2003). The possible function of these polymorphs is discussed controversially. Whereas ACC seems to play a crucial role in the initial nucleation within a biological system (Beniash et al., 1997; Weiss et al., 2002), the role of vaterite is less clear. Current hypotheses relate vaterite to repair structures in adult calcifying organisms (e.g. Watabe, 1983; Wilbur and Watabe, 1963) and to secondary shell thickening (e.g. in the freshwater bivalve *Corbicula fluminea* (Spann et al., 2010). Even though *L. elliptica* is strongly affected by iceberg rafting (Philipp et al., 2005; Smale, 2007), which can cause damage to their shells, none of the investigated individuals showed any injury in the chondrophore area and, furthermore, annual growth lines continue through all polymorphs (Fig. 5.4), suggesting simultaneous mineralization. Neither does the vaterite make the shell of the *L. elliptica* thicker; it is just part of the "normal" chondrophore structure.
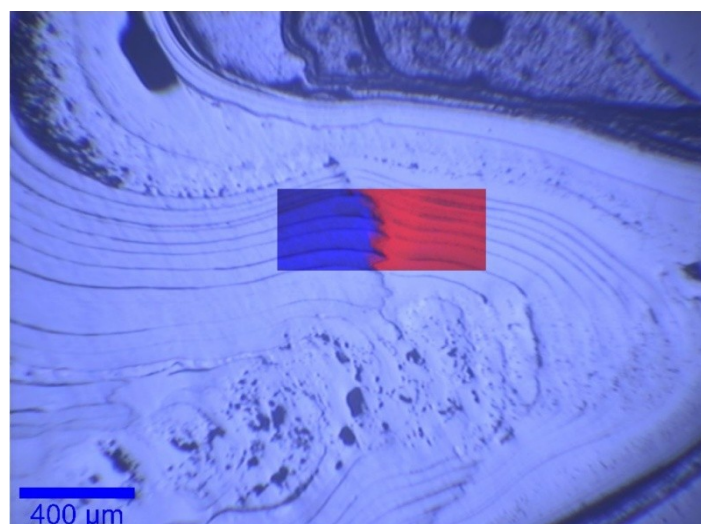
Figure 5.4: Overlay of a Raman mapping on a reflected light microscopy image (obtained on the same sample shown in figure 5.2a but in a deeper horizon after repolished following the EMP measurements), showing the growth lines continuing through the vaterite (blue) and aragonite (red) polymorph.

However, the polymorph composition of the chondrophore area of *L. elliptica* is strikingly similar to the aragonite-vaterite patterns in the otoliths of some fish species, e.g. *Oncorhynchus tshawytscha* (Chinook salmon; Gauldie, 1996) and *Salvelinus namaycush* (lake trout; Melancon et al., 2005). As in the chondrophore of *L. elliptica*, distribution and amount of vaterite varied considerably between otoliths (Melancon et al., 2005). And, as in the chondrophore of *L. elliptica* (Fig. 5.4), different polymorphs are present across annual growth bands, which is indicative of simultaneous precipitation. Furthermore, in both shell chondrophore and otoliths Mg is enriched in the vateritic (and if present calcitic) and Sr in the aragonitic areas. The polymorph dependent incorporation of Mg and Sr observed here (Fig. 5.2) and in otoliths (Melancon et al., 2005) gives further support for simultaneous

polymorph precipitation from the same fluid, e.g. the endolymph or hemolymph (please note that it is still controversially discussed from which fluid exactly the ions are transported to the site of calcification).

5.4 Conclusions

We demonstrated that the shell of the investigated specimens of *L. elliptica* is not, as previously stated, completely comprised of aragonite, but is composed of the three polymorphs aragonite, calcite and vaterite, at least in the chondrophore area. The extent to which these polymorphs are present varies between specimens. To our knowledge this is the first observation of the coexistence of these three polymorphs in a marine biogenic carbonate. The polymorph specific incorporation of elements like Sr and Mg complicates the use these elements as proxy signals. The striking similarity of the *L. elliptica* chondrophore morphology and biogeochemistry to otoliths that show co-precipitation of vaterite and aragonite requires reconsidering the current view of vaterite resulting from irregular, incomplete or failed carbonate formation. It is difficult to imagine that a complex process like biogenic calcification that developed over millions of years will be so error prone, i.e., exhibiting the same malfunction in the growth of fish otoliths and bivalve shells. However, this study emphasizes the need for high resolution analytical techniques like CRM to determine the phase composition in biogenic structures prior to reconstruct paleo-environmental conditions from chemical signals. Further work is necessary to identify the reason for the coexistence of different polymorphs of $CaCO_3$ in some biogenic structures.

6 Trace metal incorporation into the chondrophore
of *Laternula elliptica*: Indicator of change in nearshore biogeochemistry?

Harald Poigner[1], Andreas Klügel[2], Gernot Nehrke[1], Doris Abele[1], and Dorothee Wilhelms-Dick[1]

[1]Alfred Wegener Institute Helmholtz Centre for Polar and Marine Research, 27570 Bremerhaven, Germany
[2]University of Bremen, Geoscience Department, 28359 Bremen, Germany

Article in preparation for submission.

Abstract

Element contents of B, Ba, Fe, Mg, Mn, and Sr (already discussed as environmental proxies) were analyzed along continuous transects across annual growth layers of five aragonitic shells (chondrophore) of the Antarctic clam *Laternula elliptica* by laser ablation – inductively coupled plasma – mass spectrometry (LA-ICP-MS). Element variations show a pronounced seasonality with distinct winter peaks for B, Mg, Sr, and organic matter and minima for Ba. These variations probably result from sequential carbonate dissolution due to low metabolic rates and growth rates of the animals during the winter months. Increment width of the summer growth layers, which serve as approximation for average growth rate during summer, shows significant positive correlations with Ba and Sr, negative with B, and no correlations with Mg. Iron and Mn contents dropped during the first years of bivalve lifetime to values below the limits of quantification. Element patterns differed among the five individuals and can, consequently, not be attributed to environmental changes in temperature, salinity, sediment load, or food availability. These results indicate a strong physiological influence on trace metal incorporation through metabolic activity and/or growth rate in *L. elliptica*, which hampers the suitability of B, Ba, Fe, Mg, Mn, and Sr as environmental proxies for the effects in coastal waters by glacial melting.

6.1 Introduction

During the last decades the western Antarctic Peninsula (WAP) experienced a strong rise in air temperature causing substantial retreat of glaciers and loss of land ice masses (Rignot and Thomas, 2002; Vaughan et al., 2003; Braun and Hock 2004; Cook et al., 2005; Turner et al., 2005; Vaughan, 2006; Steig et al., 2009; Rueckamp et al., 2011). As a result increasing amounts of melt water and lithogenic material are released into coastal waters (Dierssen et al., 2002; Vaughan, 2006; Domínguez and Eraso, 2007). Potter Cove (King George Island, KGI) is a showcase for climate change effects in the WAP region. Rising sea surface temperatures and intensified input of freshwater affect the physical environment (e.g. sea ice duration, ice scouring, salinity, stratification, turbidity) of benthic and pelagic communities (e.g. Dierssen et al., 2002; Schloss et al., 2002; Schloss and Ferreyra, 2002; Zacher et al., 2009; Philipp et al., 2011; Piquet et al., 2011; Harper et al., 2012; Schloss et al., 2012, Bers et al., 2013; Quartino et al., 2013). Schloss et al. (2012) reported a decrease in phytoplankton biomass and/or a change in species composition (measured as chlorophyll *a*), which affect the whole food web of the Cove. In the adjacent Maxwell Bay (KGI) sediment accumulation rates have tripled during the past century, with the highest increase during the decade 1990-2000 (Monien et al., 2011). Higher amounts of inorganic suspended particulate matter in the water column also attenuate light for phytoplankton photosynthesis (Schloss et al., 2002). Lower phytoplankton biomass, which is further strongly diluted by lithogenic particles, affect the physiology and ecology of benthic filter feeders like the Antarctic soft shell clam *Laternula elliptica (King and Broderip 1832)* (e.g. Brey et al., 2011; Philipp et al., 2011; Husmann et al., 2012).

Bivalve carbonate shells are regarded as environmental archives as the incorporated trace elements (e.g. B, Ba, Fe, Mn, Mg, Sr) can be analyzed in subsequent growth layers as proxies for environmental changes. Several studies reported positive correlations between water temperature and the incorporation of Mg and Sr into shells of different species (Klein et al., 1996a; Lazareth et al., 2003; Immenhauser et al., 2005; Wanamaker et al., 2008), whereas other authors could not find an unambiguous relationship (Klein et al., 1996b; Gillikin et al., 2005; Freitas et al., 2006; Heinemann et al., 2008; Heinemann et al., 2011; Schoene et al., 2011). Distinct Ba/Ca peaks in carbonate shells were proposed as markers for phytoplankton blooms (Stecher et al., 1996; Vander Putten et al., 2000; Lazareth et al., 2003; Barats et al., 2007; Gillikin et al., 2008 and references therein; Thebault et al., 2009), whereas Ba/Ca background levels should reflect dissolved Ba concentrations of the water column (Gillikin et al., 2008; Barats et al., 2009). Several authors also proposed enhanced Mn incorporation as marker for phytoplankton blooms (Vander Putten et al., 2000; Lazareth et al., 2003; Langlet et al., 2007), whereas other authors attributed higher Mn levels in the shell matrix to a higher dissolved Mn content in

the water or to a stronger Mn release from sediments (Freitas et al., 2006; Barats et al., 2008). Earlier ecological studies related Mn and Fe contents in shells and tissues of *L. elliptica* to uptake of lithogenic particles within the glacial runoff zone (Ahn et al., 1996; Abele et al., 2008). The incorporation of B into marine carbonates and its δ^{11}B are strongly controlled by pH (e.g. Hemming and Hanson, 1992; Sanyal et al., 2000; Yu et al., 2007; Foster, 2008; Rollion-Bard and Erez, 2010; McCoy et al., 2011). As bivalves actively change the pH of the extrapallial fluid (EPF; compartment of shell formation; Crenshaw and Neff, 1969; Crenshaw, 1972), the B/Ca ratio and δ^{11}B are probably of restricted significance as proxies for environmental pH.

At present there is no consensus in the literature with respect to either the significance of environmental forcing on trace element incorporation into bivalve shells or their validity as environmental proxies, which appears to be dependent on physiology and consequently species specific. Carre et al. (2006) found only little environmental influence on the incorporation of Ba, Mg, Mn, and Sr into the aragonitic shells of the clams *Mesodesma donacium* and *Chione subrugosa*. Other authors found a biological control (e.g. vital effects, metabolic activity of the mantle, biological regulation of the crystal growth rate) on metal incorporation (e.g. Klein et al., 1996b; Gillikin et al., 2005; Heinemann et al., 2008; Takesue et al., 2008; Heinemann et al., 2011; Schoene et al., 2011), which may explain the high variability among species, but also between sampling locations. Dick et al. (2007) reported an influence of lifetime respiration mass on the incorporation of Al, Cu, Fe, Mn, Pb, and U into the chondrophore of the Antarctic soft shell clam *L. elliptica*. Further, the incorporation of Mg, Sr, and other trace elements also depends on the calcium carbonate polymorph. This is important since aragonite, calcite, and vaterite were found to compose the chondrophore of *L. elliptica* (Nehrke et al., 2012).

The condrophore of *L. elliptica* consists of seasonal layers. Brey and Mackensen (1997) validated an annual formation of the growth bands by stable isotope analysis (δ^{18}O and δ^{13}C) and found light-colored growth bands formed during summer and dark growth bands formed during winter. The shell of *L. elliptica* would only provide a time-resolved climate archive, if a clear relation between environmental change and incorporation of trace metals into the growth bands can be confirmed. Individuals of *L. elliptica* reach a maximum lifetime of ≥ 36 years (Philipp et al., 2005), but the thickness of growth bands decreases with age from ~1000 µm to smaller 50 µm (Poigner, unpublished data). Sampling these narrow growth bands is challenging and requires a method enabling high spatial resolution sampling. This is met by laser ablation - inductively coupled plasma - mass spectrometer (LA-ICP-MS) and was already used in several studies (e.g. Stecher et al., 1996; Vander Putten et al., 2000; Gillikin et al., 2005; Carre et al., 2006; Dick et al.,

2007; Jacob et al., 2008; Soldati et al., 2009; Heinemann et al., 2011). Dick et al. (2007) measured contents of Al, Fe, Mn, Cu, Pb, and U in the chondrophore of *L. elliptica* by means of LA-ICP-Quadrupole-MS (LA-ICP-Q-MS). While the wavelength of the applied system was 1064 nm, which is weakly absorbed by carbonate and many other solid materials (Durrant, 1999; Jackson, 2001), the usage of a shorter wavelength increases the ablation efficiency of solid samples (Jeffries et al., 1995; Shuttleworth, 1996) as bivalve shells. Dick et al. (2007) performed single spot ablation analysis with a spot size of about 200 µm, to ablate a sufficient amount of material to exceed the limits of detection/quantification. This provided an annual resolution for the growth bands of the first twelve years of bivalve lifetime. After this age, the annual growth layers become smaller than the ablation crater and up to four growth bands were averaged.

In the present study, we compare B, Ba, Fe, Mn, Mg, and Sr content profiles obtained by LA-ICP-Sector Field-MS (LA-ICP-SF-MS) in the chondrophores of five *L. elliptica* individuals from one location in Potter Cove. The advantage of LA-ICP-SF-MS is its higher sensitivity compared to LA-ICP-Q-MS. We worked with a wavelength of 193 nm yielding higher ablation efficiency and a smaller crater size compared to the 1064 nm wavelength used by Dick et al. (2007). This setup is suitable to ablate transects along the chondrophore and analyze isotopes in high spatial, and therefore temporal resolution. Our aims were to understand (i) if the element incorporation into the carbonate matrix shows seasonal patterns, (ii) if single element patterns can be related to environmental signals, and (iii) if five individuals from the same locations display consistent elemental patterns.

6.2 Material and methods

6.2.1 Bivalve shell sampling

Five individuals of *L. elliptica* were collected in Potter Cove, King George Island (62°14' S, 58° 40' W) in January 2010 by scuba diving at station B21 (5 m water depth; Fig. 6.1). This station is located in the discharge area of melt water streams, characterized by high contents of terrigenous material in the water column (Schloss et al., 2002).

Air dried shells were cut through the chondrophore (Figure 6.2a) with a diamond saw (Buehler, Isomet Low Speed Saw). Saw blade and samples were water cooled during cutting. The chondrophore surface of both halves was grinded using waterproof silicon carbide paper in the qualities of P1200, P2400, P4000 (Struers, Denmark). Finally, the sample surface was polished with a 3 µm diamond suspension (Dia Duo, Struers, Denmark) and with a 0.3 µm Al_2O_3 emulsion (Struers, Denmark) using an automated polishing machine (Logitech PM2A, Logitech, Great Britain). As different polymorphs in the chondrophore of *L. elliptica* affect the incorporation of Mg and Sr (Nehrke et al., 2012),

chondrophore surfaces were primarily scanned by Confocal Raman Microscopy (CRM) to characterize the polymorphal composition (aragonite, vaterite, and calcite). The investigated chondrophore surfaces of all five individuals consisted entirely of aragonite. The age of each bivalve was determined by counting the annual growth rings in the chondrophore region. Summer and winter growth increment widths were measured (in the direction of maximum growth) using a stereomicroscope (SZX12, Olympus, Japan) and a Color View Soft Imaging System according to Brey et al. (2011). The study presents the LA-ICP-SF-MS analysis of three samples (B211, B213, B214) out of five of an age of 16, 18, and 19 years.
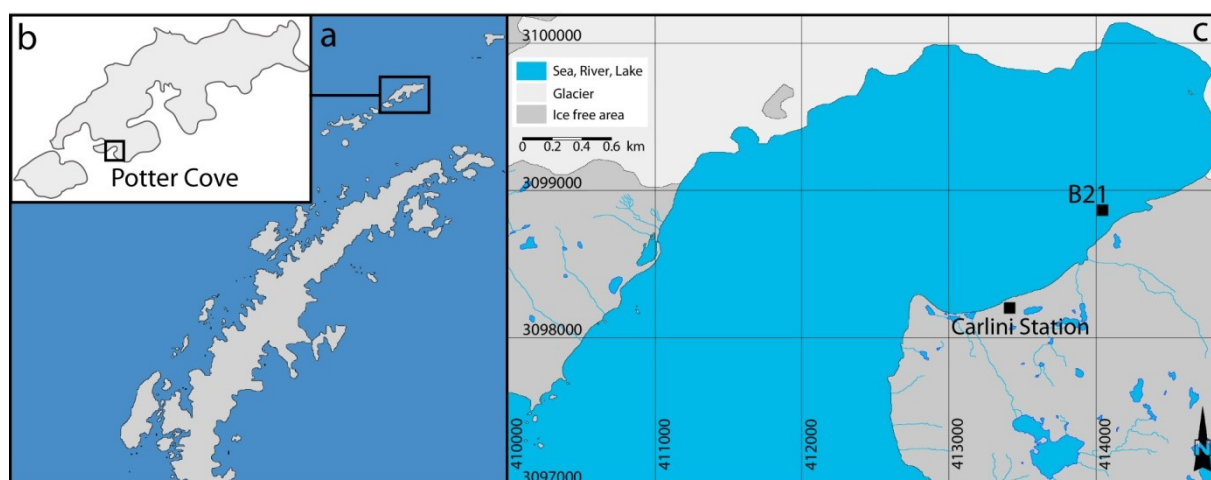
Figure 6.1: a) Map of the Antarctic Peninsula (King George Island highlighted); b) Map of King George Island; c) Map of Potter Cove including the sampling station B21 (UTM grid: zone Z21E; WGS84).

6.2.2 Laser ablation analysis

Annual growth bands of the bivalve chondrophore were sampled in continuous transects (Fig. 6.2b) by LA (Laser UP193, New Wave Research, USA) with a wavelength of 193 nm, coupled to a High resolution (HR)-ICP-MS (Element2, Thermo Finnigan, Germany); see table 6.1 for instrument settings. In a first pass ^{11}B, ^{43}Ca, ^{55}Mn, ^{57}Fe, ^{88}Sr, and ^{138}Ba were analyzed at low resolution (300; LR) to attain maximum intensities. In a subsequent second pass ^{56}Fe was analyzed together with ^{44}Ca (internal standard), and ^{88}Sr (internal indicator for annual growth cycles) in medium resolution (4000; MR). This MR mode enables a separation of Fe and interfering ArO, but at the costs of decreased signal intensity. Intensities of ^{57}Fe (mean over all five samples: 4500 cps) analyzed in the LR mode were only slightly above to the high background signal (averaged 2600 cps), so that Fe contents remained below the limit of quantification (l.o.q.), which was defined as 9x single standard deviation (SD) of the background signal. Therefore, we only show ^{56}Fe results, obtained in the MR mode. All other element intensities were distinctly higher than

the background signal. Sample surfaces were preablated to remove possible contaminations. Prior to ablation, the background signal of the system (gas blank) was measured over 20 s. For the shell samples, Ca was used as internal standard with Ca contents analog to inorganic $CaCO_3$ (40 weight%). For calibration the NIST 612 and NIST 610 standard reference materials were analyzed prior to each transect run. Reference material contents reported by Pearce et al. (1997) were adopted. Iron and Mg were calibrated using the NIST 610 and all other elements using the NIST 612. Concentrations of the second standard (for Mg and Fe: NIST 612; for B, Ba, Mn, and Sr: NIST 610) were calculated via extrapolation and revealed precisions between 2% (^{88}Sr) and 4% (^{56}Fe, ^{138}Ba), except for ^{11}B (7%) and accuracies between -10% (^{11}B) to +1% (^{88}Sr). Additionally, analytical quality was assessed by analyzing a carbonate standard (pressed pellet of NIES22 powder; Yoshinaga et al., 2000) and a basaltic glass (BCR2G; Jochum et al., 2005) along with the samples (Tab. 6.2). Even if the sample matrices between calibration standard and reference material differed, recovery rates for NIES22 were 91% for Sr, 93% for Ba, and 110% for Mg.
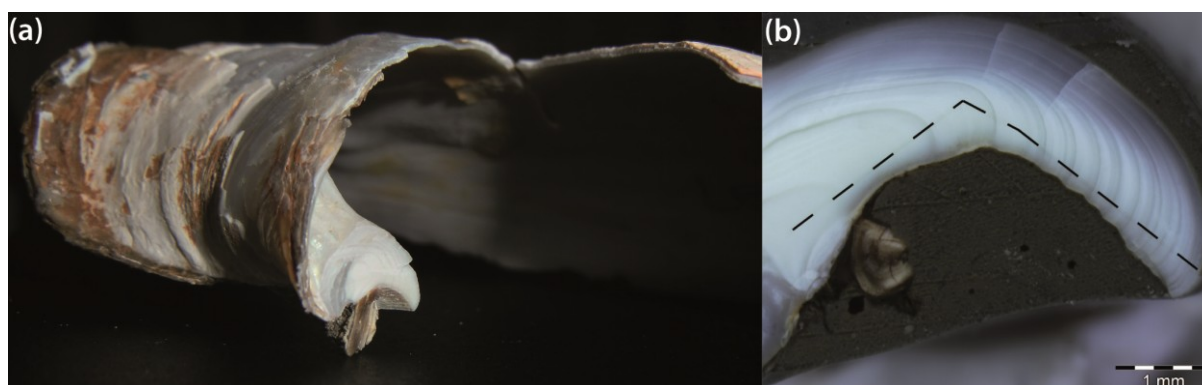
Figure 6.2: a) Shell of *L. elliptica*, cut through the chondrophore; b) Continuous laser ablation transect (black, dashed line) of the annual growth layers in the chondrophore. Dark growth bands are deposited during Austral winter and define the annual growth increments. Note that the ablated transect is not equal to the direction of increment growth, therefore, the transect does not necessarily represent the increment width in figure 6.3 and 6.4.

Table 6.1: Operation conditions of the LA-ICP-MS system.

Laser Ablation: Laser UP193 (New Wave Research)		ICP-MS: Element2 (Thermo Finnigan)	
Laser irradiance	~ 1 GW cm^{-1}	Radio frequency power	1200 W
Repetition rate	5 Hz	He sample gas	0.66 L min^{-1}
Ablation line speed	5 µm s^{-1}	auxiliary gas	0.95 L min^{-1}
Ablation spotsize	50 µm	Ar make-up gas	0.89 L min^{-1}
		Dwell time	50 ms (LR) / 200 ms (MR) per isotope

Table 6.2: Limit of quantification (l.o.q. = 9x SD of the background signal) for all elements and samples. All values in mg kg^{-1}. (LR = low resolution, 300; MR = medium resolution, 4000; N = sample size; n.d. = not determined; * = Analyses in MR were only applied to the samples B211 and B214 and stopped, due to Fe contents distinctly lower than the l.o.q.; n.c. = not certified; conc. = concentration).

Sample	^{11}B (LR) l.o.q.	^{25}Mg (LR) l.o.q.	^{55}Mn (LR) l.o.q.	^{56}Fe (MR) l.o.q.	^{88}Sr (LR) l.o.q.	^{88}Sr (MR) l.o.q.	^{138}Ba (LR) l.o.q.
B211	6.0	3.0	4.0	2.1	2.2	4.5	0.2
B212	7.0	4.5	6.0	n.d.*	1.4	n.d.*	0.2
B213	7.1	4.4	5.2	n.d.*	1.1	n.d.*	0.2
B214	5.7	2.4	4.8	2.1	1.4	4.5	0.3
B215	6.5	4.8	6.2	n.d.*	1.9	n.d.*	0.2
NIES 22 certified	conc. n.c.	conc. 21 ± 1	conc. n.c.	conc. n.c.	conc. 2360 ± 50	conc. 2360 ± 50	conc. 2.89 ± 0.08
found (N=6)	-	23 ± 3	-	-	2150 ± 90	n.d.*	2.7 ± 0.1
BCR2G certified	conc. **6.0**	conc. **21466**	conc. **1550**	conc. **96387**	conc. **342**	conc. **342**	conc. **683**
found (N=1)	6.9	24140	1550	n.d.*	313	n.d.*	573

6.2.3 Statistical analysis

The continuous LA-transects (Fig. 6.2b) diverged from the direction of maximal growth. Therefore, element contents were averaged for summer and winter bands according to the LA-transects to relate the metal content to increment width following the direction of maximum growth. The increment width of the summer growth layers was used as rough approximation for the average growth rate during the Austral summer. Increment width of winter growth layers was not used for statistical analysis, due to considerable changes of metabolism and therefore possible dissolution of the carbonate matrix (further details compare 6.4). Pearson correlation coefficients between the increment width of distinct summer layers and element contents were computed by OriginPro 8 (OriginLab Corporation, USA). Before analysis, data were tested for normal distribution by Kolmogorow-Smirnow test. An alpha level of 5% was chosen as statistically significant.

6.3 Results

Element contents derived from the LA-ICP-SF-MS analysis over ablation distance are given in figure 6.3 (B211, B213, and B214; LR; Sr, Mg, Ba, B, and Mn) and figure 6.4 (B211, B214; MR; Sr, Fe). In all five individuals Sr, Mg, and Ba contents are well above the quantification limit (l.o.q.), whereas B contents vary around or slightly above the l.o.q.. In contrast, Fe and Mn contents decline during the first years of bivalve lifetime below the l.o.q. (Fig. 6.3, 6.4). High l.o.q. for B and Mn result from high background intensities caused by spectral overlap with ^{22}Ne^{++} and ^{40}Ar^{15}N^{+} ions, respectively, that are abundant

in the plasma gas. The relatively high l.o.q. for Fe results from limited transmission in MR mode.
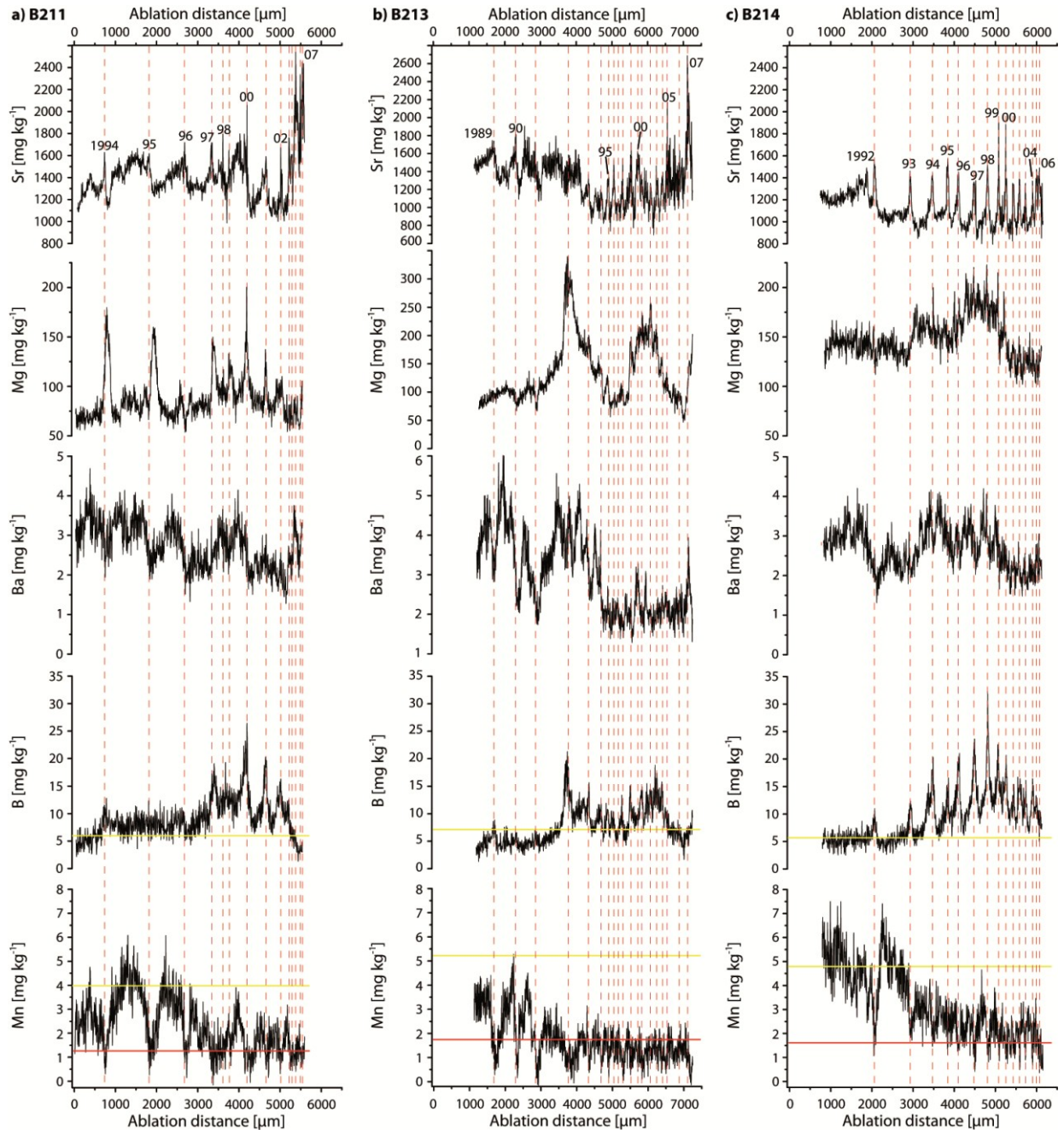
Figure 6.3: Sr, Mg, Ba, B, and Mn contents in the chondrophore of *L. elliptica* (a, B211; b, B213; c, B214) analyzed along continuous transects by LA-ICP-MS with a resolution of 300. Yellow solid lines: Limits of quantification (9x SD), red solid lines: Limits of detection (3x SD). The vertical dashed red lines highlight the winter growth layers.
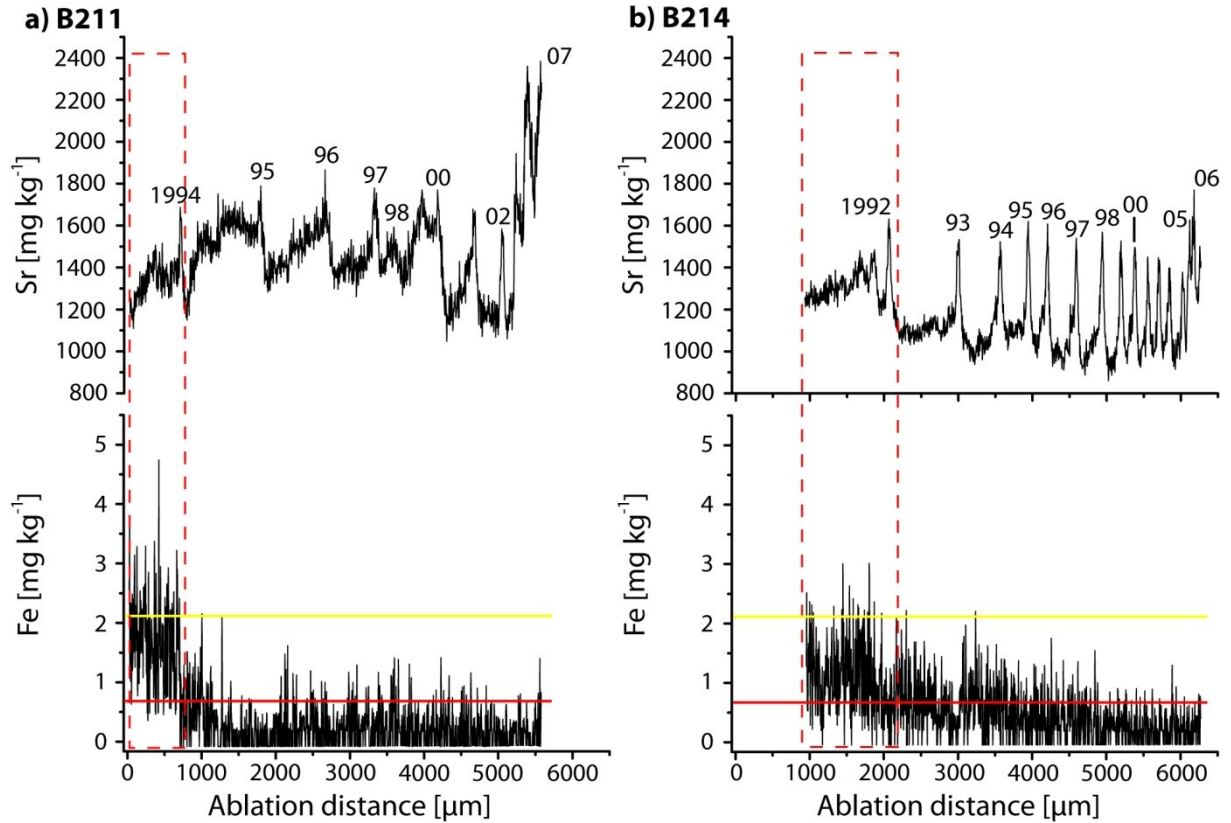
Figure 6.4: Fe and Sr contents in the chondrophore of *L. elliptica* (a, B211; b, B214) measured in continuous transects by LA-ICP-MS with an ICP-MS resolution of 4000. Yellow solid lines show the limits of quantification (9x SD) and red solid lines show the limits of detection (3x SD). The vertical dashed red frame highlight the first annual growth layer.
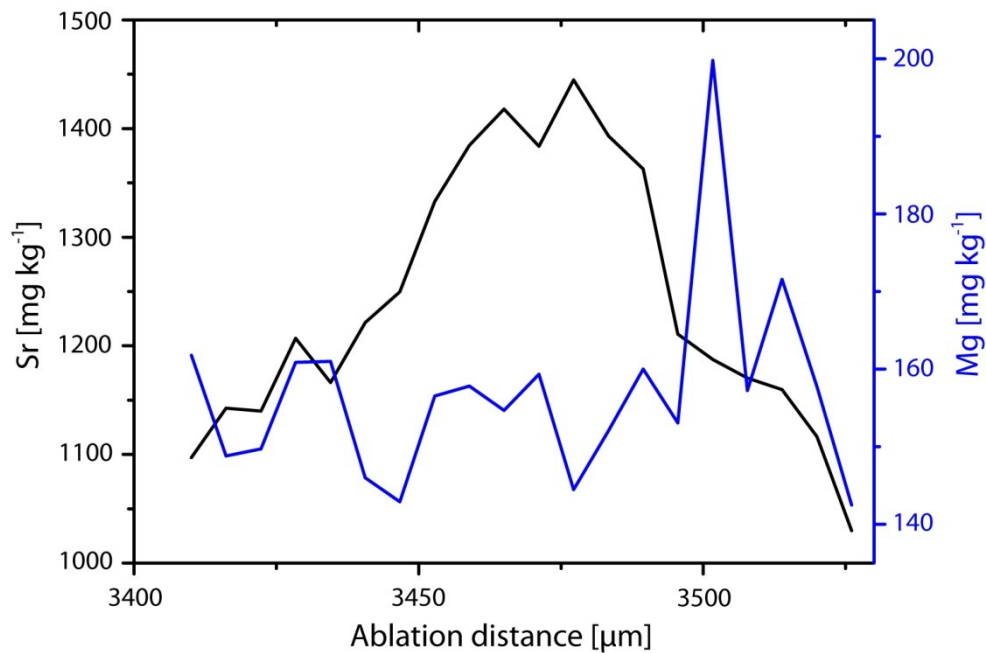
Figure 6.5: Shift of the winter Mg peak compared to the Sr peak of the winter growth layer 1997 of replicate B211. This shift cannot be explained by the sequential analyzing mode of the used ICP-MS system (compare chapter 3).

Table 6.3: Pearson correlation coefficients (r) between summer increment width (used as approximation for averaged growth rate during Austral summer) and element contents and related p-values. '*' denotes significant correlations at an alpha level of 5%. (N = sample size).

	Replicate	B211	B212	B213	B214	B215
Element	N	8	12	9	14	10
Sr	r	0.77*	0.84*	0.84*	0.58*	0.80*
	p-value	0.025*	0.001*	0.005*	0.030*	0.006*
Mg	r	-0.21	0.19	0.09	0.24	0.44
	p-value	0.624	0.562	0.818	0.418	0.204
Ba	r	0.96*	0.86*	0.86*	0.58*	0.93
	p-value	< 0.001*	< 0.001*	0.003*	0.029*	0.785
B	r	-0.60	-0.71*	-0.46	-0.68*	-0.72*
	p-value	0.117	0.009*	0.212	0.010*	0.019*

The comparison of visible seasonal growth layers and ablation transects show that B, Ba, Mg, and Sr underlie a strong seasonality (note that figure 6.3 and 6.4 contain ablation distance which may differ from increment width; compare figure 6.2b). Strontium, Mg, and B peak contents are congruent with winter growth bands (Fig. 6.3). Contrary, Ba content minima coincide with the distinct Sr peaks of the winter growth layers. Further, increment width decreases with increasing animal age, and only two replicates show rising element contents (B211: Sr, Ba; B213: Sr, Mg, Ba) within the last years of lifetime. Apart from seasonal changes, only small variations are observable, such as slight increases in the years 1992/93 (B213, B214) and 2000 to 2002 (B215). Strontium contents in sample B211 remain lower from 2000 to 2002 and Sr baseline content was nearly constant over all years. All Mg time records are dominated by seasonal oscillations except for individual B213, where Mg contents increase strongly in 1991/92 and 1998/99 and decrease in 1992/93 and 2003/04. Weaker changes – overprinted by seasonality – occur in B214 (increase in 1993/94 and 1996/97; decrease in 1999/2000). Within several winter growth layers, Mg maxima are not congruent with Sr maxima (Fig. 6.5), which cannot be explained by the sequential analysis mode by the MS (the time of 0.63 s between the analysis of Mg and Sr corresponds to 3 µm of ablation distance).

Barium baseline contents decrease over lifetime in all shell replicates, although it is less pronounced in B215. In shell B213 Ba content strongly decreases in 1993/94 followed by low contents over several years. In the shells B211 and B214 Ba contents drop during the years 1992/93 (B214), in-between 2000 and 2002 (B211), and starting with 2000 till the end of the recorded lifespan of B214. The individuals B212 and B215 (data not shown) do not display sudden changes in Ba incorporation. In all five replicates maxima in B content in winter growth layers and B base line contents increase after the first three or four years of bivalve lifetime and decrease after a few years again.

Strontium and B incorporation into summer growth layers correlate positively with increment width (approximation for growth rate), whereas Ba content is negatively correlated and Mg uncorrelated to increment width (Tab. 6.3).

Overall, the five individuals show different elemental patterns (except for B), although all individuals were sampled from the same location and were approximately of the same age.

6.4 Discussion

6.4.1 Strontium and magnesium

The Sr content of the aragonitic summer growth layers (~900 – 1800 mg kg^{-1}) of the *L. elliptica* shells in this study are of the same magnitude as found by Nehrke et al. (2012) (~2000 mg kg^{-1}), and in both studies distinct Sr maxima occur in winter growth layers. Therefore, Sr profiles can be used as an internal indicator for the annual growth cycles, as long as the sample surface consists entirely of aragonite (that was confirmed by CRM, see 6.2.1). Similarly, Mg contents are higher in winter growth layers in both studies, although in some years peak shifts among both elements were observable in the LA-ICP-MS transects. However, shifts were smaller than reported for *Arctica islandica* (Epple, 2004; Foster et al., 2008) and both element maxima appeared in winter growth bands (Foster et al., 2008, 2009)

The latter authors further found an increasing amount of organic material surrounding aragonite crystals and changing morphology (shorter, stubbier) of the aragonite within winter growth layers. Likewise, the chondrophore of *L. elliptica* displayed a higher organic molecule content in the winter growth layers deduced from the intense fluorescence in winter layers observed by Confocal Raman Microscopy (Fig. 6.6; Nehrke and Nouet, 2011; Wall and Nehrke, 2012). This study shows simultaneous enrichment of organic matter, Sr, and Mg in the winter growth bands, herein contrasting earlier works. These reported a higher Sr incorporation into organic poor layers of bivalve carbonates (compared to organic rich layers), whereas higher Mg (and Mn) contents were associated with the insoluble organic matrix of shells or pearls (e.g. Lorens and Bender, 1980; Jacob et al., 2008; Takesue et al., 2008; Schoene et al., 2010; Soldati et al., 2010). These authors, therefore, suggested a strong relation of Mg incorporation to the incorporation of organic macromolecules, whereas Sr is associated to the carbonate matrix. X ray absorption near edge structure (XANES) in *Arctica islandica* revealed that within the winter growth layers Mg is associated to the organic matrix and Sr to the carbonate matrix (Foster et al., 2008, 2009). However, the secretion of organic macromolecules from the mantle tissue (to form the organic shell matrix) is genetically determined and, therefore,

species and/or taxon specific (Jacob et al., 2008; Jackson et al., 2010). Since Mg is associated with the organic matrix of the shell, the incorporation of Mg is also species and/or taxon specific (Jacob et al., 2008). Consequently, differences in the incorporation of trace metals into winter growth layers of *L. elliptica* (Sr, Mg, B: high contents vs. Ba: low contents) compared to other species may be explained by (i) qualitative (and quantitative) differences in organic matrix composition, or (ii) by a potential carbonate dissolution due to low metabolic and growth rates during winter (discussed in 6.4.4).
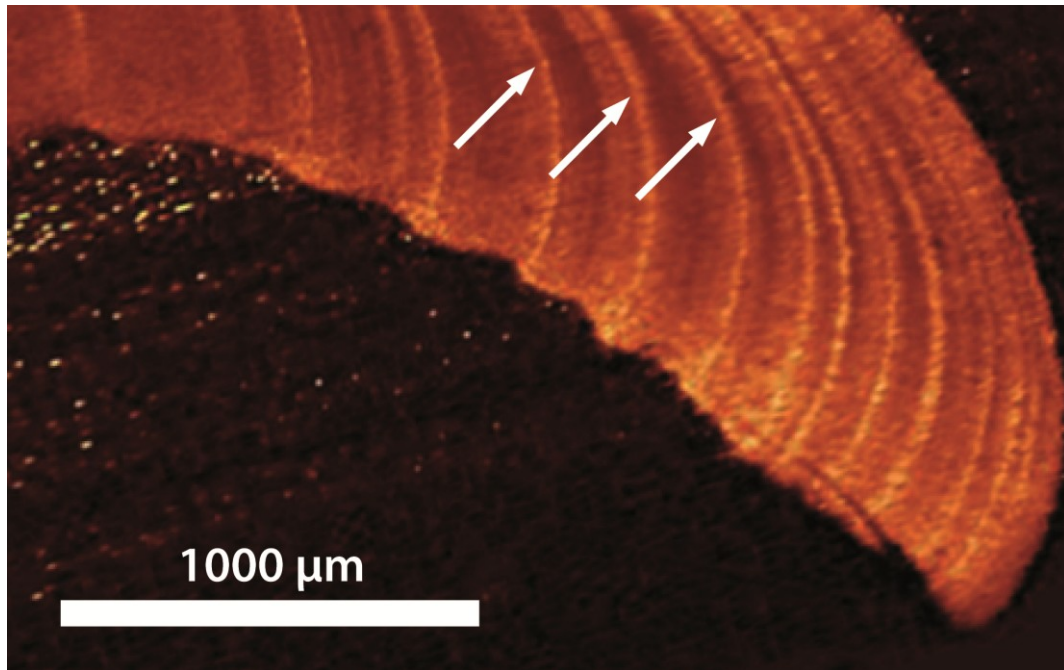
Figure 6.6: Raman fluorescence distribution map of growth layers in a chondrophore of *L. elliptica*. The white arrows point at selected winter growth layers, characterized by higher fluorescence due to higher organic matter content.

Due to the distinct differences in the organic and carbonate matrices among summer and winter growth layers and the influence the organic matrix within the winter growth layers in *L. elliptica*, only the increment width of the summer growth layers was correlated to trace metal contents within these layers (compare 6.2.3). No correlation (r_{mean} = 0.15) between the Mg content and increment width (growth rate) of summer layers was found, whereas the Sr content correlated positively (r_{mean} = 0.77) to the increment width of summer growth layers. This agrees with Carre et al. (2006) who proposed a decreasing discrimination of Sr^{2+} against Ca^{2+} by calcium channels with increasing growth rate in the clams *Mesodesma donacium* and *Chione subrugosa* (both aragonitic). Also in aragonitic shells of the clam *Saxidomus giganteus* most of the variability in Sr/Ca ratios was explained by growth rate ($0.64 < R^2 < 0.87$; Gillikin et al., 2005) and the authors excluded thermodynamic control of Sr incorporation, because of the positive correlation

$(0.09 < R^2 < 0.27)$ between Sr/Ca ratios and temperature. To the contrary, if Sr incorporation was thermodynamically controlled, it would have been negatively correlated to calcification temperature (Kinsman and Holland, 1969; Gaetani and Cohen, 2006). The positive correlation between temperature and Sr incorporation was observed in various studies of bivalve shell formation (Dodd, 1965; Stecher et al., 1996; Freitas et al., 2006) where variations in Sr contents are explained by variations of crystal growth/calcification rate (e.g. Swan, 1957; Dodd, 1965; Palacios et al., 1994; Stecher et al., 1996; Carre et al., 2006). Schoene et al. (2011) reported increasing Sr/Ca and Mg/Ca ratios with decreasing growth rate at advanced age in aragonitic *Arctica islandica* shells, but age (Sr) and growth rate (Mg) detrended data resulted in negative correlations between sea water temperature and Sr/Ca and Mg/Ca ratios. This observation agrees with inorganic precipitation experiments of aragonite (Kinsman and Holland, 1969; Gaetani and Cohen, 2006) and points towards an influence of calcification temperature on the incorporation of Sr. However, temperature explained only for up to 41% (Sr) and 27% (Mg) of the variability in element incorporation in *Arctica islandica* (Schoene et al., 2011). Contrary, in calcitic shells of *Mytilus trossulus* the skeletal Sr/Ca ratios are mainly affected by the metabolic mantle activity (Klein et al., 1996b) and salinity had only a secondary effect. Interestingly these authors also showed that mantle metabolic activity varies with shell curvature, which leads to spatial variability in Sr/Ca ratios (especially along the lateral shell margins). In the calcitic shell of *Mytilus edulis* temperature accounted for only 0.26% of overall variance in Sr/Ca ratio, whereas biological control (~41%) and salinity effects (58.5%) had a higher influence (Heinemann et al., 2011).

In *Mytilus edulis* the biological control was even stronger on the incorporation of Mg and accounted for 79% of the overall variance of the Mg/Ca ratio (Heinemann et al., 2008, 2011). Temperature explained only 21% of variability and no significant influence of salinity on the Mg/Ca ratio was observed (Heinemann et al., 2011). The authors reported a positive correlation between Mg/Ca and temperature at higher salinities (29, 34), below salinity 29 no correlation existed. Contrary, Wanamaker et al. (2008) found a more robust Mg/Ca temperature relationship in the shell of *M. edulis* only at lower salinities (23, 28). Several other authors report a positive or no correlation between Mg incorporation in the carbonate shells of different species and temperature (Klein et al., 1996a; Lazareth et al., 2003; Immenhauser et al., 2005; Foster, 2008).

In Potter Cove the seawater surface temperature (SST) ranged between +2°C and -2°C and varied among seasons (Schloss et al., 2012). Melt water discharge may cause lower salinities at the collection site of *L. elliptica* during the Austral summer, which is located at only 5 m water depth close to melt water streams. Therefore, an influence of changing temperature and salinity on the incorporation of Mg and/or Sr appears possible, but

unlikely – because in an earlier study of Nehrke et al. (2012) an individual of *L. elliptica* from a deeper station (less influenced by freshwater input and seasonal temperature changes of the bottom water < 2°C; Schloss et al., 2012) showed the same general pattern as the individuals analyzed in the present study.

However, if the incorporation of Sr and Mg into the shell of *L. elliptica* is related to environmental forces, the element profiles of all five replicates should document sudden changes similarly.

Mean SST and mean water temperatures at 30 m depth in Potter Cove increased by 0.32°C decade^{-1} between 1991 and 2009 (Schloss et al., 2012). In 2009/10 a strong El Niño event caused a cooling in summer mean SST (Schloss et al., 2012; Bers et al., 2013). Earlier El Niño events (1991/92, 1997/98) were responsible for lower SSTs and the years 2000 – 2002 were characterized by higher SSTs (Bers et al., 2013). Brey et al. (2011) reported lower growth rates than average for *L. elliptica* in Potter Cove related to strong El Niño events (1991/92, 1997/98) and higher growth rates in response to strong La Niña events (1998/99). No distinct changes related to these events occur in the Sr and Mg time records in the five individuals, except the Mg profile of replicate B213 (Fig. 6.3). Two sudden rises of Mg contents in B213 coincide to two contrarian climate events during Austral summer 91/92 (strong El Niño event) and 98/99 (strong La Niña event). The latter peak spans four years, including the warmer years 2000 – 2002. Therefore, the present study reveals no consistent pattern between temperature and Mg and Sr incorporation into five individuals from the same location.

Therefore, we suppose that beside the effect of growth rate on Sr contents in summer growth layers, other physiological parameters (e.g. changes in the chemistry of the extra pallial fluid (EPF) or shell matrix) seem responsible for the winter peaks of both elements (Sr, Mg). Overall, these results for *L. elliptica* are consistent with the results of Foster et al. (2008, 2009) for the aragonitic shell of *Arctica islandica*, who found (i) highest Mg and Sr peaks related to winter growth bands, (ii) a high variation in seasonal patterns between individuals as well as between different shell areas within one individual, (iii) no correlation between metal incorporation and SST variations (Sr, Mg), and (iv) a strong overprint by biological or kinetic processes (Sr).

6.4.2 Barium

The positive correlation (r_{mean} = 0.84) of Ba contents to increment width (growth rate) of summer layers suggests a relation of Ba incorporation to physiological processes, similarly to Sr. Consequently, the decreasing growth and metabolic rates at advanced age explains the decline in Ba content over bivalve lifetime. Minima in Ba content are found in winter growth layers enriched with organic matter. Hence, we suggest that Ba is

associated with the carbonate matrix of the shell in *L. elliptica*, as proposed by Takesue et al. (2008) for *Corbula amurensis*.

Distinct Ba peaks during summer, which could be assigned to phytoplankton blooms (compare introduction), are lacking in all five replicates. This may relate to the low light regime in Potter Cove, where high turbidity hampers intense phytoplankton blooms (Schloss et al., 2002; Schloss and Ferreyra, 2002; Schloss et al., 2012). During the last two decades chlorophyll *a* summer contents (a proxy for phytoplankton biomass) in Potter Cove decreased (Schloss et al., 2012) as well as the Ba contents of summer growth layers decrease or remain constant over life time in all replicates. Moreover, the Ba content in B214 rose during Austral summer 1993/94 but remained constant in B215 (Fig. 6.3). Low chlorophyll a contents just before and during the El Niño events in 1997/98 (Bers et al., 2013) did not result in lower Ba incorporation into the shells. Further, the phase of high chlorophyll *a* values in Potter Cove from 2000 to 2002 did not cause higher Ba contents in the shells of *L. elliptica* – in the replicates B211 and B214 contents are even lower compared to the years before.

Overall, the Ba pattern of only one shell (B213) out of five might be explained by changes in chlorophyll *a* contents and phytoplankton in the water column. Therefore we propose that changes in phytoplankton biomass do not have a significant influence on the Ba incorporation into the shell matrix of *L. elliptica*.

6.4.3 Manganese and iron

The drop in Fe and Mn contents during the first years (Fig. 6.3 and 6.4) is consistent with the results of Dick et al. (2007; for Al, Cu, Mn, Fe, Pb, and U in *L. elliptica*) and Carre et al. (2006; Mn in *Mesodesma donacium* and *Chione subrugosa*). Dick et al. (2007) showed a clear relationship between the strong decrease in metal incorporation and the progressive slowing of age-dependent metabolic rate in mature *L. elliptica* older than eight years of age (Dick et al., 2007). These results reveal a strong physiological influence through growth rate of Fe and Mn incorporation into the shell matrix of *L. elliptica*, which limits the applicability of Fe and Mn as environmental proxies (e.g. plankton blooms, sediment redox conditions, Fe and Mn flux across the benthic boundary layer, input of lithogenic material).

6.4.4 Boron

Several authors reported a control of pH on the B incorporation into the marine carbonates (e.g. inorganic carbonate, foraminifera, bivalves) and a potential use of B as proxy for pH changes of seawater (e.g. Hemming and Hanson, 1992; Sanyal et al., 2000; Yu et al., 2007; Foster, 2008; Rollion-Bard and Erez, 2010; McCoy et al., 2011) or

intensified input of freshwater (salinity-proxy; e.g. Roopnarine et al., 1998). Nevertheless, it is still discussed, if B is mainly hosted in the carbonate (similar to Ba and Sr; Takesue et al., 2008) or the organic matrix (e.g. Heinemann et al., 2012) of the shell – or just species dependent. However, several mollusks physiologically alter the pH and the chemical composition of the EPF (e.g. Crenshaw and Neff, 1969; Crenshaw, 1972; Klein et al., 1996b; Heinemann et al., 2008, 2012) out of which the bivalve carbonate shell is calcified. This raises the general question, if the B incorporation reflects the seawater pH or the pH of the EPF?

In *L. elliptica* a physiological control of B incorporation can be assumed due to the correlation (r_{mean} = -0.63) between B contents and increment width in the summer growth layers. Contrary to Sr and Ba, increasing growth rate results in decreasing B incorporation. Maximum B contents in winter growth layers (analogically to Sr and Mg) are in agreement with McCoy et al. (2011), who found that within the calcitic shell of *Mytilus californianus* distinct B/Ca peaks are associated with winter growth layers, which were also enriched in organic matter (compared to the broader summer growth bands). The authors (and references therein) explain this increased accumulation of organic matter in winter growth layers by a potential carbonate dissolution, due to low metabolic rates and growth rates during winter. Their data further did not show a strong correlation between seawater pH and B/Ca ratio in the bivalve shell (R^2 < 0.21). Together both results indicate a strong biological influence on B incorporation, which the authors relate to a physiological control over the EPF.

In the bivalves *Mercenaria mercenaria* and *Mytilus edulis* pH of the EPF decreased whereas the Ca concentration of the EPF increased during the closure of the valves (Crenshaw and Neff, 1969; Crenshaw, 1972). After the opening of the valves, pH rises and the Ca concentration of the EPF decreases. Brockington (2001) found that *L. elliptica* retracts its siphon and starves over a four months period during the Austral winter at Adelaide Island. Therefore, if a direct regulation (based on a positive correlation) of B incorporation through pH is assumed (e.g. Hemming and Hanson, 1992; Sanyal et al., 2000; Yu et al., 2007; Foster, 2008; McCoy et al., 2011), we would expect a decreasing pH of the EPF during the winter months resulting in lower B accretion into the carbonate. However, our data for *L. elliptica* shows exactly the opposite pattern.

Overall, the pattern of B incorporation in *L. elliptica* cannot be explained by changes in seawater pH. Therefore B is of restricted value as environmental proxy in *L. elliptica*.

6.5 Conclusions

The incorporation of B, Ba, Mg, and Sr into the shell of *L. elliptica* showed a strong seasonality with distinct content maxima of Sr, Mg, and B in winter growth layers coinciding with content minima of Ba. Referring to Schoene et al. (2010), we are aware of the potential overestimation of trace metal concentrations in winter growth layers through the inobservance of seasonal changes in organic matter content (and consequently the content of calcium carbonate). As analytical simplification the calcium content, which is the internal standard for the quantification of the trace metal content, was defined constant. Consequently the decrease in calcium carbonate (through the increase of organic matter) biases the trace metal quantification and would lead to an overestimation of all trace element contents in winter growth layers. Nevertheless, differing seasonal pattern among elements (Ba minima vs. B, Mg, Sr maxima) and peak shifts of Mg and Sr strongly contradict such an analytical bias. In fact, the authenticity of the distinct winter peaks of Mg and Sr was proven independently by Electron Micro Probe in an earlier study (compare Nehrke et al., 2012).

The origin of the seasonal element patterns remains unclear, but can probably be explained by the following theoretical model:

(i) Within the summer growth layers Ba and Sr accretion correlate positively and B negatively with increment width and can therefore assumed to be growth rate dependent. Consequently, the extend of trace metal incorporation into the carbonate matrix of summer growth layers is strongly influenced through growth rate (probably due to changes in ion selectivity). Contrary, Mg is reported to be associated to the organic matrix in other bivalve species, and therefore appears independent from growth rate in *L. elliptica*.

(ii) Within the winter growth layers B, Mg, and Sr are enriched, as well as organic matter. Contrary, Ba content declines during winter. Since we expect a valve closure by individuals of *L. elliptica* in Potter Cove during the winter month (similar like observed by Brockington (2001), two scenarios appear theoretically possible, as the result of a drop in pH of the EPF and dissolving carbonate (Crenshaw and Neff, 1969; Crenshaw, 1972):

(a) Carbonate dissolution during winter month result in enhanced residual organic matter (and lower carbonate content) in winter growth layers, which cause the elevated Mg winter contents. Further, species specific macromolecules possess a higher affinity to B and Sr and a lower affinity to Ba compared to the calcium carbonate matrix.

(b) Carbonate dissolution is responsible for the Mg winter peaks like described in scenario a. The other elements (in particular Ba and Sr) substitute calcium in the carbonate matrix, but differences in bonds strength to the carbonate ions result in different

solubilities during carbonat dissolution. For example, a higher solubility and higher release of Ba compared to Ca can explain the Ba minima within winter growth layers or a lower solubility of Sr compared to Ca would lead to higher residual Sr content in the winter growth layers. (B remains somewhat unclear, because it was associated to the organic or the carbonate matrix depending on the reference). Analogously, such sequential carbonate dissolution according to mineral stability is reported for inorganic calcite (aragonite was rarely considered), where dissolution is severely retarded by organic coatings and trace metals incorporated into the crystals (reviewed in Morse and Arvidson, 2002 and Morse et al., 2007).

Heinemann et al. (2012) found increasing elemental ratios (B/Ca, Mg/Ca, Sr/Ca) in the EPF of *Mytilus edulis* with increasing growth rate and decreasing ratios with shell dissolution. This observation is, however, compatible both scenarios, because the release of Ca during carbonate dissolution (Crenshaw and Neff, 1969) would lead to higher residual trace metal contents in the shell and dilute the trace metal concentrations in the EPF (Ba was unfortunately not investigated).

The results of this study revealed further that:
(i) the interpretation of Fe and Mn is restricted, because both contents remain mainly below the quantification limit. Hence, the analysis of continuous transects – to provide high spatial and temporal resolution - is not practicable for Fe and Mn, due to high background signals caused by spectral overlap and low Fe contents in the shells of *L. elliptica*. Nevertheless, the drop in Fe and Mn contents during the first years of bivalve lifetime is consistent with the results of Dick et al. (2007) who showed a strong dependence of metal incorporation on respiration mass in *L. elliptica*, which further means a strong regulation of Mn and Fe incorporation by physiological processes (respiration mass).
(ii) Especially Sr can be used as an internal indicator for the annual growth cycles, due to its pronounced winter peaks.
(iii) Differences in elemental patterns among the five replicates cannot be attributed to the external environment (e.g. temperature, salinity, sediment load, food availability), because all individuals were sampled from the same location and approximately the same age, but show different elemental pattern.

Overall, the incorporation of all elements is strongly influenced by physiological processes (metabolic activity, growth rate, and probably shell dissolution during winter) and do not provide a significant relationship to the environment of the bivalve. Therefore we

conclude, that the contents of B, Ba, Fe, Mg, Mn, and Sr (and Al, Cu, Pb, and U; Dick et al., 2007) within the shell of *L. elliptica* cannot be used as proxies for changes in the water column (e.g. sediment load, temperature, salinity, pH), induced by glacial retreat around Potter Cove.

7 Conclusions and perspectives

Biogeochemical processes related to the element assimilation and incorporation into the calcium carbonate shell of the Antarctic clam *Laternula elliptica* were studied in different aspects, especially for Fe and Mn. The primary aim of this thesis was to test the assumption, if both elements – stored within the high timely resolved carbonate shell of the bivalve - are suitable as environmental proxies for glacial retreat and input of lithogenic debris into the water column. This chapter outlines the main results of the chapters two to six, with special emphasis on the questions and aims given in chapter 1.4. Furthermore, it summarizes the main remaining problems and presents possible guidelines for future projects.

7.1 Conclusions

Aim 1: Assimilation pathways of Fe and Mn into *Laternula elliptica*

Iron concentrations in hemolymph of *L. elliptica* are strongly affected by external Fe concentrations. High initial Fe hemolymph concentrations declined rapidly during experiments under low Fe concentrations (compare chapter 3). Further, the hemolymph fluid contained on average 70% of the total hemolymphmatic Fe concentration (30% bound in hemocyte cells), which explains the fast adaptation of Fe concentrations in the bivalve hemolymph to variations of external, bioavailable Fe concentrations. Iron concentrations in the hemolymph and pore water samples from the Potter Cove were roughly within the same range, whereas seawater Fe concentrations were too low to explain the high Fe concentrations in *L. elliptica*. Therefore dissolved Fe from pore water was regarded as the main Fe source for *L. elliptica* in Potter Cove (chapter 3).

However, in chapter 3 pore water samples and bivalves were sampled from related but not exactly the same locations. Therefore, small scaled differences in pore water chemistry and distances up to 335 m among related sampling sites likely explain discrepancies in Fe concentrations of pore water and bivalve hemolymph. Nevertheless, it was remarkable that in chapter 4 hemolymph Fe concentrations did not differ significantly among two stations of different Fe pore water concentrations (5 – 120 µmol L^{-1} Fe vs. 10 – 45 µmol L^{-1} Fe within the first 5 cm of sediment depth), although pore water and bivalves were sampled from exactly the same locations. This observation contradicts an assimilation of Fe out of the pore water, at least in the dissolved state. Actually the most reasonable explanation is that dissolved Fe^{2+} (reduced during early diagensis) is transported (by diffusion or advection, e.g. bioturbation) out of the ferruginous zone into the oxic layer or into the bottom water, where it precipitates as easy soluble and highly potential bioavailable ferrihydrates (Monien et al., 2013). Due to this process the easily soluble Fe increased remarkable within the first centimeters of sediment depth (D. Monien,

85

pers. comm.), which is easily ingested by *L. elliptica*, which is clearly shown by the high amount of fine grained lithogenic material in the digestive tract of the bivalve (chapter 2). Since the easy soluble Fe fraction was defined as ascorbic acid-soluble Fe at a pH of 7.5 (modified after Maerz et al., 2008 and references therein), the ferrihydrates are very likely available to the bivalve, despite the moderate pH conditions within the bivalve digestive tract (pH 5.8 – 6.5). The comparison of stable isotopic signatures (δ^{56}Fe) of the bivalve hemolymph and environmental samples (pore water, sediment fractions) may provide further support of this interpretation, since δ^{56}Fe signatures of the hemolymph (-0.21‰ to -1.91‰) of *L. elliptica* are within the general range of pore water samples (+0.5‰ to -4.0‰; e.g. Bergquist and Boyle, 2006; Severmann et al., 2006; Homoky et al., 2009; Severmann et al., 2010). However, the δ^{56}Fe analyses of pore water samples of Potter Cove are currently in progress.

Furthermore, this process can also explain the discrepancy among very low Mn concentrations in bivalve hemolymph compared to higher concentrations of dissolved Mn in pore water. The kinetic of the oxidation of dissolved Mn^{2+} is slower compared to Fe^{2+} (Roitz et al., 2002). Hence, less precipitation of Mn within the oxic benthic boundary layer (compared to Fe) would support the export of Mn into the water column and a lower Mn assimilation by *L. elliptica*, which explains the observed low Mn concentrations in the hemolymph. This in turn implies that the assimilation of dissolved Fe through the bivalve was strongly overestimated in chapter 3, whereas it was underestimated for precipitated pore water Fe - although precipitated pore water Fe was mentioned as potential Fe source for *L. elliptica* (compare figure 3.7).

Nevertheless, the assimilation of pore water Fe and Mn (independently if dissolved or precipitated) by *L. elliptica* is not directly related to the input of lithogenic debris into coastal waters as a consequence of glacial retreat, since the dissimilatory reduction of manganese oxides and iron(hydr)oxides during early diagenesis and the related release of Fe^{2+} and Mn^{2+} are controlled by several factors (e.g. organic matter content, oxygen penetration depth, remineralization rate, bioirrigation/bioturbation). Consequently, the Fe and Mn assimilation of the bivalve does not reflect the glacigenous input of Fe and Mn into the coastal waters and both elements are, therefore, unsuitable as proxies for this environmental process.

Aim 2.1: Mineralogical impact on trace metal incorporation in the calcium carbonate shell of *L. elliptica*

The first report of the coexistence of three different calcium carbonate polymorphs, namely aragonite, calcite and vaterite, in a marine calcifying organism is the scientific highlight of this thesis (chapter 5). Further, the mineralogical composition of the chondrophore did not follow a discernible three-dimensional structure, which may explain why within the first study (chapter 5) all five individuals from three different locations along the WAP were composed of all three polymorphs, whereas it was possible to investigate entirely aragonitic section planes of five individuals from Potter Cove in chapter 6.

Nevertheless, it hampers the usability of trace metals as environmental proxies in the shell of *L. elliptica*, since (i) annual growth layers continued through the different polymorphs and (ii) the incorporation of trace metals into the carbonate matrix is polymorph dependent (shown for Mg and Sr within this thesis). Both observations were already made in other bivalve shells, pearls, and fish otholits (Gauldie, 1996; Melancon et al., 2005; Wehrmeister et al., 2007; Spann et al., 2010; Wehrmeister et al., 2011) and a polymorph dependent incorporation was also observed for Mn (e.g. Melancon et al., 2005; Jacob et al., 2008) and can be assumed for Fe.

Hence, additional, time- and cost-consuming mineralogical analyses are necessary for the determination of the mineralogical composition of the chondrophore, to exclude significant variations in trace metal incorporation due to the presence of different calcium carbonate polymorphs.

Aim 2.2: Optimization of the LA-ICP-MS setup to quantify the Fe and Mn content of the shell

Isobaric mass interferences caused by Ar and Ca (carrier gas, sample matrix) hampered an accurate quantification of Fe in the low resolution mode, due to spectral overlap (compare chapter 6). A higher resolution mode of the ICP-MS enabled a better separation of the analyte (Fe) and interfering species, but at the costs of signal intensity. Due to high background concentrations, signal intensities of Fe and Mn in the shell matrix of *L. elliptica* remained beneath the limits of quantification (l.o.q.).

Therefore, Fe and Mn contents within the shell of *L. elliptica* are too low, to enable element analysis via laser ablation sector-field ICP-MS in the required high spatial (temporal) resolution (continuous ablation transects). In consequence, trace element analysis (not restricted to Fe and Mn) should be conducted as single spot ablation analysis at the costs of spatial resolution, similar to Dick et al. (2007), to ablate sufficient sample material to exceed l.o.q.. The choice of smaller laser wave lengths and smaller spot sizes may reduce the loss in resolution.

Aim 3: Is the element incorporation (especially Fe and Mn) into the shell matrix related to environmental parameters?

Although the interpretation of incorporated Fe and Mn in the shell is restricted due to contents below the l.o.q. (compare aim 2.2) contents of both elements dropped during the first years of bivalve lifetime. This observation is consistent with the results of Dick et al. (2007), who further showed a strong dependence of metal incorporation on respiration mass in *L. elliptica.* This denotes a strong regulation of Mn and Fe incorporation by physiological processes (lifetime metabolic activity). Additionally, Fe and Mn contents declined rapidly during the first years (representing the years 1989 – 1994) and remained continuously low in shell layers of higher ages (representing the years 1995 – 2005). Monien et al. (2011) found increasing sediment mass accumulation rates during the past decades. Therefore, an increasing amount of lithogenic material is not positively correlated to Fe and Mn contents within the shell.

Furthermore, variations in element incorporation of B, Ba, Mg, and Sr in five shells (same location, same age) differed distinctly within the period between 1994 – 2006 and did not provide a significant relationship to the environment of the bivalve (temperature, salinity, sediment load, food availability). Instead, the trace metal incorporation of all investigated elements (B, Ba, Fe, Mg, Mn, and Sr) was strongly influenced by physiological processes (metabolic activity, growth rate, and probably shell dissolution during winter). In consequence, the contents of Fe and Mn (and B, Ba, Mg, and Sr, this study; Al, Cu, Fe, Mn Pb, and U, Dick et al., 2007) within the shell of *L. elliptica* cannot be used as proxies for changes in the water column (e.g. sediment load, temperature, salinity, pH) induced by glacial retreat around Potter Cove.

Overall, neither the Fe and Mn assimilation from lithogenic particulate matter derived from glacial melt waters, nor a relationship between the Fe and Mn incorporation into the calcium carbonate shell of *L. elliptica* and environmental Fe and Mn concentrations was confirmed within this thesis. Therefore, changes in melt water driven import of Fe and Mn into coastal Antarctic waters **<u>cannot</u>** be deduced from variations of trace metal contents (Fe, Mn) in the shell of the clam *Laternula elliptica*. Further, the low Fe and Mn contents disables the possibility to perform high spatial (temporal) resolution analysis within the shell of *L. elliptica* and the polymorph dependent element incorporation necessitates additional analysis to verify homogeneity in calcium carbonate polymorphs. In consequence, Fe and Mn contents in the shell of *L. elliptica* are not suited to reconstruct variations in import of glacigenous derived particulate material to coastal Antarctic waters.

7.2 Perspectives

Even though Fe and Mn contents of the carbonate shell are not practicable as environmental proxies, *Laternula elliptica* posses a high potential as a valuable study subject, with respect to:

(*i*) *the genetic regulation of shell formation by extracellular matrix proteins.*

Genes expressed in nacre forming mantle cells and secreted proteins differ extensively among bivalve and gastropod species (Jackson et al., 2010). These extracellular matrix proteins likely constitute the latter organic shell matrix (Jackson et al., 2010) and regulate the initiation, expansion, and termination of crystal growth as well as the precipitated calcium carbonate polymorph (Lowenstam, 1981; Belcher et al., 1996). The coexistence of aragonite, vaterite, and calcite in *L. elliptica* facilitates the characterization of genes and matrix proteins controlling the simultaneous mineralization of up to three different calcium carbonate polymorphs.

(ii) *the elemental and isotopic Fe metabolism of the clam.*

High Fe concentrations (clearly above the l.o.q.) of tissues and hemolymph in individuals from Potter Cove facilitate Fe isotope measurements. The analyses of δ^{56}Fe signatures of different organs may verify (a) whether a fractionation of Fe isotopes between different organs and body fluids takes place and (b) whether the δ^{56}Fe fingerprints hint to possible Fe source(s) for *L. elliptica*.

8 German-Ukranian coproject (Abstracts)

Toxicological effects of Ni^{2+} and Co^{2+} on the goldfish, *Carassius auratus*

8.1 Tissue specificity in nickel uptake and induction of oxidative stress in kidney and spleen of goldfish Carassius auratus, exposed to waterborne nickel

Abstract

Toxic and carcinogenic effects of nickel compounds are suggested to result from nickel-mediated oxida-tive damage to macromolecules and/or inhibition of cellular antioxidant defenses. We investigated the effects of waterborne Ni^{2+} (10, 25 and 50 mg L^{-1}) on the blood and blood-producing tissues (kidney and spleen) of goldfish to identify relationships between Ni accumulation and oxidative stress. Whereas the main hematological parameters (total hemoglobin and hematocrit) were unaffected, Ni^{2+} exposure had substantial influence on goldfish immune system, causing lymphopenia. Ni accumulation increased renal iron content (by 49–78%) and resulted in elevated lipid peroxide (by 29%) and protein carbonyl content (by 274–278%), accompanied by suppression of the activities of superoxide dismutase (by 50–53%), glu-tathione peroxidase (15–45%), glutathione reductase (31–37%) and glucose-6-phosphate dehydrogenase (20–44%), indicating development of oxidative stress in kidney. In contrast to kidney, in spleen the activation of glutathione peroxidase (by 34–118%), glutathione-S-transferase (by 41–216%) and glutathione reductase (by 47%), as well as constant levels of low molecular mass thiols and metals together with enhanced activity of glucose-6-phosphate dehydrogenase (by 41–94%) speaks for a powerful antioxidant potential that counteracts Ni-induced ROS production. Further, as Ni accumulation in this organ was negligible, Ni-toxicity in spleen may be minimized by efficient exclusion of this otherwise toxic metal.

8.2 Antioxidant system efficiently protects goldfish gills from Ni^{2+}-induced oxidative stress

Abstract

Fish gills are target organs for waterborne metal ions and this work aimed to investigate the effects of waterborne Ni^{2+} (10, 25 and 50 mg L^{-1}) on goldfish gills. A special focus was on the relationship between Ni uptake and the homeostasis of reactive oxygen species (ROS) in the gills, the tissue, in direct contact with the metal pollutant. Ni-accumulation in the gills occurred as a function of exposure concentration (R^2 = 0.98). The main indices of oxidative stress, namely carbonyl proteins (CP) and lipid peroxides (LOOH), decreased by 21–33% and 21–24%, as well as the activities of principal antioxidant enzymes superoxide dismutase and glutathione-dependent peroxidase, by 29–47% and 41–46%, respectively, in gills of Ni-exposed fish. One of the main players in the antioxidant defense of gills seems to be catalase, which increased by 23–53% in Ni-treated fish, and low molecular mass thiol-containing compounds (L-SH), exceeding untreated controls by 73–105% after fish exposure to 10–50 mg L^{-1} of Ni^{2+}. The increased level of L-SH, mainly represented by reduced glutathione, was supported by enhanced activities of glutathione reductase (by 27–38%), glutathione-S-transferase (56–141%) and glucose-6-phosphate dehydrogenase (by 96–117%) and demonstrates the ability of the antioxidant system of gills to resist Ni-induced oxidative stress.

8.3 Goldfish brain and heart are well protected from Ni^{2+}-induced oxidative stress

Authors: Kubrak[§], O.I., Poigner[§], H., Husak, V.V., Rovenko, B.M, Meyer, S., Abele, D., and Lushchak, V.I.

[§]Authors contributed equally.

Abstract

After 96 h goldfish exposure to 10, 25 or 50 mg L^{-1} of Ni^{2+} no Ni accumulation was found in brain and heart, but lipid peroxide concentration was by 44% elevated in brain, whereas carbonyl protein content was by 45−45% decreased in heart. High molecular mass thiol content was enhanced by 30% in heart, while in brain low molecular mass thiol content increased by 28−88%. Superoxide dismutase activity was by 27 and 35% increased in brain and heart, respectively. Glutathione peroxidase activity was lowered to 38 and 62% of control values in both tissues, whereas catalase activity was increased in heart by 15−45%, accompanied by 18−29% decreased glutathione reductase activity. The disturbances of free radical processes in brain and heart might result from Ni-induced injuries to other organs with more prominent changes in heart, because of close contact of this organ with blood, whereas blood-brain barrier seems to protect brain.

9 References

Abele, D., Atencio, A., Dick, D., Gonzalez, O., Kriews, M., Meyer, S., Philipp, E., Stoelting, I. (2008) Iron, copper and manganese discharge from glacial melting into Potter Cove and metal concentrations in *Laternula elliptica* shells. Berichte zur Polar- und Meeresforschung **571**, 39-46.

Addadi, L., Weiner, S. (1989) In: Mann, S., Webb, J., Williams, J.P. (Eds.), Biomineralization, Chemical and Biochemical Perspectives. VCH, Weinheim, pp. 133-156.

Addadi, L., Joester, D., Nudelman, F., Weiner, S. (2006) Mollusk shell formation: A source of new concepts for understanding biomineralization processes. Chemistry-a European Journal **12**, 981-987.

Ahn, I.Y. (1993) Enhanced particle flux through the biodeposition by the Antarctic suspension feeding bivalve *Laternula elliptica* in Marian Cove, King George Island. Journal of Experimental Marine Biology and Ecology **171**, 75-90.

Ahn, I.Y., Kang, J.S., Kang, S.H. (1993) Primary Food Sources for Shallow-water Benthic Fauna in Marian Cove, King George Island during an Austral Summer. Korean Journal of Polar Research **4**, 67–72.

Ahn, I.Y., Lee, S.H., Kim, K.T., Shim, J.E., Kim, D.Y. (1996) Baseline heavy metal concentrations in the Antarctic clam, *Laternula elliptica* in Maxwell Bay, King George Island, Antarctica. Marine Pollution Bulletin **32**, 592-598.

Ahn, I.Y., Chung, H., Kang, J.S., Kang, S.H. (1997) Diatom composition and biomass variability in nearshore waters of Maxwell Bay, Antarctica, during the 1992/1993 austral summer. Polar Biology **17**,123–130.

Ahn, I.Y., Shim, J.H. (1998) Summer metabolism of the Antarctic clam, *Laternula elliptica* (King and Broderip) in Maxwell Bay, King George Island and its implications. Journal of Experimental Marine Biology and Ecology **224**, 253-264.

Ahn, I.Y., Kang, J., Kim, K.W. (2001) The effect of body size on metal accumulations in the bivalve *Laternula elliptica*. Antarctic Science **13**, 355-362.

Ahn, I.Y., Surh, J., Park, Y.G., Kwon, H., Choi, K.S., Kang, S.H., Choi, H.J., Kim, K.W., Chung, H. (2003) Growth and seasonal energetics of the Antarctic bivalve *Laternula elliptica* from King George Island, Antarctica. Marine Ecology Progress Series **257**, 99-110.

Ahrland, S. (1975) Metal complexes present in seawater. In: Goldberg, E.D. (Ed.), The nature of seawater. Dahlem workshop report, Dahlem Konferenzen., Berlin, pp. 219-244.

Aizenberg, J., Addadi, L., Weiner, S., Lambert, G. (1996) Stabilization of amorphous calcium carbonate by specialized macromolecules in biological and synthetic precipitates. Advanced Materials **8**, 222–226, doi:10.1002/adma.19960080307.

Anbar, A.D., Rouxel, O. (2007) Metal stable isotopes in paleoceanography Annual Review of Earth and Planetary Sciences. Annual Reviews, Palo Alto, pp. 717-746.

Balci, N., Bullen, T.D., Witte-Lien, K., Shanks, W.C., Motelica, M., Mandernack, K.W. (2006) Iron isotope fractionation during microbially stimulated Fe(II) oxidation and Fe(III) precipitation. Geochimica et Cosmochimica Acta **70**, 622-639.

Barats, A., Pecheyran, C., Amouroux, D., Dubascoux, S., Chauvaud, L., Donard, O.F.X. (2007) Matrix-matched quantitative analysis of trace-elements in calcium carbonate shells by laser-ablation ICP-MS: application to the determination of daily scale profiles in scallop shell (*Pecten maximus*). Analytical and Bioanalytical Chemistry **387**, 1131-1140.

Barats, A., Amouroux, D., Pecheyran, C., Chauvaud, L., Donard, O.F.X. (2008) High-frequency archives of manganese inputs to coastal waters (Bay of Seine, France) resolved by the LA-ICP-MS analysis of calcitic growth layers along scallop shells (*Pecten maximus*). Environmental Science & Technology **42**, 86-92.

Barats, A., Amouroux, D., Chauvaud, L., Pecheyran, C., Lorrain, A., Thebault, J., Church, T.M., Donard, O.F.X. (2009) High frequency Barium profiles in shells of the Great Scallop *Pecten maximus*: a methodical long-term and multi-site survey in Western Europe. Biogeosciences **6**, 157-170.

Barrera, E., Tevesz, M.J.S., Carter, J.G., McCall, P.L. (1994) Oxygen and carbon isotopic composition and shell microstructure of the bivalve *Laternula elliptica* from Antarctica. Palaios **9**, 275-287.

Batenburg, S.J., Reichart, G.J., Jilbert, T., Janse, M., Wesselingh, F.P., Renema, W. (2011) Interannual climate variability in the Miocene: High resolution trace element and stable isotope ratios in giant clams. Palaeogeography Palaeoclimatology Palaeoecology **306**, 75-81.

Bates, B.C., Kundzewicz, Z.W., Wu, S., Palutikof, J.P. (eds.) (2008) Climate Change and Water. Technical Paper of the Intergovernmental Panel on Climate Change, IPCC Secretariat, Geneva, 210 pp.

Beard, B.L., Johnson, C.M., (1999) High precision iron isotope measurements of terrestrial and lunar materials. Geochimica et Cosmochimica Acta **63**, 1653-1660.

Beard, B.L., Johnson, C.M., Cox, L., Sun, H., Nealson, K.H., Aguilar, C. (1999) Iron isotope biosignatures. Science **285**, 1889-1892.

Beard, B.L., Johnson, C.M., Skulan, J.L., Nealson, K.H., Cox, L., Sun, H. (2003a) Application of Fe isotopes to tracing the geochemical and biological cycling of Fe. Chemical Geology **195**, 87-117.

Beard, B.L., Johnson, C.M., Von Damm, K.L., Poulson, R.L. (2003b) Iron isotope constraints on Fe cycling and mass balance in oxygenated Earth oceans. Geology **31**, 629-632.

Beard, B.L., Johnson, C.M. (2004) Inter-mineral Fe isotope variations in mantle-derived rocks and implications for the Fe geochemical cycle. Geochimica et Cosmochimica Acta **68**, 4727-4743.

Beck, M., Dellwig, L., Schnetger, B., Brumsack, H.J. (2008) Cycling of trace metals (Mn, Fe, Mo, U, V, Cr) in deep pore waters of intertidal flat sediments. Geochimica et Cosmochimica Acta **72**, 2822-2840.

Behrens, G., Kuhn, L.T., Ubic, R., Heuer, A.H. (1995) Raman spectra of vaterite calcium carbonate. Spectroscopy Letters **28**, 983–995, doi:10.1080/00387019508009934.

Belcher, A.M., Wu, X.H., Christensen, R.J., Hansma, P.K., Stucky, G.D., Morse, D.E. (1996) Control of crystal phase switching and orientation by soluble mollusc-shell proteins. Nature **381**, 56-58.

Belshaw, N.S., Zhu, X.K., Guo, Y., O'Nions, R.K. (2000) High precision measurement of iron isotopes by plasma source mass spectrometry. International Journal of Mass Spectrometry **197**, 191-195.

Beniash, E., Aizenberg, J., Addadi, L., Weiner, S. (1997) Amorphous calcium carbonate transforms into calcite during sea urchin larval spicule growth. Proceedings of the Royal Society. *London*, Series B **264**, 461–465, doi:10.1098/rspb.1997.0066.

Bergquist, B.A., Boyle, E.A. (2006) Iron isotopes in the Amazon River system: Weathering and transport signatures. Earth and Planetary Science Letters **248**, 54-68.

Berkman, P.A., Marks, D.S., Shreve, G.P. (1986) Winter sediment resuspension in McMurdo-Sound, Antarctica, and its ecological implications. Polar Biology **6**, 1-3.

Berner, R.A. (1981) A new geochemical classification of sedimentary environments. Journal of Sedimentary Petrology **51**, 359-365.

Bers, A.V., Momo, F., Schloss, I.R., Abele, D. (2013) Analysis of trends and sudden changes in long-term environmental data from King George Island (Antarctica): relationships between global climatic oscillations and local system response. Climatic Change **116**, 789-803.

Bevelander, G., Nakahara, H. (1969) An electron microscope study of the formation of the nacreous layer in the shell of certain bivalve molluscs. Calcified Tissue Research **3**, 84-92.

Bjerregaard, P., Depledge, M.H. (1994) Cadmium accumulation in *Littorina littorea*, *Mytilus edulis* and *Carcinus maenas* – The influence of salinity and calcium ion concentrations. Marine Biology **119**, 385-395.

Brantley, S.L., Liermann, L.J., Guynn, R.L., Anbar, A., Icopini, G.A., Barling, J. (2004) Fe isotopic fractionation during mineral dissolution with and without bacteria. Geochimica et Cosmochimica Acta **68**, 3189-3204.

Braun, M., Hock, R. (2004) Spatially distributed surface energy balance and ablation modelling on the ice cap of King George Island (Antarctica). Global and Planetary Change **42**, 45-58.

Brey, T., Mackensen, A. (1997) Stable isotopes prove shell growth bands in the Antarctic bivalve *Laternula elliptica* to be formed annually. Polar Biology **17**, 465-468.

Brey, T., Voigt, M., Jenkins, K., Ahn, I.Y. (2011) The bivalve *Laternula elliptica* at King George Island — A biological recorder of climate forcing in the West Antarctic Peninsula region. Journal of Marine Systems **88**, 542-552.

Brockington, S. (2001) The seasonal energetics of the Antarctic bivalve *Laternula elliptica* (King and Broderip) at Rothera Point, Adelaide Island. Polar Biology **24**, 523-530.

Brown, K.M., Fraser, K.P.P., Barnes, D.K.A., Peck, L.S. (2004) Links between the structure of an Antarctic shallow-water community and ice-scour frequency. Oecologia **141**, 121-129.

Bruland, K.W., Lohan, M.C. (2004) The control of trace metals in seawater. In: Holland, H.D., Turekian, K.K. (Eds.), The oceans and marine geochemistry: Treatise on geochemistry. Pergamon, Oxford, U.K., pp. 23-47.

Bullen, T.D., White, A.F., Childs, C.W., Vivit, D.V., Schulz, M.S. (2001) Demonstration of significant abiotic iron isotope fractionation in nature. Geology **29**, 699-702

Caldeira, K., Wickett, M.E. (2003) Oceanography: Anthropogenic carbon and ocean pH. Nature **425**, 365, doi:10.1038/425365a.

Canfield, D.E., Thamdrup, B., Hansen, J.W. (1993) The anaerobic degradation of organic-matter in Danish coastal sediments – Iron reduction, manganese reduction, and sulfate reduction. Geochimica et Cosmochimica Acta **57**, 3867-3883.

Canfield, D.E., Thamdrup, B. (2009) Towards a consistent classification scheme for geochemical environments, or, why we wish the term 'suboxic' would go away. Geobiology **7**, 385-392.

Carre, M., Bentaleb, I., Bruguier, O., Ordinola, E., Barrett, N.T., Fontugne, M. (2006) Calcification rate influence on trace element concentrations in aragonitic bivalve shells: Evidences and mechanisms. Geochimica et Cosmochimica Acta **70**, 4906-4920.

Carter, J. G. (1980) Environmental and biological controls of bivalve shell mineralogy and microstructure, in *Skeletal Growth of Aquatic Organisms*, D. C. Rhoads and R. A. Lutz, pp. 69–113, Plenum, New York.

Cook, A.J., Fox, A.J., Vaughan, D.G., Ferrigno, J.G. (2005) Retreating glacier fronts on the Antarctic Peninsula over the past half-century. Science **308**, 541-544.

Corbisier, T.N., Petti, M.A.V., Skowronski, R.S.P., Brito, T.A.S. (2004) Trophic relationships in the nearshore zone of Martel Inlet (King George Island, Antarctica): δ^{13}C stable-isotope analysis. Polar Biology **27**, 75-82.

Craig, H. (1961) Isotopic variations in meteoric waters. Science **133**, 1702-1703.

Crenshaw, M.A., Neff, J.M. (1969) Decalcification at the mantle-shell interface in molluscs. American Zoologist **9**, 881-885.

Crenshaw, M.A. (1972) Inorganic composition of molluscan extrapallial fluid. Biological Bulletin **143**, 506-512.

Crosby, H.A., Roden, E.E., Johnson, C.M., Beard, B.L. (2007) The mechanisms of iron isotope fractionation produced during dissimilatory Fe(III) reduction by *Shewanella putrefaciens* and *Geobacter sulfurreducens*. Geobiology **5**, 169-189

Cuif, J.-P., Dauphin, Y., Sorauf, J.E. (2011) Biominerals and Fossils through Time, Cambridge Univ. Press, Cambridge, U. K.

Cuif, J.-P., Dauphin, Y., Nehrke, G., Nouet, J., Perez-Huerta, A. (2012) Layered growth and crystallization in calcareous biominerals: Impact of structural and chemical evidence on two major concepts in invertebrate biomineralization studies. Minerals **2**, 11–39, doi:10.3390/min2010011.

Cummings, V., Hewitt, J., Van Rooyen, A., Currie, K., Beard, S., Thrush, S., Norkko, J., Barr, N., Heath, P., Halliday, N.J., Sedcole, R., Gomez, A., McGraw, C., Metcalf, V. (2011) Ocean acidification at high latitudes: Potential effects on functioning of the Antarctic bivalve *Laternula elliptica.* PLoS ONE **6**, e16069, doi:10.1371/journal.pone.0016069.

Curtosi, A., Pelletier, E., Vodopivez, C., St Louis, R., Mac Cormack, W.P. (2010) Presence and Distribution of Persistent Toxic Substances in Sediments and Marine Organisms of Potter Cove, Antarctica. Archives of Environmental Contamination and Toxicology **59**, 582-592.

Dean, R.B., Dixon, W.J. (1951) Simplified Statistics for Small Numbers of Observations. Analytical Chemistry **23**, 636-638.

Decho, A.W., Luoma, S.N. (1996) Flexible digestion strategies and trace metal assimilation in marine bivalves. Limnology and Oceanography **41**, 568-572.

Deheyn, D.D., Gendreau, P., Baldwin, R.J., Latz, M.I. (2005) Evidence for enhanced bioavailability of trace elements in the marine ecosystem of Deception Island, a volcano in Antarctica. Marine Environmental Research **60**, 1-33.

Dellwig, O., Bosselmann, K., Kolsch, S., Hentscher, M., Hinrichs, J., Boettcher, M.E., Reuter, R., Brumsack, H.J. (2007) Sources and fate of manganese in a tidal basin of the German Wadden Sea. Journal of Sea Research **57**, 1-18.

Depledge, M.H., Phillips, D.J.H. (1986) Circulation, respiration and fluid dynamics in the gastropod mollusc, *Hemifusus tuba* (Gmelin). Journal of Experimental Marine Biology and Ecology **95**, 1.

Diaz, R.J. (2004) Biological and physical processes structuring deep-sea surface sediments in the Scotia and Weddell Seas, Antarctica. Deep-Sea Research Part II-Topical Studies in Oceanography **51**, 1515-1532.

Dick, D., Philipp, E., Kriews, M., Abele, D. (2007) Is the umbo matrix of bivalve shells (*Laternula elliptica*) a climate archive? Aquatic Toxicology **84**, 450-456.

Dickens, G., Koelling, M., Smith, D., Schnieders, L., Scientists, I.E. (2007) Rhizon Sampling of Pore Waters on Scientific Drilling Expeditions: An Example from the IODP Expedition 302, Arctic Coring Expedition (ACEX). Scientific Drilling **4**, 22-25.

Dierssen, H.M., Smith, R.C., Vernet, M. (2002) Glacial meltwater dynamics in coastal waters west of the Antarctic peninsula. Proceedings of the National Academy of Sciences of the United States of America **99**, 1790-1795.

Dissard, D., Nehrke, G., Reichart, G.J., Bijma, J. (2010) The impact of salinity on the Mg/Ca and Sr/Ca ratio in the benthic foraminifera *Ammonia tepida*: Results from culture experiments. Geochimica et Cosmochimica Acta **74**, 928–940, doi:10.1016/j.gca.2009.10.040.

Domack, E., Leventer, A., Dunbar, R., Taylor, F., Brachfeld, S., Sjunneskog, C., Party, O.D.P.L.S., (2001) Chronology of the Palmer Deep site, Antarctic Peninsula: a Holocene palaeoenvironmental reference for the circum-Antarctic. Holocene **11**, 1-9.

Domínguez, C., Eraso, A. (2007) Substantial changes happened during the last years in the icecap of King George Insular, Antarctica. Karst and Cryokarst. Studies of the Faculty of Earth Sciences, University of Silesia **45**, 87-110.

Dodd, J.R. (1965) Environmental control of strontium and magnesium in *Mytilus*. Geochimica et Cosmochimica Acta **29**, 385-398.

Durrant, S.F. (1999) Laser ablation inductively coupled plasma mass spectrometry: achievements, problems, prospects. Journal of Analytical Atomic Spectrometry **14**, 1385-1403.

Elderfield, H. (1972) Effects of volcanism on water chemistry, Deception Island, Antarctica. Marine Geology **13**, M1–M6.

Elderfield, H. (1976) Manganese fluxes to the oceans. Marine Chemistry **4**, 103-132.

Elrod, V.A., Berelson, W.M., Coale, K.H., Johnson, K.S. (2004) The flux of iron from continental shelf sediments: A missing source for global budgets. Geophysical Research Letters **31**.

Epple, V. (2004) High-resolution climate reconstruction for Holocene based on growth chronologies of bivalve Arctica islandica from the North Sea. Dissertation. University of Bremen.

Epstein, S., Buchsbaum, R., Lowenstam, H., Urey, H.C. (1951) Carbonate-water isotopic temperature scale. Geological Society of America Bulletin **62**, 417-426.

Epstein, S., Buchsbaum, R., Lowenstam, H.A., Urey, H.C. (1953) Revised carbonate-water isotopic temperature scale. Geological Society of America Bulletin **64**, 1315-1326.

Estroff, L. A., Hamilton, A.D. (2001) At the interface of organic and inorganic chemistry: Bioinspired synthesis of composite materials. Chemistry of Materials **13**, 3227–3235, doi:10.1021/cm010110k.

Falini, G., Albeck, S., Weiner, S., Addadi, L. (1996) Control of aragonite or calcite polymorphism by mollusk shell macromolecules. Science **271**, 67-69.

Falter, J.L., Sansone, F.J. (2000) Hydraulic control of pore water geochemistry within the oxic-suboxic zone of a permeable sediment. Limnology and Oceanography **45**, 550-557.

Fehr, M.A., Andersson, P.S., Halenius, U., Gustafsson, O., Morth, C.-M. (2010) Iron enrichments and Fe isotopic compositions of surface sediments from the Gotland Deep, Baltic Sea. Chemical Geology **277**, 310-322.

Ferreyra, G.A., Schloss, I.R., Sahade, R., Tatián, M., Quartino, M.L., Mercuri, G., Momo, F., Fuentes, V.L., Atencio, A. (2003) Acoplamiento pelágico-bentónico: síntesis de 10 años de investigaciones en Caleta Potter (Antártida). Libro de resúmenes V Jornadas Nacionales de Ciencias del Mar y XIII Coloquio Argentino de Oceanografía, Mar del Plata, Argentina, pp. 106.

Finch, A. A., Allison, N. (2007) Coordination of Sr and Mg in calcite and aragonite. Mineralogical Magazine **71**, 539–552, doi:10.1180/minmag.2007.071.5.539.

Fisher, N.S., Teyssie, J.L. (1986) Influence of food composition on the biokinetics and tissue distribution of zinc and americium in mussels. Marine Ecology-Progress Series **28**, 197-207.

Fisher, N.S., Teyssie, J.L., Fowler, S.W., Wang, W.X. (1996) Accumulation and retention of metals in mussels from food and water: A comparison under field and laboratory conditions. Environmental Science & Technology **30**, 3232-3242.

Foster, L.C., Finch, A.A., Allison, N., Andersson, C., Clarke, L.J. (2008) Mg in aragonitic bivalve shells: Seasonal variations and mode of incorporation in *Arctica islandica*. Chemical Geology **254**, 113-119.

Foster, G.L. (2008) Seawater pH, pCO$_2$ and [CO$_3^{2-}$] variations in the Caribbean Sea over the last 130 kyr: A boron isotope and B/Ca study of planktic forminifera. Earth and Planetary Science Letters **271**, 254-266.

Foster, L.C., Allison, N., Finch, A.A., Andersson, C. (2009) Strontium distribution in the shell of the aragonite bivalve *Arctica islandica*. Geochemistry Geophysics Geosystems **10**.

Freitas, P.S., Clarke, L.J., Kennedy, H., Richardson, C.A., Abrantes, F. (2006) Environmental and biological controls on elemental (Mg/Ca, Sr/Ca and Mn/Ca) ratios in shells of the king scallop *Pecten maximus*. Geochimica et Cosmochimica Acta **70**, 5119-5133.

Frenzel, M., Harper, E.M. (2011) Micro-structure and chemical composition of vateritic deformities occurring in the bivalve *Corbicula fluminea* (Mueller, 1774). Journal of Structural Biology **174**, 321–332, doi:10.1016/j.jsb.2011.02.002.

Froelich, P.N., Klinkhammer, G.P., Bender, M.L., Luedtke, N.A., Heath, G.R., Cullen, D., Dauphin, P., Hammond, D., Hartman, B., Maynard, V. (1979) Early oxidation of organic-matter in pelagic sediments of the eastern equatorial Atlantic – Suboxic diagenesis. Geochimica et Cosmochimica Acta **43**, 1075-1090.

Gaetani, G.A., Cohen, A.L. (2006) Element partitioning during precipitation of aragonite from seawater: A framework for understanding paleoproxies. Geochimica et Cosmochimica Acta **70**, 4617-4634.

Gagnon, C., Fisher, N.S. (1997) The bioavailability of sediment-bound Cd, Co, and Ag to the mussel *Mytilus edulis*. Canadian Journal of Fisheries and Aquatic Sciences **54**, 147-156.

Gauldie, R. W. (1996) Effects of temperature and vaterite replacement on the chemistry of metal ions in the otoliths of *Oncorhynchus tshawytscha.* Canadian Journal of Fisheries and Aquatic Sciences **53**, 2015–2026, doi:10.1139/cjfas-53-9-2015.

George, S.G., Pirie, B.J.S., Coombs, T.L. (1976) The kinetics of accumulation and excretion of ferric hydroxide in *Mytilus edulis (l.)* and its distribution in the tissues. Journal of Experimental Marine Biology and Ecology **23**, 71-84.

Gili, J.M., Coma, R., Orejas, C., Lopez-Gonzalez, P.J., Zabala, M. (2001) Are Antarctic suspension-feeding communities different from those elsewhere in the world? Polar Biology **24**, 473-485.

Gillikin, D.P., Lorrain, A., Navez, J., Taylor, J.W., Keppens, E., Baeyens, W., Dehairs, F. (2005) Strong biological controls on Sr/Ca ratios in aragonitic marine bivalve shells. Geochemistry Geophysics Geosystems **6**.

Gillikin, D.P., Lorrain, A., Paulet, Y.M., Andre, L., Dehairs, F. (2008) Synchronous barium peaks in high-resolution profiles of calcite and aragonite marine bivalve shells. Geo-Marine Letters **28**, 351-358.

Gonzalez, P.M., Abele, D., Puntarulo, S. (2010) Exposure to excess dissolved iron in vivo affects oxidative status in the bivalve *Mya arenaria*. Comparative Biochemistry and Physiology C-Toxicology & Pharmacology **152**, 167-174.

Gonzalez, P.M., Puntarulo, S. (2011) Iron and nitrosative metabolism in the Antarctic mollusc *Laternula elliptica*. Comparative Biochemistry and Physiology C-Toxicology & Pharmacology **153**, 243-250.

Goodwin, D.H., Flessa, K.W., Schone, B.R., Dettman, D.L. (2001) Cross-calibration of daily growth increments, stable isotope variation, and temperature in the Gulf of California bivalve mollusk *Chione cortezi*: Implications for paleoenvironmental analysis. Palaios **16**, 387-398.

Graeve, M., Sahade, R., Fuentes, V., Tatián, M., Kattner, G. (2008) Bentho-pelagic coupling at Potter Cove, Antarctica: A fatty acid approach. Berichte zur Polar- und Meeresforschung **571**, 147 – 153.

Griscom, S.B., Fisher, N.S., Luoma, S.N. (2000) Geochemical influences on assimilation of sediment-bound metals in clams and mussels. Environmental Science & Technology **34**, 91-99.

Griscom, S.B., Fisher, N.S. (2004) Bioavailability of sediment-bound metals to marine bivalve molluscs: An overview. Estuaries **27**, 826-838.

Grossman, E.L., Ku, T.L. (1986) Oxygen and carbon isotope fractionation in biogenic aragonite – temperature effects. Chemical Geology **59**, 59-74.

Guelke, M., von Blanckenburg, F. (2007) Fractionation of stable iron isotopes in higher plants. Environmental Science & Technology **41**, 1896-1901.

Harper, E.M., Clark, M.S., Hoffman, J.I., Philipp, E., Peck, L.S., Morley, S.A. (2012) Iceberg Scour and Shell Damage in the Antarctic Bivalve *Laternula elliptica*. Plos One **7**.

Harvey, R.W., Luoma, S.N. (1985) Effect of adherent bacteria and bacterial extracellular polymers upon assimilation by *Macoma balthica* of sediment-bound Cd, Zn and Ag. Marine Ecology-Progress Series **22**, 281-289.

Hasle, G.R., Medlin, L.K. (1990) Family *Bacillariaceae*: the genus *Nitzschia* section *Fragilariopsis*. In: Medlin LK, Priddle J (eds) Polar Marine diatoms. British Antarctic Survey, National Environment Research Council, Cambridge, pp. 181–196.

Heinemann, A., Fietzke, J., Eisenhauer, A., Zumholz, K. (2008) Modification of Ca isotope and trace metal composition of the major matrices involved in shell formation of *Mytilus edulis*. Geochemistry Geophysics Geosystems **9**.

Heinemann, A., Hiebenthal, C., Fietzke, J., Eisenhauer, A., Wahl, M. (2011) Disentangling the biological and environmental control of *M. edulis* shell chemistry. Geochemistry Geophysics Geosystems **12**.

Heinemann, A., Fietzke, J., Melzner, F., Boehm, F., Thomsen, J., Garbe-Schoenberg, D., Eisenhauer, A. (2012) Conditions of Mytilus edulis extracellular body fluids and shell composition in a pH-treatment experiment: Acid-base status, trace elements and δ^{11}B. Geochemistry Geophysics Geosystems **13**.

Hemming, N.G., Hanson, G.N. (1992) Boron isotopic composition and concentration in modern marine carbonates. Geochimica et Cosmochimica Acta **56**, 537-543.

Heroy, D.C., Sjunneskog, C., Anderson, J.B. (2008) Holocene climate change in the Bransfield Basin, Antarctic Peninsula: evidence from sediment and diatom analysis. Antarctic Science **20**, 69-87.

Hoegh-Guldberg, O., Mumby, P.J., Hooten, A.J., Steneck, R.S., Greenfield, P., Gomez, E., Harvell, C.D., Sale, P.F., Edwards, A.J. , Caldeira, K., Knowlton, N., Eakin, C.M., Iglesias-Prieto, R., Muthiga, N., Bradbury, R.H., Dubi, A., Hatziolos, M.E. (2007) Coral reefs under rapid climate change and ocean acidification. Science **318**, 1737–1742, doi:10.1126/science.1152509.

Homoky, W.B., Severmann, S., Mills, R.A., Statham, P.J., Fones, G.R. (2009) Pore-fluid Fe isotopes reflect the extent of benthic Fe redox recycling: Evidence from continental shelf and deep-sea sediments. Geology **37**, 751-754.

Hotz, K., Augsburger, H., Walczyk, T. (2011) Isotopic signatures of iron in body tissues as a potential biomarker for iron metabolism. Journal of Analytical Atomic Spectrometry **26**, 1347-1353.

Hotz, K., Krayenbuehl, P.-A., Walczyk, T. (2012) Mobilization of storage iron is reflected in the iron isotopic composition of blood in humans. Journal of Biological Inorganic Chemistry **17**, 301-309.

Hotz, K., Walczyk, T. (2013) Natural iron isotopic composition of blood is an indicator of dietary iron absorption efficiency in humans. Journal of Biological Inorganic Chemistry **18**, 1-7.

Husmann, G. (2013) The bivalve *Laternula elliptica*: physiological and molecular response to changing coastal Antarctic environments. Dissertation. Institut für Klinische Molekularbiologie, Kiel.

Husmann, G., Abele, D., Monien, D., Monien, P., Kriews, M., Philipp, E. (2012) The influence of sedimentation on metal accumulation and cellular oxidative stress markers in the Antarctic bivalve *Laternula elliptica*. Estuarine Coastal and Shelf Science **111**, 48-59.

Icopini, G.A., Anbar, A.D., Ruebush, S.S., Tien, M., Brantley, S.L. (2004) Iron isotope fractionation during microbial reduction of iron: The importance of adsorption. Geology **32**, 205-208.

Immenhauser, A., Nagler, T.F., Steuber, T., Hippler, D. (2005) A critical assessment of mollusk $^{18}O/^{16}O$, Mg/Ca, and $^{44}Ca/^{40}Ca$ ratios as proxies for Cretaceous seawater temperature seasonality. Palaeogeography Palaeoclimatology Palaeoecology **215**, 221-237.

IPCC (2007) Climate Change 2007: Synthesis Report. Contribution of Working Groups I, II and III to the Fourth Assessment Report of the Intergovernmental Panel on Climate Change [Core Writing Team, Pachauri, R.K., Reisinger, A. (eds.)]. IPCC, Geneva, Switzerland, 104 pp.

Isla, E., Gerdes, D., Palanques, A., Gili, J.-M., Arntz, W. (2006) Particle fluxes and tides near the continental ice edge on the eastern Weddell Sea shelf. Deep Sea Research Part II: Topical Studies in Oceanography **53**, 866-874.

Jackson, D.J., McDougall, C., Woodcroft, B., Moase, P., Rose, R.A., Kube, M., Reinhardt, R., Rokhsar, D.S., Montagnani, C., Joubert, C., Piquemal, D., Degnan, B.M. (2010) Parallel Evolution of Nacre Building Gene Sets in Molluscs. Molecular Biology and Evolution **27**, 591-608.

Jackson, S.E. (2001) The application of Nd:YAG lasers in LA-ICP-MS. *In* Sylvester, P.J. (ed.) Laser Ablation-ICP-Mass Spectrometry in the Earth Sciences: Principles and Applications, Mineralog. Assoc. Canada (MAC) Short Course Series. Mineralogical Association of Canada, 29-45.

Jacob, D.E., Soldati, A.L., Wirth, R., Huth, J., Wehrmeister, U., Hofmeister, W. (2008) Nanostructure, composition and mechanisms of bivalve shell growth. Geochimica et Cosmochimica Acta **72**, 5401-5415.

Jacobs, S.S. (1989) Marine controls on modern sedimentation on the Antarctic continental shelf. Marine Geology **85**, 121-153.

Jeffries, T.E., Perkins, W.T., Pearce, N.J.G. (1995) Comparisons of infrared and ultraviolet-laser probe microanalysis inductively-coupled plasma-mass spectrometry in mineral analysis. Analyst **120**, 1365-1371.

Jochum, K.P., Willbold, M., Raczek, I., Stoll, B., Herwig, K. (2005) Chemical characterisation of the USGS reference glasses GSA-1G, GSC-1G, GSD-1G, GSE-1G, BCR-2G, BHVO-2G and BIR-1G using EPMA, ID-TIMS, ID-ICP-MS and LA-ICP-MS. Geostandards and Geoanalytical Research **29**, 285-302.

Johnson, C.M., Roden, E.E., Welch, S.A., Beard, B.L. (2005) Experimental constraints on Fe isotope fractionation during magnetite and Fe carbonate formation coupled to dissimilatory hydrous ferric oxide reduction. Geochimica et Cosmochimica Acta **69**, 963-993.

Johnson, C.M., Beard, B.L., Roden, E.E. (2008) The iron isotope fingerprints of redox and biogeochemical cycling in the modern and ancient Earth Annual Review of Earth and Planetary Sciences, pp. 457-493.

Kadar, E., Lowe, D.M., Sole, M., Fisher, A.S., Jha, A.N., Readman, J.W., Hutchinson, T.H. (2010) Uptake and biological responses to nano-Fe versus soluble $FeCl_3$ in excised mussel gills. Analytical and Bioanalytical Chemistry **396**, 657-666.

Kang, J.S., Kang, S.H., Lee, J.H., Lee, S.H. (2002) Seasonal variation of microalgal assemblages at a fixed station in King George Island Antarctica, 1996. Marine Ecology Progress Series **229**, 19–32.

Kiczka, M., Wiederhold, J.G., Kraemer, S.M., Bourdon, B., Kretzschmar, R. (2010) Iron Isotope Fractionation during Fe Uptake and Translocation in Alpine Plants. Environmental Science & Technology **44**, 6144-6150.

King, P., Broderip, W. (1832) Description of the Cirripedia, Conchifera and Mollusca in a collection formed by the officers of HMS Adventure and Beagle employed between the years 1826 and 1830 in surveying the southern coasts of South America, including the straits of Magalhaens and the coast of Tierra del Fuego. Zoological Journal **5**, 332-349.

Kinsman, D.J.J., Holland, H.D. (1969) The co-precipitation of cations with $CaCO_3$-IV. The co-precipitation of Sr^{2+} with aragonite between 16° and 96°C. Geochimica et Cosmochimica Acta **33**, 1-17.

Klein, R.T., Lohmann, K.C., Thayer, C.W. (1996a) Bivalve skeletons record sea-surface temperature and delta O-18 via Mg/Ca and O-18/O-16 ratios. Geology **24**, 415-418.

Klein, R.T., Lohmann, K.C., Thayer, C.W. (1996b) Sr/Ca and $^{13}C/^{12}C$ ratios in skeletal calcite of *Mytilus trossulus*: Covariation with metabolic rate, salinity, and carbon isotopic composition of seawater. Geochimica et Cosmochimica Acta **60**, 4207-4221.

Kloeser, H., Quartino, M.L., Wiencke, C. (1996) Distribution of macroalgae and macroalgal communities in gradients of physical conditions in Potter Cove, King George Island, Antarctica. Hydrobiologia **333**, 1-17.

Kloeser, H. (1998) Habitats and distribution patterns of benthic diatoms in Potter Cove (King George Island, Antarctica) and its vicinity. Berichte zur Polarforschung **299**, 95–105.

Kowalke, J. (1998) Energieumsätze benthischer Filtrierer der Potter Cove (King George Island, Antarktis), Berichte zur Polarforschung **286**. Alfred Wegener Institute for Polar and Marine Research, Bremerhaven, pp. 147.

Kowalke, J. (1999) Filtration in Antarctic ascidians - striking a balance. Journal of Experimental Marine Biology and Ecology **242**, 233-244.

Kowalski, N., Dellwig, O., Beck, M., Grunwald, M., Durselen, C.D., Badewien, T.H., Brumsack, H.J., van Beusekom, J.E.E., Boettcher, M.E. (2012) A comparative study of manganese dynamics in the water column and sediments of intertidal systems of the North Sea. Estuarine Coastal and Shelf Science **100**, 3-17.

Krayenbuehl, P.A., Walczyk, T., Schoenberg, R., von Blanckenburg, F., Schulthess, G. (2005) Hereditary hemochromatosis is reflected in the iron isotope composition of blood. Blood **105**, 3812-3816.

Laës, A., Blain, S., Laan, P., Ussher, S.J., Achterberg, E.P., Treguer, P., de Baar, H.J.W. (2007) Sources and transport of dissolved iron and manganese along the continental margin of the Bay of Biscay. Biogeosciences **4**, 181-194.

Landing, W.M., Bruland, K.W. (1987) The contrasting biogeochemistry of iron and manganese in the Pacific-ocean. Geochimica et Cosmochimica Acta **51**, 29-43.

Langebroek, P.M., Paul, A., Schulz, M. (2010) Simulating the sea level imprint on marine oxygen isotope records during the middle Miocene using an ice sheet-climate model. Paleoceanography **25**.

Langer, G., Nehrke, G., Probert, I., Ly, J., Ziveri, P. (2009) Strain-specific responses of *Emiliania huxleyi* to changing seawater carbonate chemistry. Biogeosciences **6**, 2637–2646, doi:10.5194/bg-6-2637-2009.

Langer, G., Probert, I., Nehrke, G., Ziveri, P. (2011) The morphological response of *Emiliania huxleyi* to seawater carbonate chemistry changes: An inter-strain comparison. Journal of Nannoplankton Research **23**, 29–34.

Langlet, D., Alleman, L.Y., Plisnier, P.D., Hughes, H., Andre, L. (2007) Manganese content records seasonal upwelling in Lake Tanganyika mussels. Biogeosciences **4**, 195-203.

Lazareth, C.E., Vander Putten, E., Andre, L., Dehairs, F. (2003) High-resolution trace element profiles in shells of the mangrove bivalve *Isognomon ephippium*: a record of environmental spatio-temporal variations? Estuarine Coastal and Shelf Science **57**, 1103-1114.

Lee, B.G., Luoma, S.N. (1998) Influence of microalgal biomass on absorption efficiency of Cd, Cr, and Zn by two bivalves from San Francisco Bay. Limnology and Oceanography **43**, 1455-1466.

Lohan, M.C., Statham, P.J., Peck, L. (2001) Trace metals in the Antarctic soft-shelled clam *Laternula elliptica*: implications for metal pollution from Antarctic research stations. Polar Biology **24**, 808-817.

Lorens, R.B., Bender, M.L. (1980) The impact of solution chemistry on *Mytilus edulis* calcite and aragonite. Geochimica et Cosmochimica Acta **44**, 1265-1278.

Lorius, C., Jouzel, J., Ritz, C., Merlivat, L., Barkov, N.I., Korotkevich, Y.S., Kotlyakov, V.M. (1985) A 150,000-year climatic record from Antarctic ice. Nature **316**, 591-596.

Loste, E., Wilson, R.M., Seshadri, R., Meldrum, F.C. (2003) The role of magnesium in stabilising amorphous calcium carbonate and controlling calcite morphologies. Journal of Crystal Growth **254**, 206–218, doi:10.1016/S0022-0248(03)01153-9.

Lovley, D.R., Phillips, E.J.P. (1988) Novel mode of microbial energy-metabolism – organic-carbon oxidation coupled to dissimilatory reduction of iron or manganese. Applied and Environmental Microbiology **54**, 1472-1480.

Lowenstam, H. A., Abbott, D.P. (1975) Vaterite: A mineralization product of hard tissues of a marine organism (Ascidicea). Science **188**, 363–365, doi:10.1126/science. 1118730.

Lowenstam, H.A. (1981) Minerals formed by organisms. Science **211**, 1126-1131.

Lowenstam, H. A., Weiner, S. (1989) On Biomineralization, Oxford Univ. Press, New York.

Luoma, S.N., Johns, C., Fisher, N.S., Steinberg, N.A., Oremland, R.S., Reinfelder, J.R. (1992) Determination of selenium bioavailability to a benthic bivalve from particulate and solute pathways. Environmental Science & Technology **26**, 485-491.

Lynn, D.C., Bonatti, E. (1965) Mobility of manganese in diagenesis of deep-sea sediments. Marine Geology **3**, 457-474.

Ma, Z.J., Huang, J., Sun, J., Wang, G.N., Li, C.Z., Xie, L.P., Zhang, R.Q. (2007) A novel extrapallial fluid protein controls the morphology of nacre lamellae in the pearl oyster, *Pinctada fucata*. Journal of Biological Chemistry **282**, 23253-23263.

Maerz, C., Hoffmann, J., Bleil, U., De Lange, G.J., Kasten, S. (2008) Diagenetic changes of magnetic and geochemical signals by anaerobic methane oxidation in sediments of the Zambezi deep-sea fan (SW Indian Ocean). Marine Geology **255**, 118-130.

Maksym, T., Stammerjohn, S.E., Ackley, S., Massom, R. (2012) Antarctic Sea Ice-A Polar Opposite? Oceanography **25**, 140-151.

Mangum, C.P. (1979) A note on blood and water mixing in large marine gastropods. Comparative Biochemistry *and* Physiology **63A**, 389.

Martins, V., Abrantes, I., Grangeia, C., Martins, P., Nagai, R., Sousa, S.H.M., Laut, L.L.M., Dias, J.M.A., Dias, J.M., da Silva, E.F., Rocha, F. (2012) Records of sedimentary dynamics in the continental shelf and upper slope between Aveiro-Espinho (N Portugal). Journal of Marine Systems **96-97**, 48-60.

McConnaughey, T.A., Gillikin, D.P. (2008) Carbon isotopes in mollusk shell carbonates. Geo-Marine Letters **28**, 287-299.

McCoy, S.J., Robinson, L.F., Pfister, C.A., Wootton, J.T., Shimizu, N. (2011) Exploring B/Ca as a pH proxy in bivalves: relationships between *Mytilus californianus* B/Ca and environmental data from the northeast Pacific. Biogeosciences **8**, 2567-2579.

McCrea, J.M. (1950) On the isotopic chemistry of carbonates and a paleotemperature scale. The Journal of Chemical Physics **18**, 849-857.

Melancon, S., Fryer, B.J., Ludsin, S.A., Gagnon, J.P, Yang, Z.P. (2005) Effects of crystal structure on the uptake of metals by lake trout (*Salvelinus namaycush*) otoliths. Canadian Journal of Fisheries and Aquatic Sciences **62**, 2609–2619, doi:10.1139/f05-161.

Meredith, M.P., Wallace, M.I., Stammerjohn, S.E., Renfrew, I.A., Clarke, A., Venables, H.J., Shoosmith, D.R., Souster, T., Leng, M.J. (2010) Changes in the freshwater composition of the upper ocean west of the Antarctic Peninsula during the first decade of the 21st century. Progress in Oceanography **87**, 127-143.

Michalchuk, B.R., Anderson, J.B., Wellner, J.S., Manley, P.L., Majewski, W., Bohaty, S. (2009) Holocene climate and glacial history of the northeastern Antarctic Peninsula: the marine sedimentary record from a long SHALDRIL core. Quaternary Science Reviews **28**, 3049-3065.

Middag, R., de Baar, H.J.W., Laan, P., Huhn, O. (2012) The effects of continental margins and water mass circulation on the distribution of dissolved aluminum and manganese in Drake Passage. Journal of Geophysical Research-Oceans **117**.

Millero, F.J., Yao, W., Aicher, J. (1995) The speciation of Fe(II) and Fe(III) in natural waters. Marine Chemistry **50**, 21-39.

Milliken, K.T., Anderson, J.B., Wellner, J.S., Bohaty, S.M., Manley, P.L. (2009) High-resolution Holocene climate record from Maxwell Bay, South Shetland Islands, Antarctica. Geological Society of America Bulletin **121**, 1711-1725.

Miura, H., Maemoku, H., Seto, K., Moriwaki, K. (1998) Late quaternary east Antarctic melting event in the Soya Coast region based on stratigraphy and oxygen isotopic ratio of fossil molluscs. Polar Geoscience **11**, 260-274.

Monien, P., Schnetger, B., Brumsack, H.J., Hass, H.C., Kuhn, G. (2011) A geochemical record of late Holocene palaeoenvironmental changes at King George Island (maritime Antarctica). Antarctic Science **23**, 255-267.

Monien, D., Monien, P., Bruenjes, R.M., Widmer, T., Schnetger, B. and Brumsack, H.J. (2013) Sedimentary regimes at Potter Cove, King George Island, maritime Antarctica - from source source to sink. EGU General Assembly 2013, held 7-12 April, 2013 in Vienna, Austria, Geophysical Research Abstracts **15**, pp. 7454.

Montes-Hugo, M., Doney, S.C., Ducklow, H.W., Fraser, W., Martinson, D., Stammerjohn, S.E., Schofield, O. (2009) Recent Changes in Phytoplankton Communities Associated with Rapid Regional Climate Change Along the Western Antarctic Peninsula. Science **323**, 1470-1473.

Morse, J.W., Arvidson, R.S. (2002) The dissolution kinetics of major sedimentary carbonate minerals. Earth-Science Reviews **58**, 51-84.

Morse, J.W., Arvidson, R.S., Luttge, A. (2007) Calcium carbonate formation and dissolution. Chemical Reviews **107**, 342-381.

Murphy, E.J., Hofmann, E.E., Watkins, J.L., Johnston, N.M., Pinones, A., Ballerini, T., Hill, S.L., Trathan, P.N., Tarling, G.A., Cavanagh, R.A., Young, E.F., Thorpe, S.E., Fretwell, P. (2013) Comparison of the structure and function of Southern Ocean regional ecosystems: The Antarctic Peninsula and South Georgia. Journal of Marine Systems **109**, 22-42.

Nehrke, G., Van Cappellen, P. (2006) Framboidal vaterite aggregates and their transformation into calcite: A morphological study. Journal of Crystal Growth **287**, 528–530, doi:10.1016/j.jcrysgro.2005.11.080.

Nehrke, G., Nouet, J. (2011) Confocal Raman microscopy as a tool to describe different mineral and organic phases at high spatial resolution within marine biogenic carbonates: Case study on *Nerita undata* (Gastropoda, Neritopsina). Biogeosciences **8**, 3761–3769, doi:10.5194/bg-8-3761-2011.

Nehrke, G., Poigner, H., Wilhelms-Dick, D., Brey, T., Abele, D. (2012) Coexistence of three calcium carbonate polymorphs in the shell of the Antarctic clam *Laternula elliptica*. Geochemistry Geophysics Geosystems **13**.

Nigro, M., Regoli, F., Rocchi, R., Orlando, E. (1997) Heavy metals in Antarctic molluscs. In: Battagalia, B. (Ed.), Antarctic communities species and survival. Cambridge University Press, Cambridge, pp. 409-412.

Noguchi, K., Hui, W.L.W., Gel, Y.R., Gastwirth, J.L., Miao, W. (2009) lawstat: An R package for biostatistics, public policy, and law. R package version 2.3.

Norkko, A., Thrush, S.F., Cummings, V.J., Gibbs, M.M., Andrew, N.L., Norkko, J., Schwarz, A.M. (2007) Trophic structure of coastal Antarctic food webs associated with changes in sea ice and food supply. Ecology **88**, 2810-2820.

Nudelman, F., Chen, H.H., Goldberg, H.A., Weiner, S., Addadi, L. (2007) Spiers memorial lecture: Lessons from biomineralization: comparing the growth strategies of mollusc shell prismatic and nacreous layers in *Atrina rigida*. Faraday Discussions **136**, 9-25.

Nuernberg, D., Bijma, J., Hemleben, C. (1996) Assessing the reliability of magnesium in foraminiferal calcite as a proxy for water mass temperatures. Geochimica et Cosmochimica Acta **60**, 803–814, doi:10.1016/0016-7037(95)00446-7.

Ohno, T., Shinohara, A., Kohge, I., Chiba, M., Hirata, T. (2004) Isotopic analysis of Fe in human red blood cells by multiple collector-ICP-mass spectrometry. Analytical Sciences **20**, 617-621.

Pakhornova, S.V., Hall, P.O.J., Kononets, M.Y., Rozanov, A.G., Tengberg, A., Vershinin, A.V. (2007) Fluxes of iron and manganese across the sediment-water interface under various redox conditions. Marine Chemistry **107**, 319-331.

Palacios, R., Orensanz, J.M., Armstrong, D.A. (1994) Seasonal and lifelong variation of Sr/Ca ratio in shells of *Mya arenaria* from Grays Harbor (Washington) – An ancillary criterion in demographic studies. Estuarine Coastal and Shelf Science **39**, 313-327.

Pearce, N.J.G., Perkins, W.T., Westgate, J.A., Gorton, M.P., Jackson, S.E., Neal, C.R., Chenery, S.P. (1997) A compilation of new and published major and trace element data for NIST SRM 610 and NIST SRM 612 glass reference materials. Geostandards Newsletter-the Journal of Geostandards and Geoanalysis **21**, 115-144.

Peck, L.S., Brockington, S., Vanhove, S., Beghyn, M. (1999) Community recovery following catastrophic iceberg impacts in a soft-sediment shallow-water site at Signy Island, Antarctica. Marine Ecology Progress Series **186**, 1-8.

Peck, L.S. (2005) Prospects for survival in the Southern Ocean: vulnerability of benthic species to temperature change. Antarctic Science **17**, 497-507.

Philipp, E., Brey, T., Poertner, H.O., Abele, D. (2005) Chronological and physiological ageing in a polar and a temperate mud clam. Mechanisms of Ageing and Development **126**, 598-609.

Philipp, E., Brey, T., Voigt, M., Abele, D. (2008) Growth and age of *Laternula elliptica* populations in Potter Cove, King-George-Island. Berichte zur Polar- und Meeresforschung **571**, 216-222.

Philipp, E.E.R., Husmann, G., Abele, D. (2011) The impact of sediment deposition and iceberg scour on the Antarctic soft shell clam *Laternula elliptica* at King George Island, Antarctica. Antarctic Science **23**, 127-138.

Phillips, D.J.H. (1976) Common mussel *Mytilus edulis* as an indicator of pollution by zinc, cadmium, lead and copper .2. Relationship of metals in mussel to those discharged by industry. Marine Biology **38**, 71-80.

Piquet, A.M.T., Bolhuis, H., Meredith, M.P., Buma, A.G.J. (2011) Shifts in coastal Antarctic marine microbial communities during and after melt water-related surface stratification. Fems Microbiology Ecology **76**, 413-427.

Poigner, H. (2012) Characterication of metals in hemolymph and tissues of the Antarctic bivalve *Laternula elliptica*. www.pangaea.de doi:10.1594/PANGAEA.776600.

Poigner, H., Monien, P., Monien, D., Kriews, M., Brumsack, H.J., Wilhelms-Dick, D., Abele, D. Influence of the pore water geochemistry on Fe and Mn assimilation in *Laternula elliptica* at King George Island (Antarctica). submitted to Estuarine, Coastal, and Shelf Science, under review.

Poulton, S.W., Canfield, D.E. (2005) Development of a sequential extraction procedure for iron: implications for iron partitioning in continentally derived particulates. Chemical Geology **214**, 209-221.

Pudsey, C.J. (2000) Sedimentation on the continental rise west of the Antarctic Peninsula over the last three glacial cycles. Marine Geology **167**, 313-338.

Quartino, M.L., Boraso de Zaixso, A.L. (2008) Summer macroalgal biomass in Potter Cove, South Shetland Islands, Antarctica: its production and flux to the ecosystem. Polar Biology **31**, 281-294.

Quartino, M.L., Deregibus, D., Campana, G.L., Edgar, G., Latorre, L., Momo, F.R. (2013) Evidence of Macroalgal Colonization on Newly Ice-Free Areas following Glacial Retreat in Potter Cove (South Shetland Islands), Antarctica. Plos One **8**.

R Development Core Team (2010) R: A language and environment for statistical computing. R Foundation for Statistical Computing, Vienna, Austria.

Rainbow, P.S. (1990) Heavy metal levels in marine invertebrates. In: Furness, R.W., Rainbow, P.S. (Eds.), Heavy metals in the marine environment. CRC Press, Inc., Boca Raton, pp. 67-79.

Rainbow, P.S., Wang, W.X. (2001) Comparative assimilation of Cd, Cr, Se, and Zn by the barnacle *Elminius modestus* from phytoplankton and zooplankton diets. Marine Ecology-Progress Series **218**, 239-248.

Rainbow, P.S. (2002) Trace metal concentrations in aquatic invertebrates: why and so what? Environmental Pollution **120**, 497-507.

Ralph, R., Maxwell, J.G.H. (1977) Growth of two Antarctic lamellibranchs: *Adamussium colbecki* and *Laternula elliptica*. Marine Biology **42**, 171–175, doi:10.1007/BF00391569.

Reinfelder, J.R., Wang, W.X., Luoma, S.N., Fisher, N.S. (1997) Assimilation efficiencies and turnover rates of trace elements in marine bivalves: a comparison of oysters, clams and mussels. Marine Biology **129**, 443-452.

Rey, J., Somoza, L., Martinezfrias, J. (1995) Tectonic, volcanic, and hydrothermal event sequence on Deception Island (Antarctica). Geo-Marine Letters **15**, 1-8.

Rignot, E., Thomas, R.H. (2002) Mass balance of polar ice sheets. Science **297**, 1502-1506.

Robertson, J.D. (1949) Ionic regulation in some marine invertebrates. The Journal of Experimental Biology **26**, 182-200.

Robertson, J.D. (1953) Further studies on ionic regulation in marine invertebrates. The Journal of Experimental Biology **30**, 277-296.

Roitz, J.S., Flegal, A.R., Bruland, K.W. (2002) The biogeochemical cycling of manganese in San Francisco Bay: Temporal and spatial variations in surface water concentrations. Estuarine Coastal and Shelf Science **54**, 227-239.

Rollion-Bard, C., Erez, J. (2010) Intra-shell boron isotope ratios in the symbiont-bearing benthic foraminiferan Amphistegina lobifera: Implications for δ^{11}B vital effects and paleo-pH reconstructions. Geochimica et Cosmochimica Acta **74**, 1530-1536.

Roopnarine, P.D., Fitzgerald, P., Byars, G., Kilb, K. (1998) Coincident boron profiles of bivalves from the gulf of California: Implications for the calculation of paleosalinities. Palaios **13**, 395-400.

Round, F.E., Crawford, R.M., Mann, D.G. (1990) The diatoms, biology & morphology of the genera. Cambridge University Press, Cambridge.

Rueckamp, M., Braun, M., Suckro, S., Blindow, N. (2011) Observed glacial changes on the King George Island ice cap, Antarctica, in the last decade. Global and Planetary Change **79**, 99-109.

Rutgers Van Der Loeff, M.M., Meadows, P.S., Allen, J.A. (1990) Oxygen in pore waters of deep-sea sediments. Philosophical Transactions of the Royal Society of London Series a-Mathematical Physical and Engineering Sciences **331**, 69-84.

Sachs, O., Sauter, E.J., Schlueter, M., van der Loeff, M.M.R., Jerosch, K., Holby, O. (2009) Benthic organic carbon flux and oxygen penetration reflect different plankton provinces in the Southern Ocean. Deep-Sea Research Part I-Oceanographic Research Papers **56**, 1319-1335.

Smale, D. A. (2007) Ice disturbance intensity structures benthic communities in nearshore Antarctic waters. Marine Ecology Progress Series **349**, 89–102, doi:10.3354/meps07104.

Samata, T. (2004) Recent advances in studies on nacreous layer biomineralization, molecular and cellular aspects. Thalassas **20**, 25-44.

Santos, I.R., Silva, E.V., Schaefer, C., Albuquerque, M.R., Campos, L.S. (2005) Heavy metal contamination in coastal sediments and soils near the Brazilian Antarctic Station, King George Island. Marine Pollution Bulletin **50**, 185-194.

Sanyal, A., Nugent, M., Reeder, R.J., Buma, J. (2000) Seawater pH control on the boron isotopic composition of calcite: Evidence from inorganic calcite precipitation experiments. Geochimica et Cosmochimica Acta **64**, 1551-1555.

Sato-Okoshi, W., Okoshi, K. (2008) Characteristics of shell microstructure and growth analysis of the Antarctic bivalve Laternula elliptica from Lutzow-Holm Bay, Antarctica. Polar Biology **31**, 131-138.

Schaeffer, T.E., Ionescu-Zanetti, C., Proksch, R., Fritz, M., Walters, D.A., Almqvist, N., Zaremba, C.M., Belcher, A.M., Smith, B.L., Stucky, G.D., Morse, D.E., Hansma, P.K. (1997) Does abalone nacre form by heteroepitaxial nucleation or by growth through mineral bridges? Chemistry of Materials **9**, 1731-1740.

Schloss, I.R., Ferreyra, G.A., Mercuri, G., Kowalke, J. (1999) Particle flux in an Antarctic shallow coastal environment: a sediment trap study. Scientia Marina **63**, 99-111.

Schloss, I.R., Ferreyra, G.A. (2002) Primary production, light and vertical mixing in Potter Cove, a shallow bay in the maritime Antarctic. Polar Biology **25**, 41-48.

Schloss, I.R., Ferreyra, G.A., Ruiz-Pino, D. (2002) Phytoplankton biomass in Antarctic shelf zones: a conceptual model based on Potter Cove, King George Island. Journal of Marine Systems **36**, 129-143.

Schloss, I.R., Abele, D., Moreau, S., Demers, S., Bers, A.V., Gonzalez, O., Ferreyra, G.A. (2012) Response of phytoplankton dynamics to 19-year (1991-2009) climate trends in Potter Cove (Antarctica). Journal of Marine Systems **92**, 53-66.

Schoenberg, R., von Blanckenburg, F. (2005) An assessment of the accuracy of stable Fe isotope ratio measurements on samples with organic and inorganic matrices by high-resolution multicollector ICP-MS. International Journal of Mass Spectrometry **242**, 257-272.

Schoene, B.R., Oschmann, W., Tanabe, K., Dettman, D., Fiebig, J., Houk, S.D., Kanie, Y. (2004a) Holocene seasonal environmental trends at Tokyo Bay, Japan, reconstructed from bivalve mollusk shells - implications for changes in the East Asian monsoon and latitudinal shifts of the Polar Front. Quaternary Science Reviews **23**, 1137-1150.

Schoene, B.R., Freyre Castro, A.D., Fiebig, J., Houk, S.D., Oschmann, W., Kroencke, I. (2004b) Sea surface water temperatures over the period 1884-1983 reconstructed from oxygen isotope ratios of a bivalve mollusk shell (*Arctica islandica*, southern North Sea). Palaeogeography, Palaeoclimatology, Palaeoecology **212**, 215-232.

Schoene, B.R., Zhang, Z., Jacob, D., Gillikin, D.P., Tutken, T., Garbe-Schoenberg, D., McConnaughey, T., Soldati, A. (2010) Effect of organic matrices on the determination of the trace element chemistry (Mg, Sr, Mg/Ca, Sr/Ca) of aragonitic bivalve shells (*Arctica islandica*)-Comparison of ICP-OES and LA-ICP-MS data. Geochemical Journal **44**, 23-37.

Schoene, B.R., Zhang, Z.J., Radermacher, P., Thebault, J., Jacob, D.E., Nunn, E.V., Maurer, A.F. (2011) Sr/Ca and Mg/Ca ratios of ontogenetically old, long-lived bivalve shells (*Arctica islandica*) and their function as paleotemperature proxies. Palaeogeography Palaeoclimatology Palaeoecology **302**, 52-64.

Seeberg-Elverfeldt, J., Schlueter, M., Feseker, T., Kolling, M. (2005) Rhizon sampling of porewaters near the sediment-water interface of aquatic systems. Limnology and Oceanography-Methods **3**, 361-371.

Severmann, S., Johnson, C.M., Beard, B.L., McManus, J. (2006) The effect of early diagenesis on the Fe isotope compositions of porewaters and authigenic minerals in continental margin sediments. Geochimica et Cosmochimica Acta **70**, 2006-2022.

Severmann, S., Lyons, T.W., Anbar, A., McManus, J., Gordon, G. (2008) Modern iron isotope perspective on the benthic iron shuttle and the redox evolution of ancient oceans. Geology **36**, 487-490.

Severmann, S., McManus, J., Berelson, W.M., Hammond, D.E. (2010) The continental shelf benthic iron flux and its isotope composition. Geochimica et Cosmochimica Acta **74**, 3984-4004.

Shackleton, N. (1967) Oxygen Isotope Analyses and Pleistocene Temperatures Re-assessed. Nature **215**, 15-17.

Shumway, S.E. (1977) Effect of salinity fluctuation on osmotic-pressure and Na^+, Ca^{2+} and Mg^{2+} ion concentrations in hemolymph of bivalve mollusks. Marine Biology **41**, 153-177.

Shuttleworth, S. (1996) Optimisation of laser wavelength in the ablation sampling of glass materials. Applied Surface Science **96**, 513-517.

Simkiss, K., Mason, A.Z. (1983) Metal Ions: Metabolic and Toxic Effects. In: Hochachka, P.W., Wilbur, K.M. (Eds.), The Mollusca: Environmental biochemistry and physiology. Academic Press, Inc., New York, pp. 101-164.

Slomp, C.P., Malschaert, J.F.P., Lohse, L., Van Raaphorst, W.(1997) Iron and manganese cycling in different sedimentary environments on the North Sea continental margin. Continental Shelf Research **17**, 1083-1117.

Smale, D.A., Barnes, D.K.A. (2008) Likely responses of the Antarctic benthos to climate-related changes in physical disturbance during the 21st century, based primarily on evidence from the West Antarctic Peninsula region. Ecography **31**, 289-305.

Smith, C.R., DeMaster, D.J., Thomas, C., Srsen, P., Grange, L., Evrard, V., DeLeo, F. (2012) Pelagic-benthic coupling, food banks, and climate change on the West Antarctic Peninsula Shelf. Oceanography **25**, 188-201.

Soldati, A. L., Jacob, D.F., Wehrmeister, J., Hofmeister, W. (2008) Structural characterization and chemical composition of aragonite and vaterite in freshwater cultured pearls. Mineralogical Magazine **72**, 579–592, doi:10.1180/minmag.2008.072.2.579.

Soldati, A.L., Jacob, D.E., Schoene, B.R., Bianchi, M.M., Hajduk, A. (2009) Seasonal periodicity of growth and composition in valves of *Diplodon chilensis patagonicus* (d'Orbigny, 1835). Journal of Molluscan Studies **75**, 75-85.

Soldati, A.L., Goettlicher, J., Jacob, D.E., Vilas, V.V. (2010) Manganese speciation in *Diplodon chilensis patagonicus* shells: a XANES study. Journal of Synchrotron Radiation **17**, 193-201.

Solomon, S., Qin, D., Manning, M., Chen, Z., Marquis, M., Averyt, K.B., Tignor, M., Miller, H.L. (eds.) (2007) Climate Change 2007: The Physical Science Basis. Contribution of Working Group I to the Fourth Assessment Report of the Intergovernmental Panel on Climate Change. Cambridge University Press, Cambridge, United Kingdom and New York, NY, USA.

Spann, N., Harper, E.M., Aldridge, D.C. (2010) The unusual mineral vaterite in shells of the freshwater bivalve *Corbicula fluminea* from the UK. Naturwissenschaften **97**, 743–751, doi:10.1007/s00114-010-0692-9.

Stammerjohn, S.E., Martinson, D.G., Smith, R.C., Iannuzzi, R.A. (2008) Sea ice in the western Antarctic Peninsula region: Spatio-temporal variability from ecological and climate change perspectives. Deep-Sea Research Part II-Topical Studies in Oceanography **55**, 2041-2058.

Stammerjohn, S., Massom, R., Rind, D., Martinson, D. (2012) Regions of rapid sea ice change: An inter-hemispheric seasonal comparison. Geophysical Research Letters **39**.

Stastna, M., Lamb, K.G. (2008) Sediment resuspension mechanisms associated with internal waves in coastal waters. Journal of Geophysical Research: Oceans **113**, C10016.

Staubwasser, M., von Blanckenburg, F., Schoenberg, R. (2006) Iron isotopes in the early marine diagenetic iron cycle. Geology **34**, 629-632.

Stecher, H.A., Krantz, D.E., Lord, C.J., Luther, G.W., Bock, K.W. (1996) Profiles of strontium and barium in *Mercenaria mercenaria* and *Spisula solidissima* shells. Geochimica et Cosmochimica Acta **60**, 3445-3456.

Steig, E.J., Schneider, D.P., Rutherford, S.D., Mann, M.E., Comiso, J.C., Shindell, D.T. (2009) Warming of the Antarctic ice-sheet surface since the 1957 International Geophysical Year (vol 457, pg 459, 2009). Nature **460**, 766-766.

Steinberg, D.K., Martinson, D.G., Costa, D.P. (2012) Two decades of pelagic ecology of the Western Antarctic Peninsula. Oceanography **25**, 56-67.

Strauss, J., Grossman, E.L., DiMarco, S.F. (2012) Stable isotopes in mollusk shells as indicators of benthic respiration and freshwater penetration on the Texas-Louisiana Shelf. Bulletin of Marine Science **88**, 817-842.

Sundby, B., Silverberg, N. (1981) Pathways of manganese in an open estuarine system. Geochimica et Cosmochimica Acta **45**, 293-307.

Sundby, B., Silverberg, N. (1985) Manganese fluxes in the benthic boundary-layer. Limnology and Oceanography **30**, 372-381.

Swan, E.F. (1957) The meaning of strontium-calcium ratios. Deep Sea Research (1953) **4**, 71.

Syvitski, J.P.M. (1989) On the deposition of sediment within glacier-influenced fjords: Oceanographic controls. Marine Geology **85**, 301-329.

Tada, Y., Wada, H., Miura, H. (2006) Seasonal stable oxygen isotope cycles in an Antarctic bivalve shell (*Laternula elliptica*): a quantitative archive of ice melt runoff. Antarctic Science **18**, 111-115.

Takesue, R.K., Bacon, C.R., Thompson, J.K. (2008) Influences of organic matter and calcification rate on trace elements in aragonitic estuarine bivalve shells. Geochimica et Cosmochimica Acta **72**, 5431-5445.

Tatián, M., Sahade, R., Esnal, G.B. (2004) Diet components in the food of Antarctic ascidians living at low levels of primary production. Antarctic Science **16**, 123-128.

Tatián, M., Sahade, R., Mercuri, G., Fuentes, V.L., Antacli, J.C., Stellfeldt, A., Esnal, G.B. (2008) Feeding ecology of benthic filter-feeders at Potter Cove, an Antarctic coastal ecosystem. Polar Biology **31**, 509-517.

Teal, L.R., Bulling, M.T., Parker, E.R., Solan, M. (2008) Global patterns of bioturbation intensity and mixed depth of marine soft sediments. Aquatic Biology **2**, 207-218.

Thebault, J., Chauvaud, L., L'Helguen, S., Clavier, J., Barats, A., Jacquet, S., Pecheyran, C., Amouroux, D. (2009) Barium and molybdenum records in bivalve shells: Geochemical proxies for phytoplankton dynamics in coastal environments? Limnology and Oceanography **54**, 1002-1014.

Thomas, C.A., Bendell-Young, L.I. (1998) Linking the sediment geochemistry of an intertidal region to metal bioavailability in the deposit feeder *Macoma balthica*. Marine Ecology-Progress Series **173**, 197-213.

Torre, L., Servetto, N., Eory, M.L., Momo, F., Tatián, M., Abele, D., Sahade, R. (2012) Respiratory responses of three Antarctic ascidians and a sea pen to increased sediment concentrations. Polar Biology **35**, 1743-1748.

Turekian, K.K., Bacon, M.P. (2003) Geochronometry of marine deposits. In: Elderfield, H. (Ed.), The oceans and marine geochemistry. Elsevier Ltd.

Turner, A., Olsen, Y.S. (2000) Chemical versus enzymatic digestion of contaminated estuarine sediment: Relative importance of iron and manganese oxides in controlling trace metal bioavailability. Estuarine Coastal and Shelf Science **51**, 717-728.

Turner, J., Colwell, S.R., Marshall, G.J., Lachlan-Cope, T.A., Carleton, A.M., Jones, P.D., Lagun, V., Reid, P.A., Iagovkina, S. (2005) Antarctic climate change during the last 50 years. International Journal of Climatology **25**, 279-294.

Urban, H.J., Mercuri, G. (1998) Population dynamics of the bivalve *Laternula elliptica* from Potter Cove, King George Island, South Shetland Islands. Antarctic Science **10**, 153-160.

Urey, H.C., Lowenstam, H.A., Epstein, S., McKinney, C.R. (1951) Measurement of paleotemperatures and temperatures of the upper cretaceous of England, Denmark, and the southeastern United States. Geological Society of America Bulletin **62**, 399-416.

van Haren, H., Gostiaux, L. (2012) Energy Release Through Internal Wave Breaking. Oceanography **25**, 124-131.

Vander Putten, E., Dehairs, F., Keppens, E., Baeyens, W. (2000) High resolution distribution of trace elements in the calcite shell layer of modern *Mytilus edulis*: Environmental and biological controls. Geochimica et Cosmochimica Acta **64**, 997-1011.

Vaughan, D.G., Marshall, G.J., Connolley, W.M., Parkinson, C., Mulvaney, R., Hodgson, D.A., King, J.C., Pudsey, C.J., Turner, J. (2003) Recent rapid regional climate warming on the Antarctic Peninsula. Climatic Change **60**, 243-274.

Vaughan, D.G. (2006) Recent trends in melting conditions on the Antarctic Peninsula and their implications for ice-sheet mass balance and sea level. Arctic Antarctic and Alpine Research **38**, 147-152.

Waite, T.D. (2001) Thermodynamics of the Iron System in Seawater. In: Turner, D.R., Hunter, K.A. (Eds.), The Biogeochemistry of Iron in Seawater. John Wiley & Sons Ltd., West Sussex, England, pp. 291-342.

Walczyk, T., von Blanckenburg, F. (2002) Natural Iron Isotope Variations in Human Blood. Science **295**, 2065-2066.

Walczyk, T., von Blanckenburg, F. (2005) Deciphering the iron isotope message of the human body. International Journal of Mass Spectrometry **242**, 117-134.

Wall, M., Nehrke, G. (2012) Reconstructing skeletal fiber arrangement and growth mode in the coral *Porites lutea* (Cnidaria, Scleractinia): a confocal Raman microscopy study. Biogeosciences **9**, 4885-4895.

Wanamaker, A.D., Kreutz, K.J., Wilson, T., Borns, H.W., Introne, D.S., Feindel, S. (2008) Experimentally determined Mg/Ca and Sr/Ca ratios in juvenile bivalve calcite for *Mytilus edulis*: implications for paleotemperature reconstructions. Geo-Marine Letters **28**, 359-368.

Wang, W.X., Fisher, N.S. (1996) Assimilation of trace elements by the mussel *Mytilus edulis*: Effects of diatom chemical composition. Marine Biology **125**, 715-724.

Wang, W.X., Fisher, N.S., Luoma, S.N. (1996) Kinetic determinations of trace element bioaccumulation in the mussel *Mytilus edulis*. Marine Ecology-Progress Series **140**, 91-113.

Wang, W.X., Fisher, N.S. (1999) Delineating metal accumulation pathways for marine invertebrates. Science of the Total Environment **238**, 459-472.

Watabe, N. (1974) Crystal growth of calcium carbonate in biological systems. Journal of Crystal Growth **24–2**5, 116–122, doi:10.1016/0022-0248(74)90288-7.

Watabe, N. (1983) Shell repair, in *The Mollusca*, edited by A. S. M. Saleuddin and K. M. Wilbur, pp. 289–316, Academic, London.

Wehrmeister, U., Jacob, D.E., Soldati, A.L., Haeger, T., Hofmeister, W. (2007) Vaterite in freshwater cultured pearls from China and Japan. Journal of Gemmology **30**, 399-412.

Wehrmeister, U., Jacob, D.E., Soldati, A.L., Loges, N., Haeger, T., Hofmeister, W. (2011) Amorphous, nanocrystalline and crystalline calcium carbonates in biological materials. Journal of Raman Spectroscopy **42**, 926-935.

Weiss, I. M., Tuross, N., Addadi, L., Weiner, S. (2002) Mollusc larval shell formation: Amorphous calcium carbonate is a precursor phase for aragonite. Journal of Experimental Zoology **293**, 478–491, doi:10.1002/jez.90004.

Weiss, I.M. (2010) Jewels in the Pearl. Chembiochem **11**, 297-300.

Weyer, S., Schwieters, J. (2003) High precision Fe isotope measurements with high mass resolution MC-ICPMS. International Journal of Mass Spectrometry **226**, 355-368.

White, W.M., Albarede, F., Telouk, P. (2000) High-precision analysis of Pb isotope ratios by multi-collector ICP-MS. Chemical Geology **167**, 257-270.

Wilbur, K. M., Watabe, N. (1963) Experimental studies on calcification in molluscs and the algea *Coccolithus Huxleyi*. Annals of the New York Academy of Sciences **109**, 82–112, doi:10.1111/j.1749-6632.1963.tb13463.x.

Willmer, P., Stone, G., Johnston, I.A. (2000) Environmental Physiology of Animals. Blackwell Science Ltd., Oxford, U.K.

Willows, R.I. (1992) Optimal digestive investment – A model for filter feeders experiencing variable diets. Limnology and Oceanography **37**, 829-847.

Yeats, P.A., Sundby, B., Bewers, J.M. (1979) Manganese recycling in coastal waters. Marine Chemistry **8**, 43-55.

Yoon, H.I., Park, B.-K., Kim, Y., Kang, C.Y. (2002) Glaciomarine sedimentation and its paleoclimatic implications on the Antarctic Peninsula shelf over the last 15,000 years. Palaeogeography, Palaeoclimatology, Palaeoecology **185**, 235-254.

Yoshinaga, J., Nakama, A., Morita, M., Edmonds, J.S. (2000) Fish otolith reference material for quality assurance of chemical analyses. Marine Chemistry **69**, 91-97.

Yu, J., Elderfield, H., Hoenisch, B. (2007) B/Ca in planktonic foraminifera as a proxy for surface seawater pH. Paleoceanography 22.

Zacher, K., Rautenberger, R., Hanelt, D., Wulff, A., Wiencke, C. (2009) The abiotic environment of polar marine benthic algae. Botanica Marina **52**, 483-490.

Zajaczkowski, M., Wlodarska-Kowalczuk, M. (2007) Dynamic sedimentary environments of an Arctic glacier-fed river estuary (Adventfjorden, Svalbard). I. Flux, deposition, and sediment dynamics. Estuarine, Coastal and Shelf Science **74**, 285-296.

Zhu, X.K., Guo, Y., Williams, R.J.P., O'Nions, R.K., Matthews, A., Belshaw, N.S., Canters, G.W., de Waal, E.C., Weser, U., Burgess, B.K., Salvato, B. (2002) Mass fractionation processes of transition metal isotopes. Earth and Planetary Science Letters **200**, 47-62.

Danksagung

Am Ende meiner Dissertation möchte ich bei all jenen Menschen bedanken, die diese Dissertation unterstützt und erst ermöglicht haben, allen voran PD Dr. Doris Abele und Dr. Dorothee Wilhelms-Dick. Liebe Doris, liebe Doro, vielen Dank für das familiäre Arbeitsklima, Eure Unterstützung in den letzten Jahren und für Euer Vertrauen, mich eigene Ideen und Fragestellungen verfolgen zu lassen. Ebenso weiß ich Eure fast endlose Geduld während der Verbesserung meines englischen Schreibstils zu schätzen.

Prof. Dr. Hans-Jürgen Brumsack danke ich für die Begutachtung meiner Dissertation und die Möglichkeit an der Universität Oldenburg zu promovieren.

Dr. Dagmar Kieke danke ich für ihre großartige Unterstützung als externe Mentorin. Liebe Dagmar, herzlichen Dank fürs zuhören und deine Ratschlage wann immer die Realität von meinen Erwartungen und Vorstellungen abgedriftet ist – sowohl fachlich als auch privat. Deinen Einsatz für mich als Person bzw. auf Grund meiner Person empfinde ich als höchstmögliche Wertschätzung für die ich dir, wie auch für das Vertrauen während der gemeinsamen Forschungsfahrten vor meiner Doktorandenzeit, gar nicht genug danken kann!

Stefanie Meyer, Ilsetraut Stölting, Kerstin Beyer und Claudia Daniel bin ich für ihr großartiges Engagement und ihre geduldige Hilfestellung im Labor und während der Expeditionsvorbereitungen dankbar.

Dr. Michael Kriews danke ich für die zahlreichen Gespräche, die mich nicht nur fachlich in dieser Zeit unterstützt haben, und für die Unterstützung, die Labore seiner Arbeitsgruppe für die Probenaufbereitung und Analyse intensiv nutzen zu können.

Prof. Dr. Thomas Brey, Dr. Gernot Nehrke, Prof. Dr. Michael Staubwasser und PD Dr. Andreas Klügel danke ich für die Möglichkeit, die Infrastruktur ihrer Arbeitsgruppen für die Analyse meiner Proben nutzen zu können, sowie für ihre Unterstützung während der Analysen und um den Manuskripten den letzten Feinschliff zu verleihen.

Der AWI Logistik danke ich für die Organisation meiner beiden Forschungsreisen ins Dallmann-Labor, insbesondere Dirk (Mengedoht) und Eberhard (Dr. Eberhard Kohlberg) für die kurzweilige und unterhaltsame Zeit im antarktischen sowie im alpinen Schnee.

Der argentinischen Crew und den Tauchern der Carlini Station (bzw. Jubany) danke ich für die großartige logistische Unterstützung und die *Laternula*-Probennahme in der Antarktis.

Bei meiner Arbeitsgruppe möchte ich mich besonders für das familiäre Arbeitsklima bedanken.

Besonderer Dank gebührt ein paar engen Freunden, die mich durch die teilweise turbulente Doktorandenzeit getragen haben:

Liebe Susann, trotz deines fluchtartigen Bürowechsels während meiner Dienstreise danke ich dir für die gemeinsame Bürozeit in Bremerhaven, Expeditionszeit in der Antarktis und Laborzeit in Köln. Deine Fröhlichkeit konnte meine Laune meistens heben.

Liebe Anneli, lieber Felix, euch danke ich für die schöne gemeinsame Zeit, egal ob in Bremerhaven, auf Expedition oder in den Alpen, aber vor allem bei den häufigen Kaffee (& Kuchen) Pausen, die (dank der vielen Mehlspeisen) den akuten und chronischen Arbeitsfrust etwas vergessen ließen.

Liebe Donata, lieber Patrick, euch danke ich für die langjährige Freundschaft sowie für die intensive Zusammenarbeit, die diese fächerübergreifende Dissertation erst ermöglich hat. An die gemeinsame Zeit auf Expedition oder Konferenzen (und natürlich während des Studiums in Oldenburg) denke ich gerne zurück.

Liebe Christiane, liebe Judith, lieber Torben, danke für die gemeinsame Zeit bei Kaffee/Bier/Wien, ob als Mitbewohner oder „Leidensgenosse", die das Leben im Norden heimischer gemacht hat.

Zum Schluss möchte ich mich noch besonders bei meiner Familie und meiner Frau Irina bedanken, die mich in dieser langen Zeit großartig unterstützt haben, auch wenn es auf Grund der großen geographischen Distanz zu ihrem verzogenen Einzelkind/-enkel/-gatten für sie selbst nicht immer einfach war.

Danke!

CURRICULUM VITAE

Harald Poigner
Dipl. Umweltwiss.

Date of Birth	May 21th, 1984
Place of Birth	Vienna
Marital status	married
Nationality	Austrian

Since Sep 2009	PhD Thesis Alfred Wegener Institute Helmholtz Centre for Polar and Marine Research, Bremerhaven, Germany "Iron and manganese in Antarctic bivalves: Indicators of change in near-shore biogeochemistry?"
Sep 2009 – Dec 2012	Scientific associate within the department "Functional Ecology" at the Alfred Wegener Institute Helmholtz Centre for Polar and Marine Research
May 2009	Diploma in Marine Environmental Sciences University of Oldenburg, Germany
Oct 2008 – May 2009	Diploma Thesis Faculty of Geo- and Atmospheric Sciences University of Innsbruck "Impact of the weather on short-term dynamics of the stratification of the Piburger Lake (Austria)"
Oct 2004 – May 2009	Studies at the Institute for Chemistry and Biology of the Marine Environment (ICBM, Oldenburg, Germany) Marine Environmental Sciences Date of intermediate diploma: September 19th, 2006
Sep 2003 - Sep 2004	University of Applied Sciences (Vienna) Marketing & Sales
June 2003	A-Levels (Horticultural College; Vienna)

Erklärung

Hiermit versichere ich, Harald Poigner, dass ich die vorliegende Arbeit selbstständig und ohne unerlaubte Hilfe unter der Verwendung der angegebenen Quellen und Hilfsmittel verfasst habe. Die den benutzten Werken wörtlich oder inhaltlich entnommenen Stellen sind als solche erkenntlich gemacht worden. Im Rahmen der Promotion wurden die Leitlinien guter wissenschaftlicher Praxis an der Carl von Ossietzky Universität befolgt und weder kommerzielle Vermittlungsdienste noch Beratungsdienste in Anspruch genommen. Darüber hinaus erkläre ich, dass diese Dissertation weder in ihrer Gesamtheit noch in Teilen einer anderen wissenschaftlichen Hochschule zur Begutachtung in einem Promotionsverfahren vorliegt oder vorgelegen hat. Teile der Dissertation (ensprechend gekennzeichnet) wurden bereits veröffentlicht.

Harald Poigner